# The individual and combined effects of creatine monohydrate and lithium chloride supplementation on brain creatine uptake in male and female rats.

Jensen Murphy, BSc Hons.

Applied Health Sciences

Submitted in partial fulfillment of the requirements for the degree of

Master of Science (Kinesiology)

Faculty of Applied Health Sciences, Brock University, St. Catharines, Ontario

# Abstract

During ischemia and traumatic brain injuries (TBIs), phosphocreatine (PCr) acts as a temporal energy buffer preventing rapid decreases in intracellular ATP concentrations. Though, the brain has limited stored creatine and it therefore relies heavily on exogenous substrates. Moreover, creatine monohydrate (CrM) supplementation can significantly increase brain total creatine concentration (TCr). Creatine's ability to enter the brain is dependent on creatine transporters, and limited evidence suggests lithium (Li), through GSK3 inhibition, upregulates this transport. Therefore, the purpose of this research was to investigate the individual and combined influences of *in vivo* creatine monohydrate and lithium chloride on creatine concentrations in the rat brain. 64 Sprague-Dawley rats (32 males, 32 females), given *ad libitum* access to a pelleted 14% certified protein rodent maintenance diet, were randomized into four experimental groups: control (CON), creatine (Cr), lithium (Li), and creatine-lithium (Cr-Li). CrM at 5g/L (0.412g/kg/day) and lithium chloride (LiCl) at 0.2g/L (0.018g/kg/day) were supplemented in the reverse osmosis drinking water. Brain [TCr] was greater with LiCl ($p=0.0002$), irrespective of CrM, and greater with CrM ($p<0.0001$), irrespective of LiCl. For slc6a8 mRNA expression, there was a trend for increased expression with LiCl ($p=0.12$). The female Li group also had a trend greater ($p=0.06$) than the Cr group. Relative daily CrM consumption was higher without LiCl ($p<0.0001$) and higher in females ($p=0.0001$). Relative daily LiCl consumption was higher among females than males ($p<0.0001$). LiCl inhibited GSK3 activity through an increase in pGSK3α, pGSK3β, ratio of pGSK3α:GSK3α, and ratio of pGSK3β:GSK3β and there was a trend for reduced total GSK3 activity ($p=0.11$) with LiCl. In conclusion, this study demonstrated that CrM and LiCl supplementation alone and in combination similarly increased brain TCr, with no synergistic or additive effects when combined.

# Table of Contents

# List of Tables and Figures

## Tables



## Figures

# List of Abbreviations and Nomenclature

| | |
|---|---|
| ABI | anoxic brain injury |
| AGAT | L-arginine:glycine aminotransferase |
| ADP | adenosine diphosphate |
| AMP | adenosine monophosphate |
| AMPA | D-amino-3-hydroxy-5-methyl-4-isoxazole-propionic acid |
| AP | area postrema |
| ATP | adenosine triphosphate |
| [ATP]/[ADP] | ratio of adenosine triphosphate to adenosine diphosphate |
| BBB | blood brain barrier |
| BCA | bicinchoninic acid |
| BSA | bovine serum albumin |
| $Ca^{2+}$ | calcium ion |
| CCAC | Canadian Council on Animal Care |
| CK | creatine kinase |
| CNS | central nervous system |
| CON | control group |
| Cr | creatine |
| Cr-Li | creatine and lithium |
| CrM | creatine monohydrate |
| CRT | creatine transporter |
| CSF | cerebrospinal fluid |
| CT | computed tomography scan |
| DNA | deoxyribonucleic acid |
| DMSO | dimethyl sulfoxide |
| EAA | excitatory amino acid |
| GAA | guanidinoacetic acid |
| GAMT | guanidinoacetate methyltransferase |
| GCS | Glasgow Coma Scale |
| GSK3α | glycogen synthase 3 alpha |
| GSK3β | glycogen synthase 3 beta |
| g | grams |
| HPLC | high performance liquid chromatography |
| HRP | horseradish peroxidase |
| HRT | cardiac tissue |
| HSD | honestly significant difference |
| $K^{+}$ | potassium ion |
| KCl | potassium chloride |
| kDa | kilodaltons |
| kg | kilograms |
| L | litres |
| LDH | lactate dehydrogenase |
| Li | lithium |
| LiCl | lithium chloride |
| mBar | millibar |

| | |
|---|---|
| mg | milligrams |
| $MgCl_2$ | magnesium chloride |
| mL | millilitres |
| mol | moles |
| mM | millimoles per litre |
| mmol | millimoles |
| MRI | magnetic resonance imagine |
| mRNA | messenger ribonucleic acid |
| mTBI | mild traumatic brain injury |
| mTOR | mammalian target of rapamycin |
| N | newtons |
| NAD | nicotinamide adenine dinucleotide |
| NADH | nicotinamide adenine dinucleotide + hydrogen |
| $N^+/K^+$-ATPase | sodium/potassium pump |
| NMDA | N-methyl-D-aspartic acid |
| PCr | phosphocreatine |
| PEP | phosphoenolpyruvate |
| p-GSK3α | phospho-glycogen synthase 3 alpha |
| p-GSK3β | phospho-glycogen synthase 3 beta |
| Pi | inorganic phosphate |
| PK | pyruvate kinase |
| PMSF | phenylmethylsulfonyl fluoride |
| RT-PCR | reverse transcription-polymerase chain reaction |
| PVDF | polyvinylidene difluoride |
| RAAS | renin-angiotensin-aldosterone-system |
| RNA | ribonucleic acid |
| ROS | reactive oxygen species |
| Ser9 | serine 9 |
| slc6a8 | creatine transporter gene |
| TBI | traumatic brain injury |
| TBS | tris-buffered saline |
| TBS-T | tris-buffered saline-tween |
| TCr | total creatine |
| [TCr] | total creatine concentration |
| TIA | transient ischemic attack |
| Tyr216 | tyrosine 216 |
| WGAS | white gastrocnemius |
| WHO | World Health Organization |

# 1. Literature Review

## 1.1. Neurological Conditions

### 1.1.1. Traumatic Brain Injury

A traumatic brain injury (TBI) is defined as an alteration of brain function caused by an external force (Menon, Schwab, Wright, & Maas, 2010). External forces can result in either open or closed head TBIs. Open head injuries are characterized by an external force of an object breaking the skull and dura mater, entering the brain. An example of this is a gunshot wound to the head that exposes the brain to the surrounding air. Closed head injuries, on the other hand, are classified as scenarios in which the skull is not penetrated by an external force. Possible external forces for a closed head TBI include: the brain undergoing a type of acceleration or deceleration movement, the head being struck by or striking an object, and forces due to an explosion (Menon et al., 2010).

Closed head TBIs are more common than open head injuries, as determined by Ginsburg & Huff (2011). Of the closed head TBIs experienced in the United States, falls are the most common cause accounting for over 52%, followed by motor vehicle injuries at 20% (Centers for Disease Control and Prevention, 2019). Motor vehicle TBIs are the result of the acceleration and deceleration forces experienced by the individual involved in the collision. Under stationary conditions, the brain is suspended within the skull in cerebrospinal fluid (CSF). If someone is driving a car at a constant speed and comes to a complete stop by hitting a stationary median, they may suffer from a TBI as a result of this external force. As per Newtons Second Law, the force an object exerts on another object is equal to the mass of the object times its acceleration (Barth, Freeman, Broshek, & Varney, 2001). This is represented by the equation F=ma, where ‘m’ is the mass of the car in kilograms, ‘a’ is the acceleration of the car in meters per second squared, and

'F' is the force of the car acting on the median, expressed in Newtons (N). If this force is great enough, it can cause the individual driving the car to jolt forward, accordingly causing the brain to accelerate forward in the CSF and hit the front of the skull. As per Newton's Third Law of Motion, every action has an equal and opposite reaction (Press, 1987). Therefore, the force in which the car acts on the median, also experiences a force equal and opposite in magnitude of the median acting on the car. This reactionary force can further cause the driver to jolt backwards in their seat. The suspended brain can then accelerate in the opposing direction, known as deceleration, hitting the back of the skull. The individual driving the car who hit the median therefore experiences damage to both frontal and occipital lobes of their brain. An acceleration of ~30 $m^2/s$ or greater in motor vehicle collisions is estimated to result in irreparable brain damage (Barth et al., 2001).

Those suffering from a TBI typically have damaged neurons and bruising of the brain at the site of impact. It is also possible for the brain to swell at the area of injury. Patients may experience decreased or loss of consciousness, memory loss before or after the injury, neurological deficits, and mental state alterations such as confusion or disorientation at the time of the injury (Menon et al., 2010). Loss of consciousness is not necessary for a head injury to be diagnosed as a TBI (Giza & Hovda, 2001). Other common symptoms include unsteadiness, dizziness, headache, visual disturbances and nausea (Giza & Hovda, 2001; Prince & Bruhns, 2017). These symptoms and possible bruising of the brain are used in diagnosing the injury as a TBI.

Initial diagnosis of TBI most commonly involves neuroimaging such as computerized tomography (CT) or magnetic resonance imaging (MRI). A CT scan uses cross-sectional x-ray imaging to determine if the brain has any swelling, bleeding, or is bruised. It is the more cost effective and time sensitive option to evaluate the brain, typically used during the first 24h after injury (Lee & Newberg, 2005). MRI is more sensitive and detailed than CT in its ability to (Lee

& Newberg, 2005). This type of imaging uses radio waves and magnetic fields to capture a full image of the blood flow and tissue health of the brain. MRIs are more time consuming than CTs and are therefore not typically used for the initial diagnosis of head trauma in the Emergency Department or Intensive Care Unit. However, 48-72h after injury of the brain, a MRI scan may be used to obtain a more accurate analysis to guide the treatment process (Lee & Newberg, 2005).

Depending on the case, a TBI can be diagnosed as mild, moderate, or severe. Mild and moderate cases oftentimes do not present as abnormal when conducting initial neuroimaging. This is why the structural imaging techniques mentioned previously for diagnosis are usually paired with the Glasgow Coma Scale (GCS). The GCS is a method used to objectively describe the consciousness level of a patient suffering from a head trauma. It assesses patients based on three categories of responsiveness: eye-opening, motor, and verbal responses (Iverson & Bryan, 2020). Responsiveness is 'scored' in each of these sections from 1 (no response), to 4 (best eye response), 5 (best verbal response), and 6 (best motor response) (Iverson & Bryan, 2020). The lowest a patient can 'score' is 3, with no eye opening, verbal response, or motor response, and the highest is 15 indicating the best responsiveness in the three categories (Iverson & Bryan, 2020). Mild TBIs are indicated by a score of 13-15 on the GCS and normal brain imaging. A TBI is diagnosed as moderate if the patient scores between 9-12 and has either normal or abnormal brain images. Severe TBIs usually have an abnormal outcome in brain images and are classified by a GCS score of 3-8 (Brasure et al., 2012).

There is currently no gold standard treatment for those suffering from a TBI (Prince & Bruhns, 2017). Treatment for TBI is determined on a case-to-case basis. For mild TBI, treatment is based on symptom management. Relative rest 24-48 hours post-injury is recommended to alleviate symptoms and decrease metabolic demand on the brain (Silverberg et al., 2020). This

most commonly includes reduced physical activity levels, limited cognitive activities, and decreased amount of time spent using screen. Lying in a dark room with no sensory stimuli is usually not recommended for mild TBI cases as it does not accelerate recovery (Silverberg et al., 2020). Following relative rest and symptom relief, normal daily activities can be progressively resumed as long as there is no worsening of symptoms. Approximately 1 in 5 patients experience symptoms from an mild TBI that last longer than 1 month (Silverberg et al., 2020). These persisting cases are often related to pre-existing health conditions such as previous TBIs. The other 80% of mild TBI cases are usually resolved within a few weeks of following the necessary steps to return to normal life activities (Silverberg et al., 2020). Moderate and severe TBIs take longer to resolve and often require further and prolonged medical interventions.

TBIs are a significant public health issue as they are recognized as a significant cause of death and disability worldwide (Whiteneck, Cuthbert, Corrigan, & Bogner, 2016). In Canada, an estimated 25,000 hospital visits and 10,000 deaths occur each year due to TBIs (Fu, Jing, McFaull, & Cusimano, 2015). By 2031, TBIs are expected to be among the most common neurological conditions suffered by Canadians (The Government of Canada, 2014). Although there has been an increase in the amount of traumatic brain injuries, the number of deaths related to TBIs has decreased (Galgano et al., 2017). This is likely due to increased awareness and technological advancement in diagnosis. Due to the increased incidence, but lower deaths, there are likely a large population suffering from disabilities related to TBI.

### 1.1.2. Anoxic Injury

An anoxic brain injury (ABI) is caused by a deprivation of oxygen to the brain. Some causes resulting in oxygen deprivation include: stroke, transient ischemic attack, a lack of oxygen at birth, and anything causing obstruction to the trachea (Shah et al., 2004). The extent of oxygen

deprivation depends on the injury; with some injuries limiting oxygen and blood flow, and others completely disallowing any oxygen to the brain. Apoptosis (programmed cell death) of neural cells begins to occur and can further lead to diminished brain function.

The most common anoxic brain injury is stroke, the 3rd leading cause of death in Canada and the 5th leading cause of death in the United States (Bulmer, Volders, & Kamal, 2021; Randolph, 2016). Each year, ~5.5 million people die from a stroke, with mortality rates as high as 60-80% (Caffes, Kurland, Gerzanich, & Marc Simard, 2015). Strokes are responsible for ~130,000 deaths in the United States and a cause of long-term disability (Randolph, 2016). Approximately 87% of strokes that occur are due to blockage in the arteries supplying blood to the brain, more commonly referred to as ischemic stroke (Marsh & Keyrouz, 2010). Such blockages can occur due to narrowing of the arteries or blockage from atherosclerotic plaques. Ischemic stroke can also occur when a blood clot moves from another part of the body to the vessels in the brain, known as an embolism. The second type of stroke that can occur is a hemorrhagic stroke. This happens when a blood vessel in the brain leaks or ruptures, leading to hemorrhage. The two categories of hemorrhagic stroke are intracerebral and subarachnoid. Intracerebral stoke is responsible for 9% of stroke cases and classified as bleeding into the brain parenchyma, the functional tissue of the brain (Marsh & Keyrouz, 2010; Naidech, 2011). Bleeding between the pia and arachnoid membranes is characterized as a subarachnoid stroke, which occurs 4% of the time (Marsh & Keyrouz, 2010; Naidech, 2011). The third type of stroke is classified as a *mini stroke* called a transient ischemic attack (TIA). It is characterized by a blockage of blood flow to the brain for only a short period of time (Navis, Garcia-Santibanez, & Skliut, 2019). Although it is less severe than ischemic and hemorrhagic strokes, it is known as a precursor to the development of a more severe stroke (Navis et al., 2019).

Onset of a stroke is primarily known for its signs and symptoms. Some of these include: slurred speech, face droop, paralysis or numbness in limbs (typically on one side), trouble walking, blurred or blackened vision, and sudden severe onset of a headache (Yew & Cheng, 2009). Following clinical evaluation of these symptoms, further testing such as neuroimaging may take place to rule out other CNS lesions and identify the type of stroke (Yew & Cheng, 2009). A CT scan can be used to detect acute hemorrhage or other mass lesions but may not be sensitive enough to rule out ischemic stroke. An MRI can then be done to detect a possible ischemic stroke as this method is more sensitive (Yew & Cheng, 2009).

The risk of stroke increases with age, with the incidence doubling each decade after 45 years of age (Kelly-Hayes, 2010). Based on the Framingham study cohort, an estimated 1 in 5 women and 1 in 6 men over age 55 years of age will experience a stroke (Petrea et al., 2009) while over 70% of stroke cases are known to occur after the age of 65 years (Kelly-Hayes, 2010). Although strokes are largely observed in the older population, it is still possible to suffer from stroke at a younger age. Between 2000 and 2010, there was a 44% increase in stroke cases amongst those aged 25-44 (Randolph, 2016).

Current prevention of stroke is limited to the management of cardiovascular disease and healthy lifestyle choices (Caffes et al., 2015; Kelly-Hayes, 2010; Marsh & Keyrouz, 2010). Treatment for stroke is time-dependent from the onset of symptoms. Thrombolysis using intravenous recombinant-tissue plasminogen activator (IV r-TPA) is the gold-standard treatment for acute ischemic stroke (Jivan, Ranchod, & Modi, 2013). It is most effective when administered no longer than three hours from the onset of stroke (Jivan et al., 2013). A mechanical thrombectomy can also be used in combination with IV r-TPA for large clots that are not fully dissipated. This involves threading a catheter to the affected brain area and blasting the clot to

allow for clearance from the brain (Jivan et al., 2013). For hemorrhagic stroke, medication can be given to manage blood pressure in cases of hypertension (Unnithan & Mehta, 2021). Surgery, such as craniotomy, decompressive craniectomy, stereotactic aspiration, endoscopic aspiration, or catheter aspiration may also be required to stop or remove the bleeding (S. Chen, Zeng, & Hu, 2014). Although there are treatment methods available, long-term prognosis remains of concern. In patients that visited acute care hospitals in Sweden, over 66% of ischemic stroke cases and 75% of intracerebral stroke cases were estimated to be dependent, if not deceased (Sennfält, Norrving, Petersson, & Ullberg, 2019).

Another common ABI is birth asphyxia, which is the lack of oxygen to the baby at the time of birth. Birth asphyxia is responsible for ~23% of newborn deaths worldwide and is also the leading cause of neurological complications such as cerebral palsy (Olivieri, Rampakakis, Gilbert, Fezoua, & Wintermark, 2021). Not only can birth asphyxia cause direct injury to the brain, but it can also impair the myelination of neurons. Olivieri et al., 2021, investigated the difference of myelination in healthy infants versus infants who experienced asphyxia at birth. They found asphyxia lead to impaired myelination in brain regions that normally become myelinated during or after birth (Olivieri et al., 2021). Impairment of this developmental process can lead to disturbances in motor, sensory, and cognitive functions (Saab, Tzvetanova, & Nave, 2013). Since this condition occurs during developmental process at birth, resulting conditions are treated based on symptom management.

Due to the prevalence of ABI's and the long-term disability associated, further research involving the prevention and treatment of these conditions is required. Increasing creatine (Cr) in the brain through supplementation may be helpful in combatting against neurological injury through the buffering capacity of the phosphocreatine energy system.

### 1.1.3. Brain Injury in Adolescent Population

Traumatic brain injuries specific to the adolescent-aged population have been a global public health issue in the past decade (Ilie et al., 2020). Approximately 1 in 5 of these individuals, who range from age 10-19 as classified by the World Health Organization (WHO), sustain a TBI in their lifetime in North America (Ilie et al., 2020). Of the TBI-related Emergency Department visits in the United States from 1995-2001, adolescents ages 15-19 years old accounted for the second highest proportion at 661.1 per 100,000 cases (Langlois, J.; Rutland-Brown, W.; Thomas, 2006). Galgano et al., (2017), also identified adolescents to experience some of the highest rates of suffering from a TBI, with falls and motor vehicle accidents being the two leading causes. Of all the age groups who experience long-term disability from a TBI, the adolescent age population has the highest incidence (Dewan, Mummareddy, Wellons, & Bonfield, 2016). This may be related to the crucial brain development that takes place during this stage of life.

The adolescent brain has high neuroplasticity, meaning it is more easily influenced by outside factors through formation of neural connections. The brain does not complete its development until approximately age 25, with the frontal cortex being the last brain region to mature (Arain et al., 2013; Casey, Jones, & Hare, 2008). This is therefore the brain region of interest in terms of TBI, as most of the rewiring takes place at this location up until age 24 (Arain et al., 2013). The frontal cortex is responsible for memory, emotions, and problem solving (Arain et al., 2013). Injury to the frontal cortex of the adolescent brain can lead to developmental delays. Although adolescents differ in their symptoms, injury patterns, and outcomes when suffering a TBI, they often get grouped in with either children or adult populations (Christensen, Eyolfson, Salberg, & Mychasiuk, 2021).

Given the high incidence of TBIs experienced by this age cohort and the differences from other age groups in injury patterns and outcomes, this is an important population to target in terms of clinical care. The propencity for developmental delay due to injury further exemplifies the importance of studying the adolescent aged brain when looking into preventative and treatment regimes.

### 1.1.4. Neurometabolic Cascade Associated with Brain Injury

Cellular damage in the brain as a result of TBI and ABI can be attributed to a chain of metabolic events that occur due to mechanical injury. These events can be classified as the "neurometabolic cascade", resulting in energetic stress (Giza & Hovda, 2001). Following a TBI, there are a few biochemical disruptions that occur leading to an efflux of potassium ($K^+$). Neuronal membranes can become disrupted, axons stretch, and voltage-gated potassium ($K^+$) channels open, all leading to an increase in $K^+$ outside the cells. Due to this $K^+$ increase, non-specific depolarization occurs leading to extensive release of glutamate, an excitatory amino acid. The extensive release of glutamate further exacerbates the movement of $K^+$ out of the cells through its activation of kainite, N-Methyl-D-aspartic acid (NMDA), and D-amino-3- hydroxy-5-methyl-4-isoxazole-propionic acid (AMPA) receptors. Under normal conditions glial cells can maintain homeostasis through their uptake of excess $K^+$. In the case of TBI or ABI where extracellular $K^+$ excess is much greater, glial cells are not able to keep up. This requires sodium potassium pumps ($Na^+/K^+$-ATPase) to activate in attempt to pump $K^+$ back into the cells. Since these pumps require ATP to function, they trigger an increase in glucose use in attempt to generate more ATP. This leads to hyperglycolysis and eventually lactate accumulation in the effected brain area.

A second factor of the cascade following concussive or ischemic brain injury is the excessive uptake of calcium ($Ca^{2+}$). The activation of excitatory amino acids (EAAs) from the

potassium efflux and non-specific depolarization in the brain leads to an influx of $Ca^{2+}$ into the surrounding cells. This occurs due to the ability of calcium to travel through pores, which are formed from the activation of NMDA receptors. With $Ca^{2+}$ increasing intracellularly, some of it further enters into the mitochondria of each cell to accommodate for the influx (Giza & Hovda, 2014). If $Ca^{2+}$ levels in the mitochondria go above the critical threshold (~1μM), this can lead to calcium overload in the mitochondria. This disruption of homeostasis within the mitochondria can decrease its ability to generate ATP, or lead to mitochondrial induced apoptosis, worsening the energy crisis (Figure 1).

Increased intracellular $Ca^{2+}$ can also lead to axonal damage within the surrounding neurons as a result of excessive $Ca^{2+}$ present in the axons. Neurofilament side-arms can become phosphorylated and lose their structure, interfering with transport through the axon. In severe cases of brain injury, normal neurotransmission can become disrupted, leading to axon disconnection. Creatine may provide a temporal energy buffer by preventing a rapid fall in ATP concentrations through the adenosine triphosphate-phosphocreatine (ATP-PCr) system.

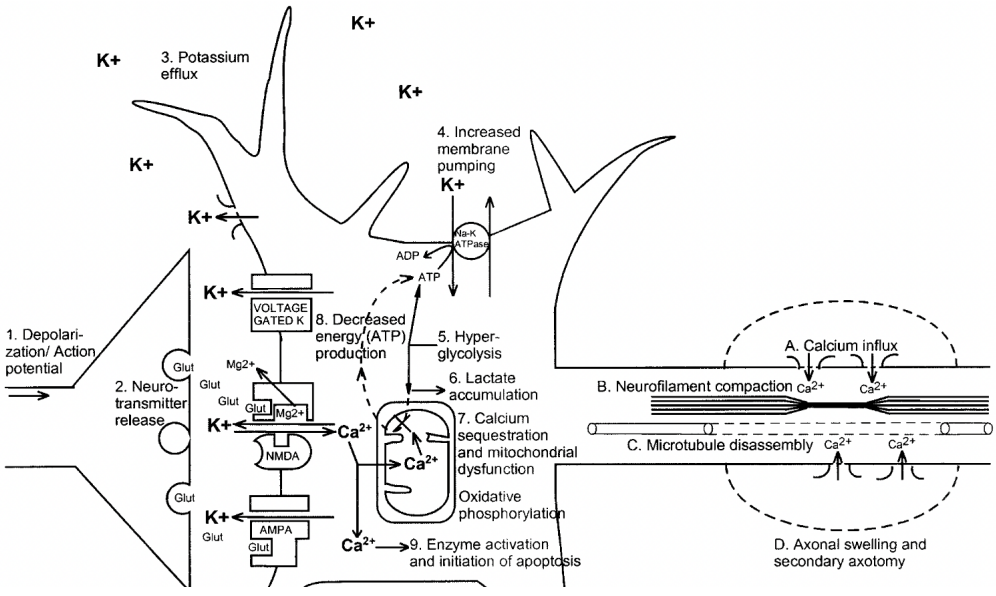


Figure 1. Neurometabolic cascade following traumatic injury. (1) Nonspecific depolarization and initiation of action potentials. (2) Release of excitatory neurotransmitters (EAAs). (3) Massive

efflux of potassium. (4) Increased activity of membrane ionic pumps to restore homeostasis. (5) Hyperglycolysis to generate more adenosine triphosphate (ATP). (6) Lactate accumulation. (7) Calcium influx and sequestration in mitochondria leading to impaired oxidative metabolism. (8) Decreased energy (ATP) production. (9) Calpain activation and initiation of apoptosis. Adapted from Giza et al., 2001.

## 1.2. Creatine Background

### 1.2.1. Creatine Overview

Creatine is an organic compound found in vertebrates which can be obtained through a combination of endogenous synthesis and diet. Humans consuming a Western diet obtain on average half of their creatine from their diet while the other half is synthesized endogenously in the kidney and liver (Borchel, Verleih, Kühn, Rebl, & Goldammer, 2019; da Silva, Nissim, Brosnan, & Brosnan, 2009). Dietary creatine is found in foods such as fresh meat, fish, and some dairy products (Andres, Ducray, Schlattner, Wallimann, & Widmer, 2008; M. E. Brosnan & Brosnan, 2016). Loss of creatine occurs due to the spontaneous conversion of Cr and phosphocreatine to creatinine, which is then expelled in the urine (da Silva et al., 2009). A typical 70 kg male with a total body Cr pool of ~120 g loses ~1.91 g per day due to its spontaneous conversion to creatinine (J. T. Brosnan, da Silva, & Brosnan, 2011). Based on this loss, synthesis and/or dietary intake of Cr is therefore required to maintain adequate levels (da Silva et al., 2009). Endogenous Cr synthesis occurs primarily in the kidneys and liver respectively, producing approximately 1 g per day (Cooper, Naclerio, Allgrove, & Jimenez, 2012; Wyss & Kaddurah-Daouk, 2000). This means more Cr is lost than endogenously synthesized, requiring humans to obtain some Cr through the diet. Synthesis of Cr begins in the kidney with L-arginine:glycine aminotransferase (AGAT) which functions to convert amino acids arginine and glycine to guanidinoacetic acid (GAA) and L-ornithine. GAA is then methylated in the liver by guanidinoacetate methyltransferase (GAMT) with S-adenosylmethionine as the methyl donor

to form creatine (da Silva et al., 2009). Cr is transported through the blood stream, with the majority (~95%) being taken up into skeletal muscle via the creatine transporter (M. E. Brosnan & Brosnan, 2016; Cooper et al., 2012). The remainder is primarily distributed amongst the brain, liver, kidneys, heart, and testes (Balestrino, 2021; Cooper et al., 2012). Small amounts of creatine transporter are also expressed in microcapillary endothelial cells at the blood-brain-barrier allowing creatine to pass slowly from the circulation into the brain (Braissant, 2012).

Creatine monohydrate (CrM) has been previously determined to increase blood creatine concentrations for ~3-4 h following oral ingestion (Antonio et al., 2021). It is also well established that ~99% of orally supplemented CrM is up taken by the tissues or excreted in the urine as creatinine (Antonio et al., 2021). Other forms of creatine such as creatine ethyl ester, creatine nitrate, and creatine dipeptides have little evidence to suggest that they are more effective or safer than CrM (Jäger, Purpura, Shao, Inoue, & Kreider, 2011). Furthermore, CrM is thought to have a greater physiological impact in creatine stores and performance than these other forms (Antonio et al., 2021).

### 1.2.2. Creatine Uptake in the Brain

The creatine transporter is responsible for the uptake of creatine in a variety of cells: neuronal cells, skeletal and cardiac muscle cells, and intestinal and kidney epithelial cells (Li et al., 2010a). Specific to the brain, gene expression of the transporter, slc6a8, is in microcapillary endothelial cells of the blood brain barrier (BBB) (Hanna-El-Daher & Braissant, 2016) (Figure 2). This allows for creatine to enter into the central nervous system from the blood stream. One of the reasons the brain has less Cr than skeletal muscle is due to the BBB having low permeability for Cr as creatine transporters are not present in astrocytes (Figure 2). In order to increase brain Cr content, the brain could potentially increase endogenous synthesis through the

AGAT and GAMT pathway or via increased uptake through the creatine transporter, which could also potentially be upregulated (Hanna-El-Daher & Braissant, 2016). Through intravenous administration of creatine in a mouse model, Ohtsuki et al., 2002, identified the creatine transporter (CRT) to be a major pathway in supplying the brain with creatine. Northern blot and immunoblot analyses demonstrated the expression of CRT in immortalized mouse brain capillary endothelial cells (TM-BBB) (Ohtsuki et al., 2002). High expression of CRT was also observed in capillaries in the brain following creatine administration. The CRT is important for the uptake of creatine, as the brain has high energy demands compared to tissues capable of synthesizing creatine such as the kidneys and liver (Christie, 2007).

*In vivo* rodent models have investigated creatine uptake in the brain through the CRT. Ipsiroglu et al., 2001, determined 4 weeks of CrM supplementation in female rats at 2 g/kg/day to significantly increase whole brain creatine concentrations. In female mice, 2 weeks of this same dose demonstrated a significant increase in brain creatine (Ipsiroglu et al., 2001). Dunham et al., 2021, conducted a study on 12-week-old male and female rats supplemented CrM over 8 weeks at 0.224 g/kg/day, 0.412 g/kg/day, and 0.794 g/kg/day. The findings indicated a significant increase in total brain creatine concentrations at each dose, with 0.412 g/kg/day having a saturating effect. (Dunham et al., 2021).

In humans, Dechent et al., 1999, demonstrated significant increases in TCr concentrations in various brain regions (grey matter, white matter, cerebellum, and thalamus) following supplementation of 20 g/day CrM in both male and female participants (Dechent, Pouwels, Wilken, Hanefeld, & Frahm, 1999). Another study in humans using the same CrM dose for 7 days determined TCr concentrations increased in the cerebral cortex (Turner, Byblow, & Gant, 2015a).

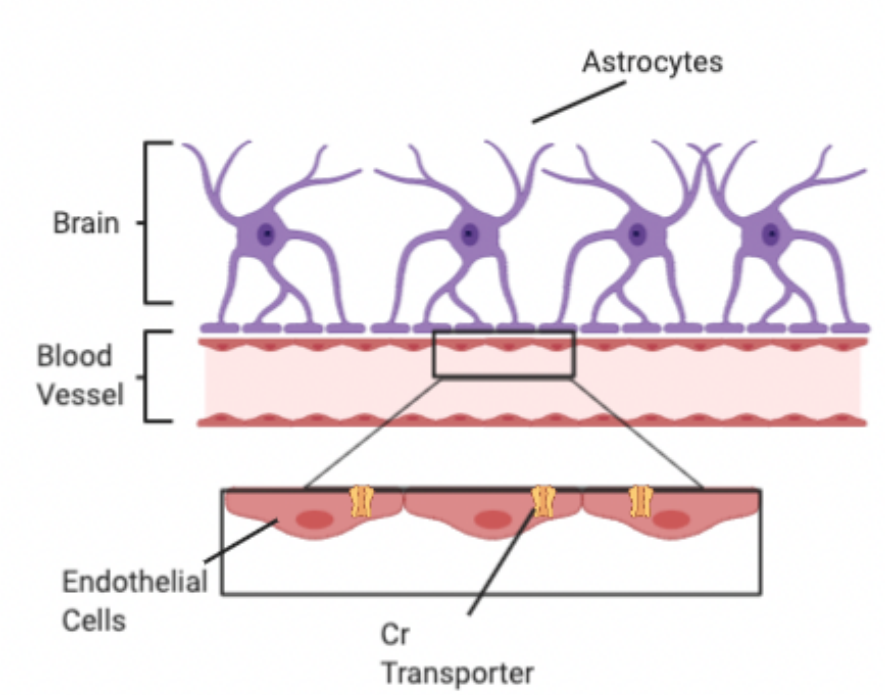


**Figure 2.** Cr transporter location on endothelial cells lining the blood brain barrier.

### 1.2.3. ATP-PCr System

Adenosine triphosphate (ATP) is the energy source for use at the cellular level of an organism. It is composed of a nitrogenous base (adenine), a ribose sugar, and three bonded phosphate groups (Dunn & Grider, 2020). Energy is stored between the phosphates, which are linked together by a phosphodiester bond. To release energy for use, this bond must be broken through the energetically favourable hydrolysis reaction yielding adenosine diphosphate (ADP) and an inorganic phosphate (Pi). ADP can be further hydrolyzed to yield adenosine monophosphate (AMP) and Pi's; however, this reaction is not favoured as minimal energy is released for use. Some of the major uses of ATP hydrolysis are DNA and RNA synthesis, intracellular signalling, synaptic signalling, active transport, and muscle contraction (Dunn & Grider, 2020). Humans depend on the hydrolysis of approximately 100-150 moles of ATP per day to ensure these functions can occur (Dunn & Grider, 2020).

Once inside cells, Cr gets transformed to its phosphorylated form, phosphocreatine (PCr), by the enzyme creatine kinase (CK). CK is primarily expressed in the heart, brain, and skeletal muscle. It catalyzes the reaction of Cr to PCr through the use of ATP, yielding ADP. PCr functions as a reserve of high energy phosphates to resynthesize ATP (Alraddadi, Lillico, Vennerstrom, Lakowski, & Miller, 2018) (Figure 3). It is responsible for the regeneration of ADP to ATP through the transfer of its phosphate group. The generation of ATP is catalyzed by the reverse CK reaction, using ADP and PCr (Figure 3).

The pool of PCr acts as a temporal energy buffer preventing a rapid fall in intracellular ATP concentrations upon sudden stress or during cellular work (Andres et al., 2008). PCr diffuses into the cytoplasm where it is catalyzed by creatine kinase (CK) to be dephosphorylated, generating ATP and Cr in regions of the cell with elevated rates of energy turnover (Guimarães-Ferreira, 2014). ADP can then be transferred directly back into the matrix of the mitochondria in preparation to be re-phosphorylated to ATP (Wyss & Kaddurah-Daouk, 2000). Cr produced through the CK reaction returns to the mitochondria while ATP is used by ATPases in its vicinity (Guimarães-Ferreira, 2014). The specific mitochondrial and cytosolic compartmentalization of isoenzymes therefore allow for a high cytosolic [ATP]/[ADP] ratio near cellular ATPases, and conversely a low [ATP]/[ADP] ratio in the mitochondrial matrix promotes oxidative phosphorylation (Uwe Schlattner, Tokarska-Schlattner, & Wallimann, 2006). CK isoenzymes therefore contribute to the maintenance of cellular energy homeostasis.

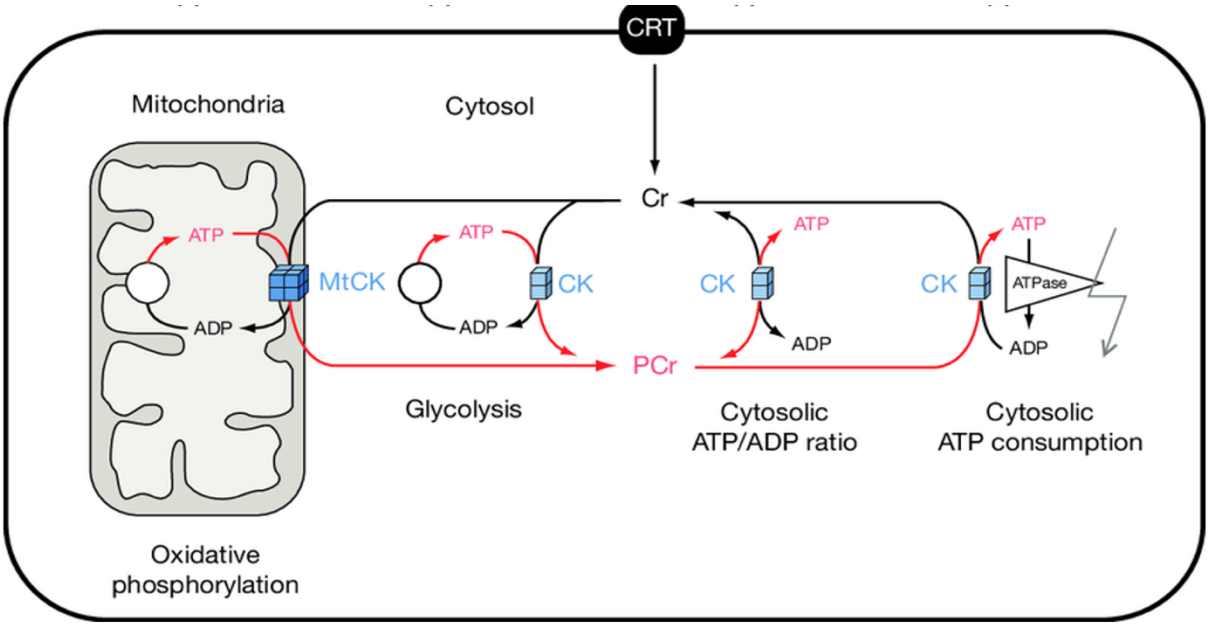


**Figure 3.** ATP-PCr system upon entry of Cr from the CRT. Adapted from U. Schlattner, Tokarska-Schlattner, & Wallimann, 2013.

### 1.2.4. Creatine and Neurological Injury

Due to the buffering capacity of the phosphocreatine energy system and low levels of Cr present in the brain, increasing brain creatine concentrations may be helpful in combatting against neurological injury. In a mouse stroke ABI model involving the occlusion of the middle cerebral artery, Prass et al., 2007, examined the effects of creatine supplementation. A supplemented creatine dose of 1% and 2% of the diet improved cerebral vascular flow by preserving vascular cell function post-stroke (Prass et al., 2007). These findings suggested that Cr may preserve brain homeostasis when under stress through stimulation of mitochondrial ATP production. A study conducted on humans undergoing acute oxygen deprivation determined that oral CrM supplementation at 20g/day for 7 days led to increased brain Cr levels, increased corticomotor excitability, and prevented decline in attention (normally observed during oxygen deficit) (Turner et al., 2015). Moreover, cortical damage following TBI was reduced by 36% in mice and 50% in

rats who were supplemented with CrM at 0.1ml/10g BW (Sullivan, Geiger, Mattson, & Scheff, 2000). More specifically, mitochondrial membrane potential was increased, ROS levels were decreased, and ATP levels were maintained following supplementation (Sullivan et al., 2000). Cr supplementation at 184 mg/kg following cerebral ischemia in mice prevented the worsening imbalance between autophagy and mTOR signalling, as well as decreased the size of infarct in the brain (Chen et al., 2021). These experiments suggest supplementation with Cr may provide neuroprotection when cellular energy is altered due to neurological injury.

There are also several investigations that examine the impact of creatine on general brain health. A double-blind placebo-control cross-over study on humans examined the effect of CrM supplementation (5g/L) for 6 weeks on intelligence test scores and working memory performance (Rae, Digney, McEwan, & Bates, 2003). Cr intervention had a significant positive effect on both measurements, suggesting that Cr plays an important role in brain energy capacity. Another study showed a significant improvement in spatial memory of female mice supplemented with 3% CrM compared to mice supplemented with 1% CrM and control mice (Allahyar, Akbar, & Iqbal, 2017). Collectively, these findings suggest that increasing brain creatine levels may help to buffer energy stores in the brain and improve neuronal function leading to added protection against possible neurological injury.

## 1.3. Lithium Background

### 1.3.1. Lithium Overview

Lithium (Li) is a naturally occurring alkali metal present in the human body at low levels. It can be consumed through diets consisting of vegetables and grains and can also be present in tap water at trace amounts. Schrauzer, (2002) estimated that the average American ingests 0.6 to 3.1 mg per day from their diet. Lithium is also available as a nutritional supplement in the form of

syrups, solutions, and capsules with less than 5mg/day advised to be a safe dose (Schrauzer, 2002). Lithium is currently used clinically in the treatment of psychiatric disorders such as bipolar disorder, depression, and schizophrenia by acting as a mood stabilizer through anti-manic properties (Ishii & Terao, 2018). The therapeutic dose for psychiatric disorders is between 600-1200 mg per day. Lithium toxicity can occur at doses upwards of 1500 mg per day resulting in neurological effects such as tremor or nystagmus, renal toxicity, cardiovascular consequences such as T wave flattening, and inhibition of thyroid hormone synthesis leading to hyperthyroidism (Hedya, Avula, & Swoboda, 2020). If recognized early on, these symptoms can be revised with adjusting the current dose administered. However, if not recognized, coma and brain damage are possible, leading to death (Hedya et al., 2020). The recommended therapeutic range for lithium in humans is between 0.5-1.2 mmol/L and without experiencing symptoms of toxicity (Mitchell, 2000). To manage these effects, serum Li concentration is frequently monitored to ensure it is below the toxic level.

### 1.3.2. GSK3β and Creatine Transport

Glycogen synthase kinase (GSK3) is a serine/threonine kinase originally known for its role in insulin receptor signalling (Freland & Beaulieu, 2012). Since then, it has been identified to aid in the regulation of several biological processes including development, immunity, neurotransmission, and cancer (Freland & Beaulieu, 2012). GSK3 is a critical downstream element of the PI3K/Akt cell survival pathway whose activity can be inhibited by Akt-mediated phosphorylation at Ser21 (GSK3α) and Ser9 (GSK-3β). Its two isoforms, GSK3α and GSK3β, differ structurally in their N- and C-terminus regions (Liang & Chuang, 2006). GSK3β can be positively regulated through tyrosine phosphorylation (Tyr216) and negatively regulated through serine phosphorylation (Ser9) (Freland & Beaulieu, 2012). Increased expression of GSK3β has

been previously observed in a *Xenopus laevis* oocytes cell model to be associated with a significant decrease in the influx of creatine through downregulation of the activity of slc6a8 transporters (Fezai et al., 2016).

Lithium inhibits both isoforms of GSK3 directly and indirectly (Freland & Beaulieu, 2012). Direct forms of GSK3β inhibition by lithium ions occur through the competition of magnesium ions which are known to be co-factors for a number of enzymes (Freland & Beaulieu, 2012). Indirect inhibition of GSK3β is possible through lithium's activation of Akt (Freland & Beaulieu, 2012). This increases the inhibitory phosphorylation of GSK3 and decreases its activation in neurons (Freland & Beaulieu, 2012). GSK3β is the only protein kinase inhibited by therapeutically tolerable concentrations of lithium (Timothy O'Brien & Klein, 2009). This means lithium does not have a significant effect on other kinases in the body when administered at therapeutically tolerable concentrations (Timothy O'Brien & Klein, 2009). Supplementation with lithium may have a positive effect on the creatine uptake into cells. Since lithium inhibits GSK3β, and GSK3β downregulates the slc6a8 transporters, lithium could potentially increase the uptake of creatine into tissues that contain the slc6a8 transporters, therefore leading to greater amounts of creatine uptake into these specific tissues.

### 1.3.3. Lithium Chloride Dosage

A study conducted on male mice 3-6 months of age supplemented 10 mg $kg^{-1}$ $day^{-1}$ LiCl in the drinking water for 6 weeks, lead to a serum lithium concentration of 0.02 mmol (Hamstra et al., 2020). This dose was adequate to impose physiological benefits across various tissues, without producing any signs of discomfort or aversion to consumption of water (Hamstra et al., 2020). In heart tissue, improved SERCA function was observed by increasing the SERCA2a:PLN ratio (Hamstra et al., 2020). In bone tissue from the same cohort of mice, GSK3β inhibition was

observed leading to downstream activation of osteogenic signalling pathways (Kurgan et al., 2019). In skeletal muscle, LiCl-mediated GSK3 inhibition led to contractile benefits (Whitley et al., 2020). Similarly, a study in a different cohort of mice 10 weeks of age using the same LiCl dose, found GSK3β to be inhibited in the aorta, leading to the prevention of high-fat diet-induced obesity (Choi et al., 2010). This low dose of LiCl of 10 mg $kg^{-1}$ $day^{-1}$ in mice therefore appears to be well-tolerated and can impose physiological benefits across several tissues.

## 1.4. Knowledge Gap

The brain is characterized by a high metabolic demand compared to other organs (Annoni et al., 2021). Due to the minimal storage capacity for creatine in the brain, it relies heavily on the systemic energetic supply, making it less able to protect against ischemia or a TBI. Following injury, therapeutic options have been targeted in attempt to reduce brain damage and speed up the healing process, however, the current options are not ideal. Discovery of beneficial therapeutic interventions is crucial to the development of novel treatments and prophylactic strategies.

PCr is known to act as a temporal energy buffer preventing a rapid fall in intracellular ATP concentrations upon sudden stress or during cellular work (Andres et al., 2008). Creatine monohydrate has previously been demonstrated to result in a significant increase in brain creatine concentration. The dose which elicited this response was 5 g/L in male and female rats over a period of 8 weeks (Dunham et al., 2021).

Creatine's ability to enter the brain is facilitated through the presence of CRT in the endothelial cells of the blood brain barrier. One mechanism in which these transporters become downregulated is through GSK3β phosphorylation. Lithium has been demonstrated to inhibit GSK3β in oocytes (Fezai et al., 2016). The potential of lithium to influence the expression of CRT

in the brain has not yet been investigated, and this area also lacks research using mammalian *in vivo* models.

### 1.5. Purpose

The purpose of this study was to investigate the individual and combined influences of creatine monohydrate and lithium chloride on creatine concentrations in the *in vivo* male and female rat brain. It was hypothesized that supplementing rats with creatine would lead to increases in brain creatine concentrations compared to no creatine supplementation. Supplementation with creatine and lithium was hypothesized to result in the greatest increase in brain creatine concentrations compared to creatine or lithium supplementation alone (Figure 4).

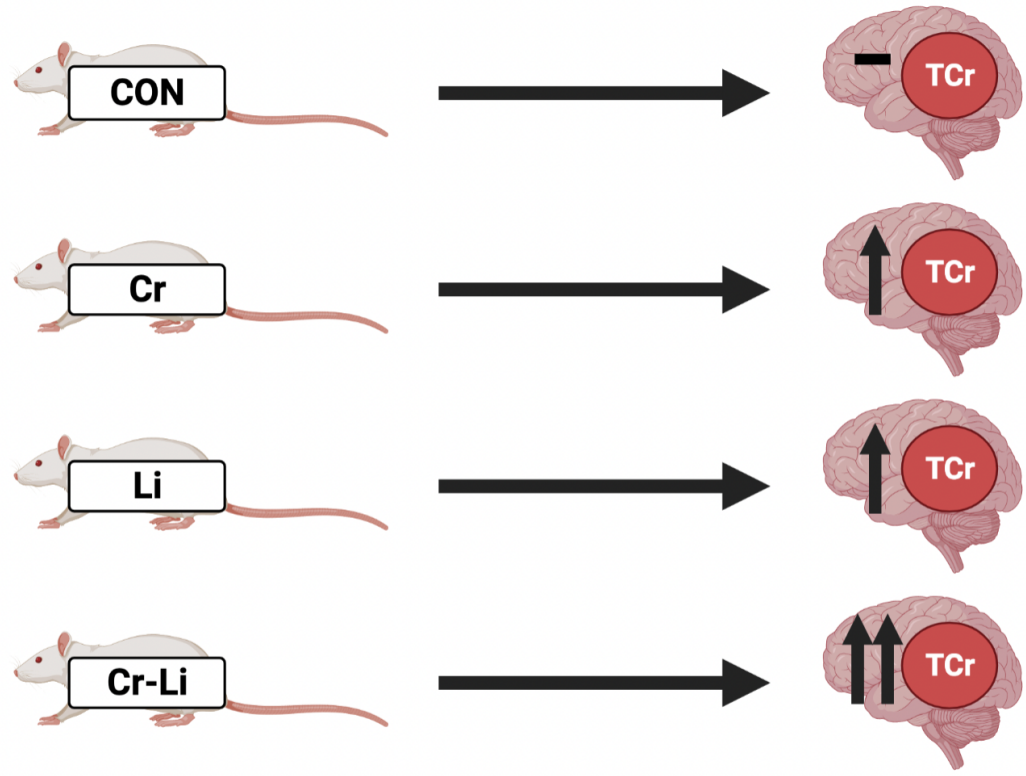


**Figure 4.** Hypothesis of brain total Cr concentration between supplementation groups.

# 2. Methodology

## 2.1. Experimental Model and Design

Sprague-Dawley outbred rats were purchased from Charles River Laboratories Inc. between 3-4 weeks of age. Outbred strains of rodents are often used in studies involving nutritional supplementation due to their genetic trait variation, compared to inbred strains, making them more relatable to genetic variation in humans (Brekke, Steele, & Mulley, 2018). Study supplementation began at 6 weeks of age, allowing 2 weeks for the animals to acclimatize to their housing conditions. Supplementation lasted for 6 weeks, bringing the rats to a total age of 12 weeks old by the end of experimentation. Rats aged 6-12 weeks have reached sexual maturity (~7 weeks), but are still far from reaching adulthood (~30 weeks) (Agoston, 2017). Therefore, the rats in the current study were considered to be of early adolescent age. In the current model, we focused on an adolescent aged cohort, as humans in this age cohort suffer a high incidence of TBIs. This study was carried out in adherence to the Canadian Council on Animal Care (CCAC) guidelines and was approved by the Brock University Animal Care Committee (AUP 20-09-02).

Initial sample size determinations were based on a power calculation for the primary outcome variable to determine the required sample size for the study. Previous brain TCr data was used with males and females computed separately, both yielding a suggested sample size of n=5/group (Dunham et al., 2021). In order to account for any possible loss of samples or any other unforeseen issues, the current study employed a sample size of n=64, with n=8/group.

## 2.2. Groups and Supplementation with Creatine and Lithium

Upon arrival to the Brock University Animal Facility, 64 Sprague-Dawley rats (32 male and 32 female) were randomly assigned into one of four experimental groups: control (CON), creatine (Cr), lithium (Li), and creatine-lithium (Cr-Li) (Table 1). CrM was administered in the

drinking water at a dose of 5 g/L, to reach 0.412g/kg/day. This dose has been previously observed to elicit a significant increase in brain and skeletal muscle total creatine concentrations in Sprague-Dawley rats (Dunham et al., 2021). Lithium chloride was also administered via drinking water at a concentration of 0.2 g/L. Based on average water consumption in this population of rats, it was estimated that the 0.2 g/L LiCl would result in a serum lithium concentration of ~0.1-0.15 mM. This concentration is below the therapeutic range of 0.5-1.2 mM, and is therefore considered to be a low dose (Mitchell, 2000). Each of the four experimental groups included 0.5% sucrose in water for palatability and to encourage consumption (Dunham et al., 2021; Ipsiroglu et al., 2001). Rats were housed in same-sex pairs, under a 12:12 light-dark cycle. They were given *ad libitum* access to their appropriate water from a 300 ml water bottle. Reverse osmosis water solutions were mixed and changed twice a week for the 6-week period. Rats were also given *ad libitum* access to a pelleted 14% certified protein rodent maintenance diet (Teklab Global, Envigo). This diet was verified to not contain any form of creatine or lithium.

**Table 1.** Experimental groups with appropriate dose of supplement in drinking water.

| Group | Creatine Monohydrate (g/L) | Lithium Chloride (g/L) | Sucrose % |
|---|---|---|---|
| CON | 0 | 0 | 0.5 |
| Cr | 5 | 0 | 0.5 |
| Li | 0 | 0.2 | 0.5 |
| Cr-Li | 5 | 0.2 | 0.5 |

## 2.3. Body Mass, Food and Water

The body mass of each rat, as well as cage food and water consumption were measured 3 times per week (every Monday, Wednesday, and Friday) for the duration of the study. These outcomes were also measured the morning before their respective endpoints.

## 2.4. Tissue Collection

Rats were anesthetized with isoflurane gas and then blood was collected via cardiac puncture using a 16-gauge needle, acquiring ~4.5-7.5 mL of blood, resulting in euthanasia. Rats were then decapitated using a guillotine so the brain could be removed. The brain was separated into 8 sections: 4 even pieces of the frontal lobe, left and right hemisphere, as well as left and right cerebellum. Of the 4 pieces of the frontal lobe, the left anterior piece from each rat was used for TCr analysis, the right anterior for CRT gene expression, the left posterior for GSK3 activity, and the right posterior for GSK3 protein expression. All tissue was placed into separate Eppendorf tubes and flash frozen in liquid nitrogen. At the end of each day, tissues were moved to -80ºC for long-term storage. Endpoints occurred over a period of four consecutive days. On each of these days, one cage from each of the four groups for both sexes were selected to total 16 rats per day.

## 2.5. Measurement of Total Creatine Concentration

High-energy phosphate concentrations were quantified using enzymatic fluorometric assays. Phosphate concentrations allowed for both phosphocreatine and free creatine concentrations to be computed. These assays have been previously used to determine high-energy phosphate concentrations in both muscle and brain tissue (Dunham et al., 2021; Tarnopolsky & Parise, 1999).

Brain tissue preparation included freeze drying a piece of the frontal lobe. This was done using a lyophilizer (FreeZone 4.5, Labconco) at a pressure of 0.004 mBar overnight. Freeze-dried tissues were then crushed into a fine powder and 3-5 mg of the powder was weighed. 600 µL of precooled 0.5 M perchloric acid (PCA) was added to each sample while on ice to extract metabolites. Samples were vortexed intermittently for 10 minutes before being centrifuged at 15,000 g at 0ºC for 10 minutes. 540 µL of supernatant was then removed and stored at -20ºC for 15 minutes, allowing samples to refreeze. 135 µL of 2.3 M potassium carbonate was then added

to neutralize the samples. Samples were then centrifuged for 10 minutes at 0ºC at 15,000 g before ~550 µL of supernatant was removed and used to measure metabolites.

Phosphocreatine concentration was determined by an ATP/PCr fluorometric assay. Reagent was prepared using 50 mM Tris, 1.0 mM $MgCl_2$, 0.5 mM D.T.T., 100 µM Glucose, and 50 µM NADP. This reagent was diluted with double distilled water and adjusted to a pH of 8.1 before 0.02 U/mL G6PDH was added. 1mL of reagent was added to 10µL of sample and vortexed. A fluorometer (Trilogy®, Turner Designs) set to an excitation wavelength of 350 nm and an emission wavelength range of 410-490 nm was used to analyze samples. The first measurement (R1) served as a baseline measurement. 25 µL of dilute hexokinase (0.014 U/mL hexokinase in 1mL of reagent) was then added to each tube, vortexed, and placed in the dark for 60 minutes. 20 µL of dilute creatine kinase (2 mg ADP, 2mg 3.6 U/mL creatine kinase, and 10 µL of 10% BSA in 1 mL of reagent) was then added to each tube, vortexed, and placed in the dark for 105 minutes. Following incubation, tubes were measured again (R2) using the fluorometer. Sample measurements were compared to 'blank' tubes consisting of 10µL of doubly distilled water in place of sample, as well as 'standard' tubes with 10 µL of a 500 µM PCr standard which were used to calculate sample concentrations. To calculate the PCr concentration present, the average baseline reading (R1) was subtracted from the average second reading (R2) for each sample. The average of the 'blank' readings was then subtracted from the average of the PCr calculation for both samples and standards. The ratio of sample-to-standard was then multiplied by the known standard concentration (500 µM PCr) and divided by the known extract concentration to yield the unknown PCr value for each sample.

Free creatine concentration was determined using a free creatine fluorometric assay. Reagent was prepared consisting of 50 mM Imidazole, 5 mM $MgCl_2$, 30 mM KCl, 25 µM PEP,

200 μM ATP, and 45 μM NADH. Doubly distilled water was added to bring the reagent to the appropriate volume, and pH adjusted to 7.5. Lactate dehydrogenase (LDH)(0.24 U/mL) and pyruvate kinase (PK)(0.75 U/mL) were then added. Then, 1 mL of reagent was added to 10 μL of sample, 'blank' tubes, or 500 μM Cr standard in triplicate. All tubes were then vortexed and left to sit for 15 minutes before the baseline reading (R1) was obtained using the fluorometer. Dilute creatine kinase (10 μL of 10% BSA and 5 mg of creatine kinase in 1 mL of reagent) was added to all samples at 25 μL per tube. Tube racks were then vortexed and placed in the dark to incubate for 60 minutes. The second time point (R2) was measured using the fluorometer with the previous settings. Sample measurements were compared to 'blank' tubes as well as known Cr standard tubes. Free creatine concentrations were determined by subtracting the average R1 per sample from the average R2. Average 'blank' readings were then subtracted from the average Cr standard, as well as from the calculated free Cr concentrations per sample. The sample-to-standard ratio was then multiplied by the known standard concentration (500 μM Cr) and divided by the known extract concentration to yield the unknown free Cr value for each sample.

To determine the concentration of total creatine (TCr) for each sample, PCr and free Cr values were added together.

## 2.6. Protein Isolation and Quantification

Protein expression was determined through western blotting. Proteins of interest included: total β-Catenin, total GSK3α, total GSK3β, phospho-GSK3α (p-GSK3α), and phospho-GSK3β (p-GSK3β).

Tissue homogenization was performed by chipping a piece of frozen frontal lobe of the brain, weighing it (20-30 mg), and placing the tissue into 2mL homogenization tubes with enough silica beads to cover the sample. Buffer was prepared (10 mL lysis buffer, 50 μL protease inhibitor,

and 34 µL PMSF) and added to sample tubes at a 1:20 dilution factor. Tubes were then put in the Fast Prep and homogenized for 45 seconds at speed 6.5, until fully liquefied. The resulting homogenate was then transferred into 1.5mL tubes. Samples were centrifuged at 10,000 g for 10 minutes at 4ºC, and supernatant was transferred to new 1.5mL tubes and stored at -80ºC.

Total protein was quantified in the homogenized samples by conducting a Bicinchoninic Acid (BCA) protein assay. BSA was serially diluted starting at 1mg/mL to 0mg/mL to serve as protein standards. Samples were also diluted at a 1:50 ratio in new 1.5mL tubes. Standards and samples were then vortexed and 10 µL were added to a 96 well plate in triplicate. BCA solution was prepared (2% (v/v) copper (II) sulfate in BCA) and 200 µL was added to each well. The plate was incubated at 37ºC for 30 minutes before reading in Spectramax M2 at 527 nm. SoftMax Pro software was used to compute total protein by assigning known protein standards and interpolating the values of the samples.

Samples were prepared for blotting by using BCA protein concentration values and diluting with doubly distilled water to 3 µg/µL. 7.5 µL of 4x Laemmli sample buffer was added to each sample, bringing the total volume of sample to 30µL.

Solubilized proteins were then loaded on TGX Bio-Rad PreCast 7.5% gradient gels in amounts of 5 µL to yield ~15 µg of protein. 4 µL of all blue pre-stained protein standard was loaded in the first well to serve as the ladder. Gels were then run for 22 minutes at 240 V, 3 A, and 300 W in running buffer (50 mL of Tris/glycine buffer in 450 mL of doubly distilled water). Polyvinyldine difluoride (PVDF) membranes were activated in methanol for 5 minutes on the rocker before placing into transfer buffer (100 mL Trans-Blot turbo buffer, 100 mL ethanol, in 300 mL doubly distilled water). Transfer to membranes was conducted using a Trans-Blot Turbo Transfer System (Bio-Rad Laboratories) which was run for 3 minutes, twice. Membranes were

then blocked with 3% BSA in tris-buffered saline tween solution (TBS-T) for 1 hour and then immunoprobed with their corresponding primary antibodies overnight (Table 2). The membranes were washed with TBS-T before incubation in anti-rabbit secondary antibody for 1 hour. TBS-T was used to wash membranes before imaged after applying Millipore Immobilon Chemiluminescent HRP Substrate or Clarity Max HRP substrate on a Bio-Rad Chemi Doc Imager. ImageLab was used to quantify optical densities that were normalized to total protein visualized on PVDF membranes with a Ponceau stain.

**Table 2.** Western blot proteins of interest, corresponding antibodies, and bands in kilodaltons.

| | **Primary Antibody** | | **Secondary Antibody** | | |
|---|---|---|---|---|---|
| **Protein of Interest** | Antibody | Concentration | Antibody | Concentration | **Band Level (kDa)** |
| B-Catenin | B-Catenin Rabbit | 1/10000 | Anti-rabbit | 1/2000 | 92 |
| GSK3a | GSK3a Rabbit | 1/2000 | Anti-rabbit | 1/10000 | 51 |
| p-GSK3a | p-GSK3a Rabbit | 1/2000 | Anti-rabbit | 1/10000 | 51 |
| GSK3b | GSK3b Rabbit | 1/2000 | Anti-rabbit | 1/10000 | 47 |
| p-GSK3b | p-GSK3b Rabbit | 1/2000 | Anti-rabbit | 1/10000 | 47 |

## 2.7. Creatine Transporter Gene (Slc6a8) Expression

The expression of the creatine transporter gene (slc6a8) was determined through Reverse Transcription Polymerase Chain Reaction (RT-qPCR). Messenger Ribonucleic Acid (mRNA) was first extracted from brain samples. Frozen brain samples were chipped, weighed (20-40 mg) and placed in 2mL homogenization tubes with just enough silica beads to cover the sample. 1mL of TRIzol Reagent was added to each tube in the fume hood. Tubes were then put in the Fast Prep

and homogenized for 45 seconds at speed 6.5, until fully liquefied. Homogenate was then transferred into 1.5 mL tubes. Samples were centrifuged at 12,000 xg for 10 minutes at 4ºC, and supernatant was transferred to new 1.5mL tubes and incubated for 5 minutes at room temperature. 200 µL of chloroform was added to each tube in the fume hood and shaken by hand for 15 seconds to mix. Tubes were then left to incubate at room temperature for 15 minutes before centrifugation at 12,000 xg for 15 minutes at 4ºC. The clear phase of the supernatant was transferred to a new 1.5 mL tube. 600 µL of isopropanol was added to each tube and inverted by hand until fully mixed. 700 µL of this solution was then transferred into a Qiagen RNeasy spin column. Spin columns with sample were then centrifuged at 12,000 xg for 1 minute before discarding the flow-through and patting the column dry with a Kimwipe. Remaining sample was then added to the column and centrifuged at 12,000 xg for 1 minute. Flow through was discarded, the column patted dry, and then 350 µL of Wash Buffer RW1 was added to the column. This step was repeated twice. The spin column was then transferred to a new collection tube, and 500 µL of Buffer RPE was added to the column. Tubes were centrifuged at 12,000 xg for 1 minute, flow-through was discarded, and the columns patted dry. 500 µL of Buffer RPE was added to the column before centrifugation at 12,000 xg for 2 minutes. Following this, spin columns were patted dry and transferred to a new collection tube. 35 µL of RNase free water was added to the column, incubated at room temperature for 1 minute, and then centrifuged at 12,000 xg for 1.5 minutes. The flow-through was then transferred from the collection tube to a 1.5 mL tube.

Each sample underwent DNA free treatment to remove any genomic DNA contamination. 3.5 µL of 10x DNase Buffer was added to each of the samples and mixed with a pipette. 1 µL of rDNase was then added to the sample and then incubated for 20 minutes at 37ºC. DNase Inhibitor was then added in amounts of 3.5 µL per sample, and gently mixed. These samples were then

centrifuged at 10,000 xg for 10 minutes and then supernatant transferred to a new 1.5 mL tube. Sample concentration (ng/μL) and absorption (A260/280) were measured and recorded for each sample using the Nanodrop Spectrophotometer. Extracted mRNA samples were then stored at -80ºC.

The creation of cDNA samples began with diluting mRNA samples with RNase free water to 1μg in a new tube based on the concentration obtained from the Nanodrop Spectrophotometer. A primer mix was prepared using Random Primers and samples of dNTP, and 2μL of this mix was added to each diluted RNA sample. The samples were then put into the thermocycler and run using the pre-set protocol (MacPherson RT1) for 5 minutes. A master mix was prepared with Invitrogen products of 4 μL of 5x FSB, 2 μL of DTT, 1 μL of RNase Out, and 1 μL of SSII, multiplied by the number of RNA samples. The master mix was then added to each RNA sample in amounts of 8 μL and then put back into the thermocycler and run for 1 hour 15 minutes using a pre-set protocol (MacPherson protocol RT2). cDNA samples were them removed from the thermocycler and stored at -20ºC until further use.

RT-PCR analysis involved the dilution of 20 μL of cDNA samples with 80 μL of RNase free water in duplicate. A master mix was prepared using 10 μL of Quanta (Taqman master mix multiplex assay), 4 μL RNase free water, and 1 μL of gene expression (slc6a8 or GAPDH) per sample of cDNA. GAPDH was used as the reference gene, as this has been previously used as a reference gene in brain tissue (Livak & Schmittgen, 2001). Master mix containing slc6a8 (active gene) was added to a 96-well plate in amounts of 15 μL, as was master mix with GAPDH. Each diluted sample of cDNA was added in 5 μL to a well with slc6a8, and a duplicate well with GAPDH. The 96-well plate was then covered and spun using a plate reader (*Labnet Mini Plate*

*Reader)* before being placed in an RT-PCR system (*Applied Biosciences RT-PCR System)* and run for ~1 hour 20 minutes.

Final gene expression values were calculated by using the $2^{-\Delta\Delta Ct}$ method . This method involves using the untreated control as the calibrator and has been previously described and reported by Livak et. al., 2001.

## 2.8. GSK3 Activity Measurement

GSK3 activity was measured in the brain using an enzyme-linked spectrophotometric assay that linked GSK3-mediated ATP hydrolysis to NADH oxidation by using pyruvate kinase (PK) and lactate dehydrogenase (LDH). Samples were measured at 340 nm as this is the optimal absorbance wavelength of NADH.

Tissue homogenization and protein content determination was performed in the same manner as described previously for western blotting. Homogenate was then added to tubes in 20 µL amounts in duplicate. Dimethyl sulfoxide (DMSO) was added to half of the sample tubes in amounts of 2.5 µL to serve as the condition without an inhibitor. The other half of the samples served as a GSK3 inhibited condition, receiving 2.5 µL each of 5mM stock CHIR (dissolved in DMSO). All tubes are then incubated on ice for 1 hour while vortexed in 15-minute intervals. During this incubation, buffer was prepared consisting of 200 mM KCl, 20 mM HEPES, 10 mM $NaN_3$, 1 mM EGTA, 15 mM $MgCl_2$, 5 mM ATP, and 10 mM phosphoenolpyruvate (PEP). Master mix was prepared using 10 mL of buffer, 36 µL PK, and 29 µL LDH, then added to each tube in 300 µL amounts. Tubes were then vortexed and 90 µL was added to a 96-well plate in triplicate. The plate was read using a spectrophotometric plate reader (M2 Multimode Reader, Molecular Devices) set to 37ºC at 340 nm. NADH was then quickly added to each of the wells using a repeater pipette set to 4 µL, followed by the addition of 5 µL GSK3 substrate to each well. The plate was

then read a second time for 30 minutes using the previously mentioned settings. The samples containing CHIR served as the baseline for GSK3 activity measurement and was subtracted from its DMSO counterparts to yield the activity slopes. The concentration of NADH was calculated using the molar extinction coefficient 6.22 $mM^{-1} \bullet cm^{-1}$ and was indicative of ATP hydrolysis in a 1:1 ratio. Total ATP hydrolysis was inferred from the rate of NADH disappearance over the 30-minute time interval.

Previously calculated protein concentrations for each sample were divided by their determined NADH concentrations from the GSK3 assay to yield ATP present per milligram of protein. These values were indicative of the GSK3 activity in each sample.

## 2.9. Statistical Analysis

Statistical analyses were conducted using Prism version 9. Outliers were pre-defined and identified as values that were +/- 2 standard deviations of the mean for the group and removed from further analysis. Two-way ANOVAs were performed using factors sex and dosing groups. One-way ANOVAs for combined sex were performed on dose when no statistical significance was present between males and females. When significant difference was present between dosing groups, post-hoc Tukey HSD adjusted two-tailed t-tests were performed to determine where the difference occurred. Repeated measure ANOVAs were conducted when analyzing multiple time points. Statistical significance was assumed at $p \leq 0.05$. Symbols indicate statistical difference between groups: *p<0.05, **p<0.01, ***p<0.001, ****p<0.0001. Trends were considered to be between p=0.051 and p=0.15. All data shown in tables and graphs is shown as the mean of group data with error bars representing standard deviation (±SD).

# 3. Results

## 3.1. Animal Body Mass

Analysis of body mass at the end of the study had a main effect of sex ($F(1, 56) = 490.4$, $p<0.0001$), with males (467.5g) being heavier than females (270.5 g) (Figure 5A). There was also a main effect of group ($F(3, 56) = 2.952$, $p=0.04$), and a trend for an interaction between sex and group ($F(3, 56) = 2.269$, $p=0.0905$). CON males (509.3 g) were significantly heavier than Li males (447.3 g, $p=0.0058$) and Cr-Li males (450.4 g, $p=0.0098$) (Figure 5B). CON males were trending higher than the Cr male group (463.13 g, $p=0.0571$). No differences were present between female groups (Figure 5C).

Analysis of body mass during supplementation demonstrated a significant difference over time ($F(5, 280) = 2453.854$, $p<0.0001$), between sex ($F(1, 56) = 315.295$, $p<0.0001$), and between groups ($F(3, 56) = 3.699$, $p=0.017$). Male (322.262 g) body mass was significantly higher than female (218.825 g) on average over time (Figure 6). Within males over time, a difference was present between groups ($F(15, 140) = 2.267$, $p=0.007$) with CON body mass (344.458 g) significantly higher than both Li (303.708 g, $p=0.008$) and Cr-Li (315.278 g, $p=0.049$) groups. Within females over time, there were no significant differences present between groups ($F(3, 28) = 0.826$, $p=0.813$).

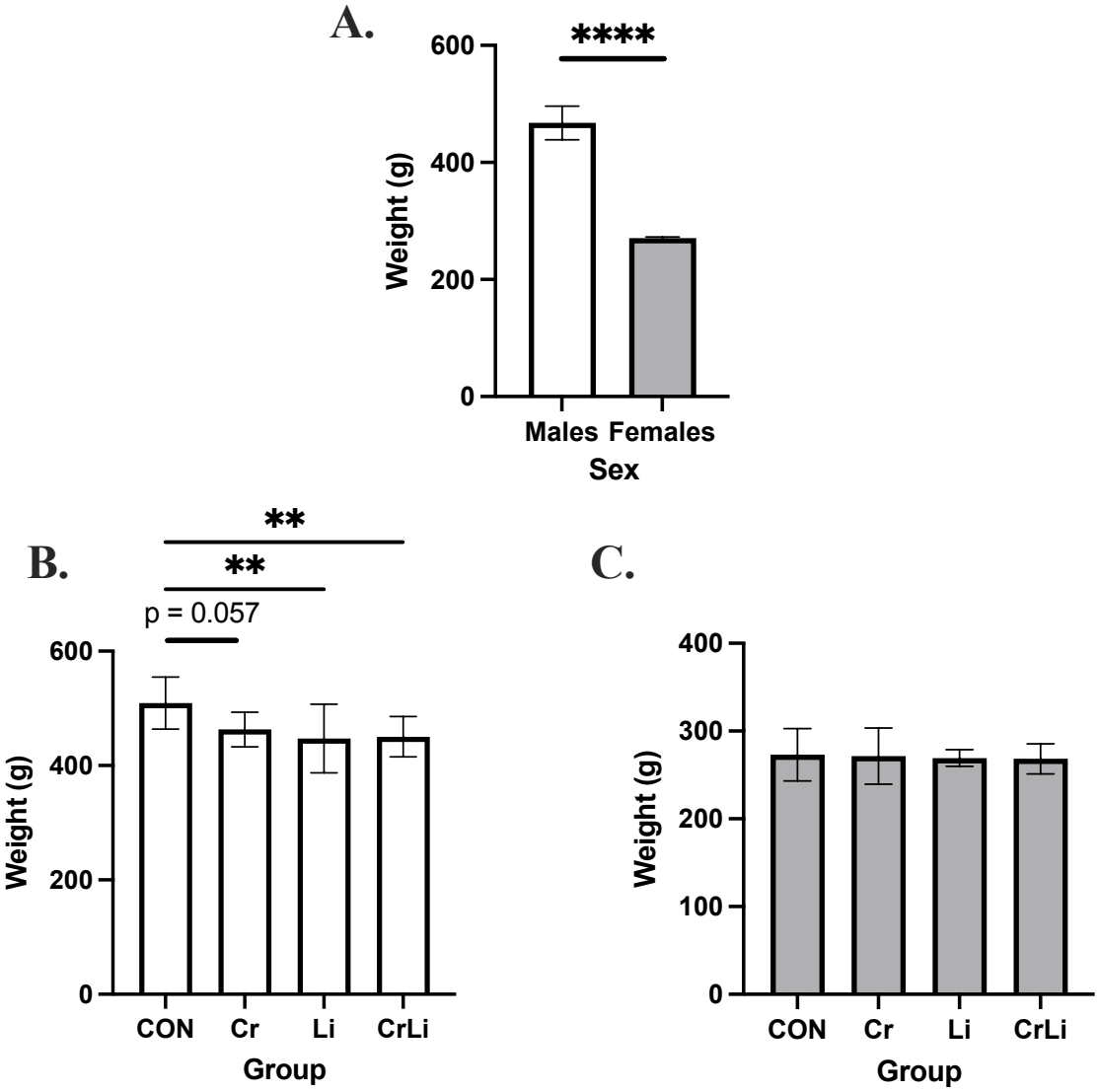


**Figure 5.** Post-supplementation weight of rats **(A)** Between sex (n=32/group), **(B)** Between male groups (n=8/group), and **(C)** Between female groups (n=8/group). Symbols indicate statistical differences between groups: **p<0.01, ****p<0.01 (Tukey's Test). Data expressed as group means +/- SD.

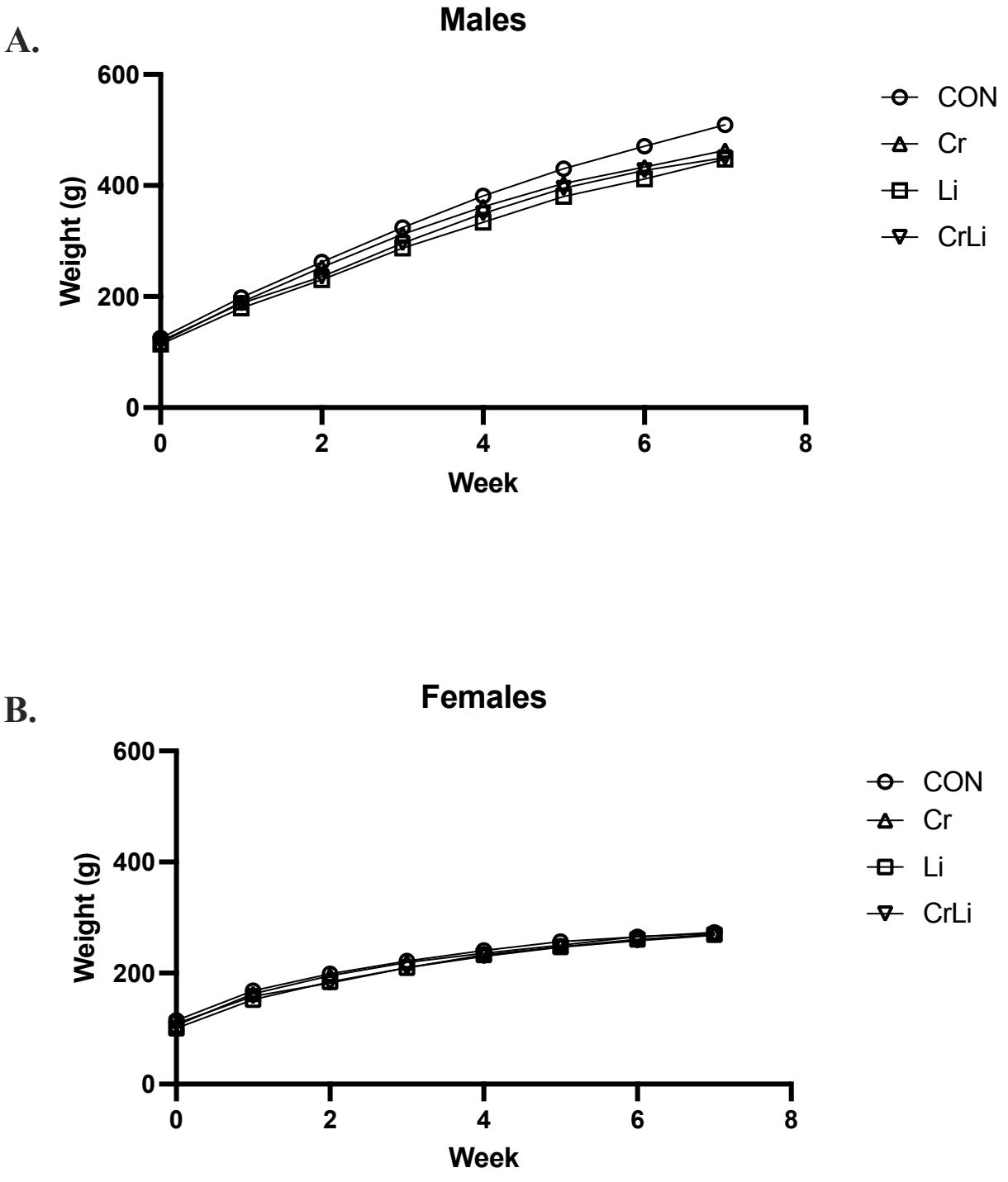


**Figure 6.** Growth curves of rats at the beginning of (week 0) and throughout the supplementation period for **(A)** Males and **(B)** Females. The average weight per week was computed for each group and plotted for each sex. Data expressed as group means with n=8/group.

### 3.2. Food and Water Consumption

Analysis of average daily food consumption per cage identified a significant difference between sex ($F(1, 24) = 309.1$, $p<0.0001$) with males (56.16 g/day) consuming more food than females (37.63 g/day) (Figure 7A). There was no significant difference between groups ($F(3, 24) = 1.803$, $p=0.1736$).

Analysis of daily food consumption relative to body weight identified a significant difference between sex ($F(1, 56) = 46.97$, $p<0.0001$) with female consumption (69.82 g/kg/day) higher than male consumption (60.49 g/kg/day) (Figure 7B). There was no difference between treatment groups within a sex ($F (3, 56) = 0.6101$, $p=0.6112$).

Analysis of food consumption over time yielded a significant difference over time ($F(5, 280) = 264.858$, $p<0.0001$), between sex ($F(1, 56) = 752.596$, $p<0.0001$), and between groups ($F(3, 56) = 3.886$, $p=0.014$). Males (378.385 g) consumed significantly more food on average over time than females (250.729 g). Within males, a difference was present between groups ($F(3, 28) = 7.409$, $p=0.01$), with CON males (402.667 g) significantly higher than Cr males (379.958 g, $p=0.022$), Li males (360.833 g, $p<0.0001$), and Cr-Li males (370.083 g, $p=0.002$). Cr males also consumed significantly more food than Li males ($p=0.05$). Within females, there was no significant difference between groups ($F(3, 28) = 574.972$, $p=0.840$).

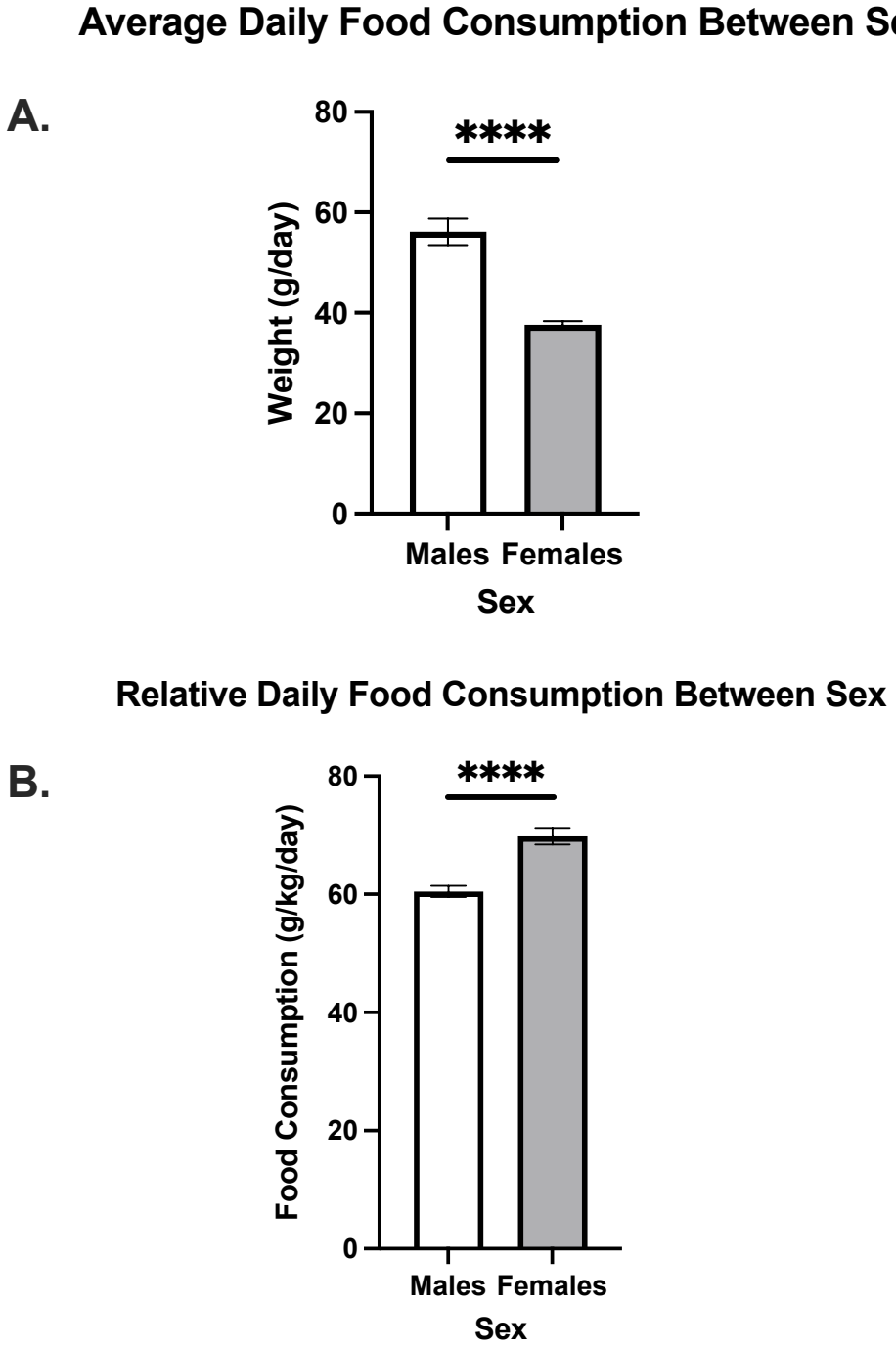


**Figure 7. (A)** Average daily food consumption per cage in grams between male and female rats (n=16/group). **(B)** Relative daily food consumption per rat in grams per kilogram body weight between male and female rats (n=32/group). The average food consumption data was calculated per cage. Consumption data per cage was used to estimate relative consumption per rat. Symbols indicate statistical differences between groups: ****$p<0.01$ (Tukey's Test). Data expressed as group means +/- SD.

Analysis of total water consumption yielded a difference between sex ($F(1, 56) = 76.83$, $p<0.0001$) with males consuming (2.299 L) significantly more than females (1.634 L). There was also a difference between groups ($F(3, 56) = 23.99$, $p<0.0001$). For the males, analysis identified water consumption in the CON group to be significantly higher than Li ($p<0.0001$) and Cr-Li ($p<0.0001$) groups. The Cr group also drank more than the Li ($p=0.0007$) and Cr-Li ($p=0.0004$) groups. For the females, CON drank significantly more than Cr-Li group ($p=0.0242$). The Cr group drank more than Li ($p=0.0383$) and Cr-Li ($p=0.0144$) groups. CON was also trending towards significance in terms of higher consumption compared to the Li group ($p=0.0620$).

Average daily water consumption was different between sexes ($F(1, 24) = 80.05$, $p<0.0001$). Males (56.76 mL) consumed significantly more water on average compared to females (40.41 mL) (Figure 8A). There was also a difference between groups ($F(3, 24) = 22.77$, $p<0.0001$). In males, CON consumed more than Li ($p<0.0001$) and Cr-Li ($p<0.0001$) (Figure 8B). Consumption was also higher in the Cr group compared to Li ($p=0.0020$) and Cr-Li groups ($p=0.0017$) (Figure 8B). In females, the CON group consumed significantly more water daily compared to Li ($p=0.0213$) and Cr-Li ($p=0.0162$) groups (Figure 8C). The Cr group was also higher than the Li ($p=0.0288$) and Cr-Li ($p=0.0220$) groups (Figure 8C).

Analysis of relative daily water consumption identified a significant difference between sex ($F(1, 56) = 50.14$, $p<0.0001$) with female consumption (74.98 mL/kg/day) higher than males (60.78 mL/kg/day) (Figure 9A). There was also a difference present between groups ($F(3, 56) = 26.47$, $p<0.0001$). In males, the CON group consumed more water than the Li ($p=0.0042$) and Cr-Li ($p=0.0021$) groups (Figure 9B). The Cr group also had a higher consumption compared to Li ($p=0.0050$) and Cr-Li ($p=0.0025$) males (Figure 9B). For females, the CON group had a higher

intake than the Li ($p<0.0001$) and Cr-Li ($p<0.0001$) groups (Figure 9C). The Cr group also consumed more than the Li ($p<0.0001$) and Cr-Li ($p<0.0001$) groups (Figure 9C).

Analysis of water consumption over time yielded a significant difference over time ($F(5, 280) = 75.689$, $p<0.0001$), between sex ($F(1, 56) = 179.260$, $p<0.0001$), and between groups ($F(3, 56) = 55.966$, $p<0.0001$). Males (383.083 mL) drank significantly more water on average over time than did females (272.344 mL). Within males, a significant difference was present between groups ($F(3, 28) = 35.340$, $p<0.0001$). For males, the CON group (470.583 mL) drank significantly more than the Li (317.958mL, $p<0.0001$) and Cr-Li (310.875mL, $p<0.0001$) groups. The Cr group (432.917 mL) also drank more than the Li ($p<0.0001$) and Cr-Li ($p<0.0001$) groups. CON males were trending towards significance in consuming more than Cr males ($p=0.06$). Within females, there was a difference between groups $F(3, 28) = 21.642$, $p<0.0001$). The CON group (307.208 mL) consumed more than the Li (240.083 mL, $p<0.0001$), and Cr-Li (229.167 mL, $p<0.0001$) groups. The Cr group drank more than the Cr (312.917 mL), Li ($p<0.0001$), and Cr-Li ($p<0.0001$) groups.

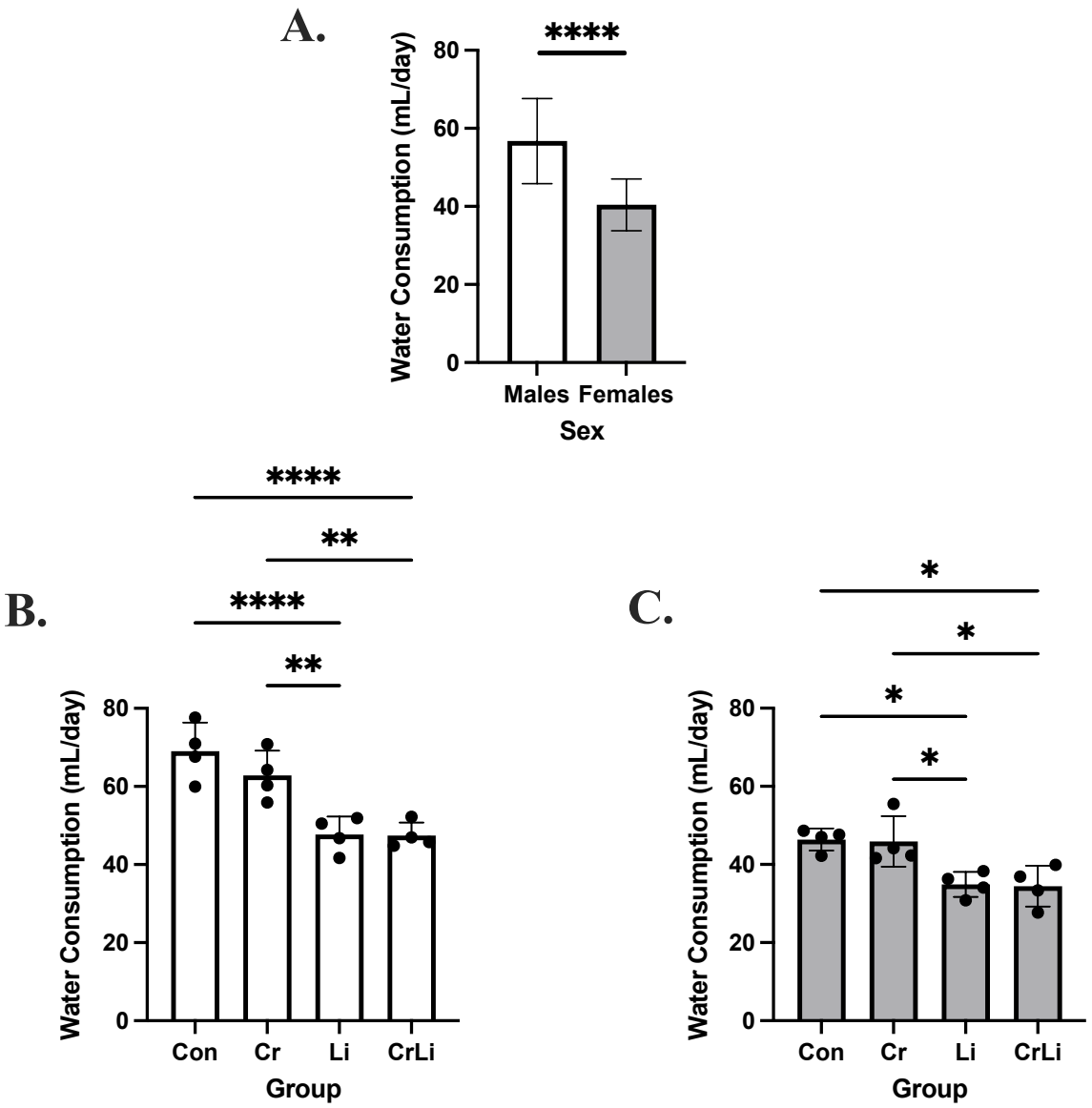


**Figure 8.** Average daily water consumption in millilitres **(A)** Between all male and female rats (n=16/group), **(B)** Between male groups (n=4/group), and **(C)** Between female groups (n=4/group). Average daily water consumption was calculated per cage. Symbols indicate statistical differences between groups: *p<0.05, **p<0.01, ****p<0.0001 (Tukey's Test). Data expressed as group means +/- SD.

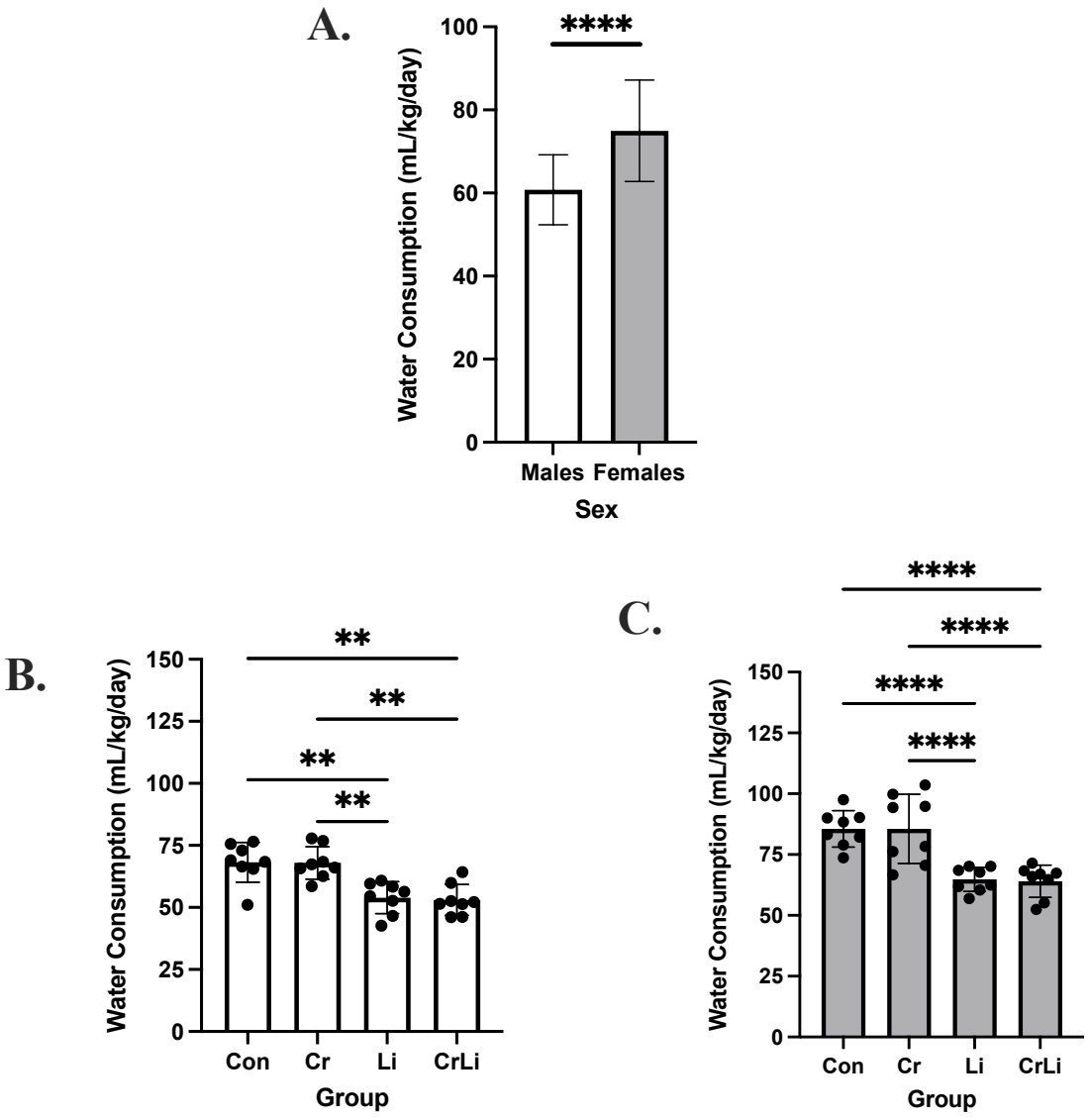


**Figure 9.** Relative water consumption in millilitres per kilogram of body weight **(A)** Between all male and female rats (n=32/group), **(B)** Between male groups (n=8/group), and **(C)** Between female groups (n=8/group). The average consumption data per cage was used to estimate relative consumption per rat. Symbols indicate statistical differences between groups: **p<0.01, ****p<0.0001 (Tukey's Test). Data expressed as group means +/- SD.

### 3.3. Creatine and Lithium Consumption

Absolute daily CrM consumption had a main effect of sex ($F(1, 28) = 69.20$, $p<0.0001$), irrespective of LiCl, with males (0.0689 g/day) higher than females (0.0502 g/day) (Figure 10A). There was also a main effect of LiCl ($F(1, 28) = 55.62$, $p<0.0001$), irrespective of sex, with the +LiCl group (0.1024 g/day) lower than the -LiCl group (0.1359 g/day) for CrM consumption (Figure 10A). There was no significant interaction between LiCl and sex ($F(1, 28) = 1.195$, $p=0.2837$).

Analysis of relative daily CrM consumption with and without LiCl identified a main effect of sex ($F(1, 28) = 19.97$, $p=0.0001$), irrespective of LiCl, with female consumption (0.3740 g/kg/day) significantly higher than males (0.3025 g/kg/day) (Figure 10B). There was also a main effect of LiCl ($F(1, 28) = 32.37$, $p<0.0001$), irrespective of sex, with LiCl fed rats (0.2927 g/kg/day) significantly lower than rats without LiCl (0.3838 g/kg/day) (Figure 10B). There was no significant interaction between LiCl and sex ($F(1, 28) = 1.053$, $p=0.3137$).

A main effect for sex was also observed for absolute daily LiCl consumption with and without CrM ($F(1, 28) = 89.77$, $p<0.0001$), irrespective of CrM, with males (0.004756 g/day) greater than females (0.003467 g/day) (Figure 11A). There was no main effect of CrM ($F(1, 28) = 0.0656$), $p=0.7998$) or interaction between sex and CrM ($F(1, 28) = 0.0040$, $p=0.9500$).

Relative daily LiCl consumption with and without CrM had a main effect of sex ($F(1, 28) = 25.63$, $p<0.0001$), irrespective of CrM, with females (0.01288 g/kg/day) greater than males (0.01070 g/kg/day) (Figure 11B). There was no main effect of CrM ($F(1, 28) = 0.1444$, $p=0.7068$) or interaction between sex and CrM ($F(1, 28) = 0.0014$, $p=0.9707$).

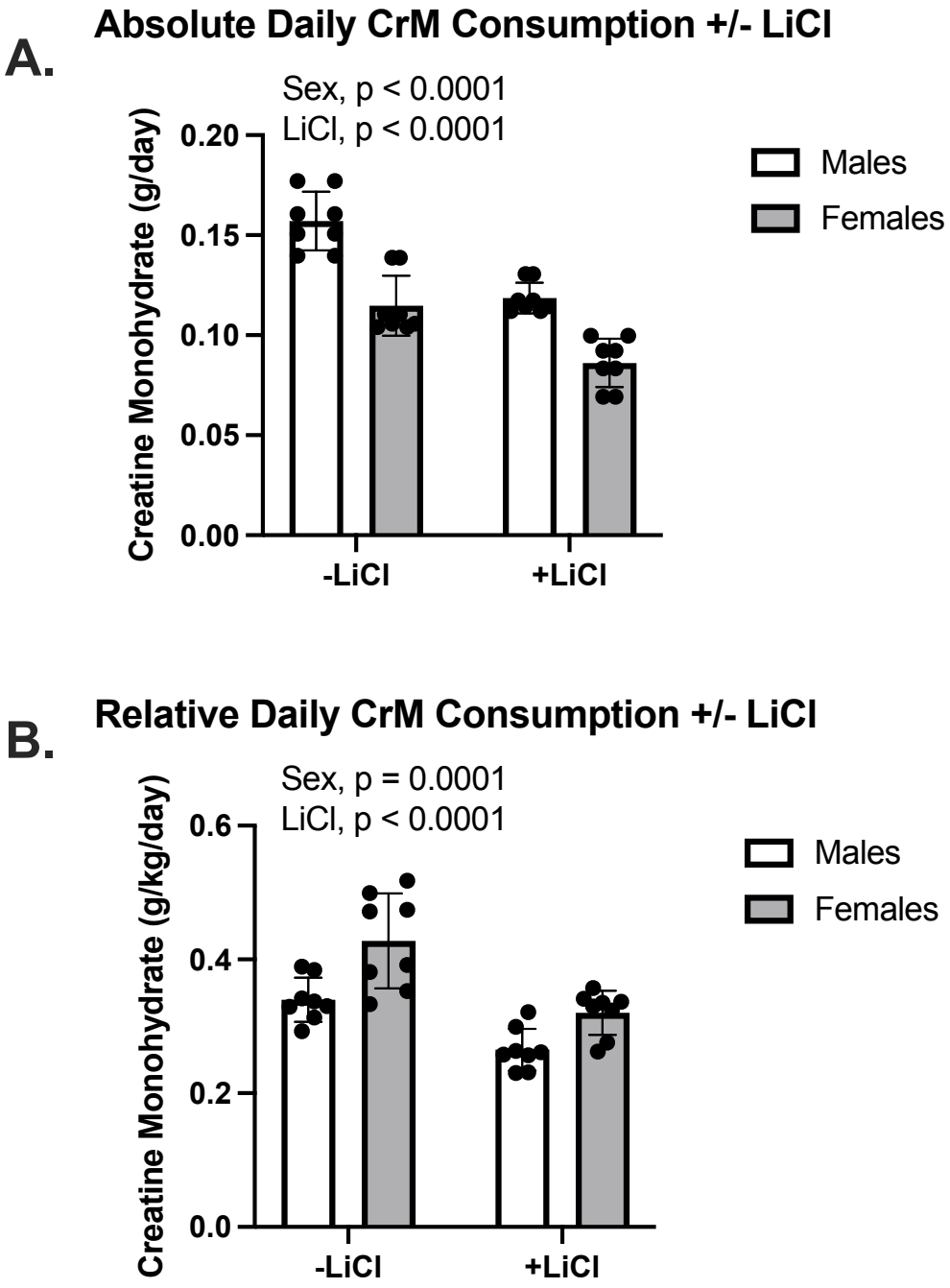


**Figure 10. (A)** Relative daily and **(B)** Absolute daily CrM consumption in grams per kilogram of body weight +/- LiCl in rats. The average consumption data per cage was used to estimate relative consumption per rat. For A & B, a two-way ANOVA was used to test the main effects of CrM, LiCl, and their potential interaction. Text indicates significant main effects with their corresponding p-values. Data expressed as group means +/- SD with n=8/group.

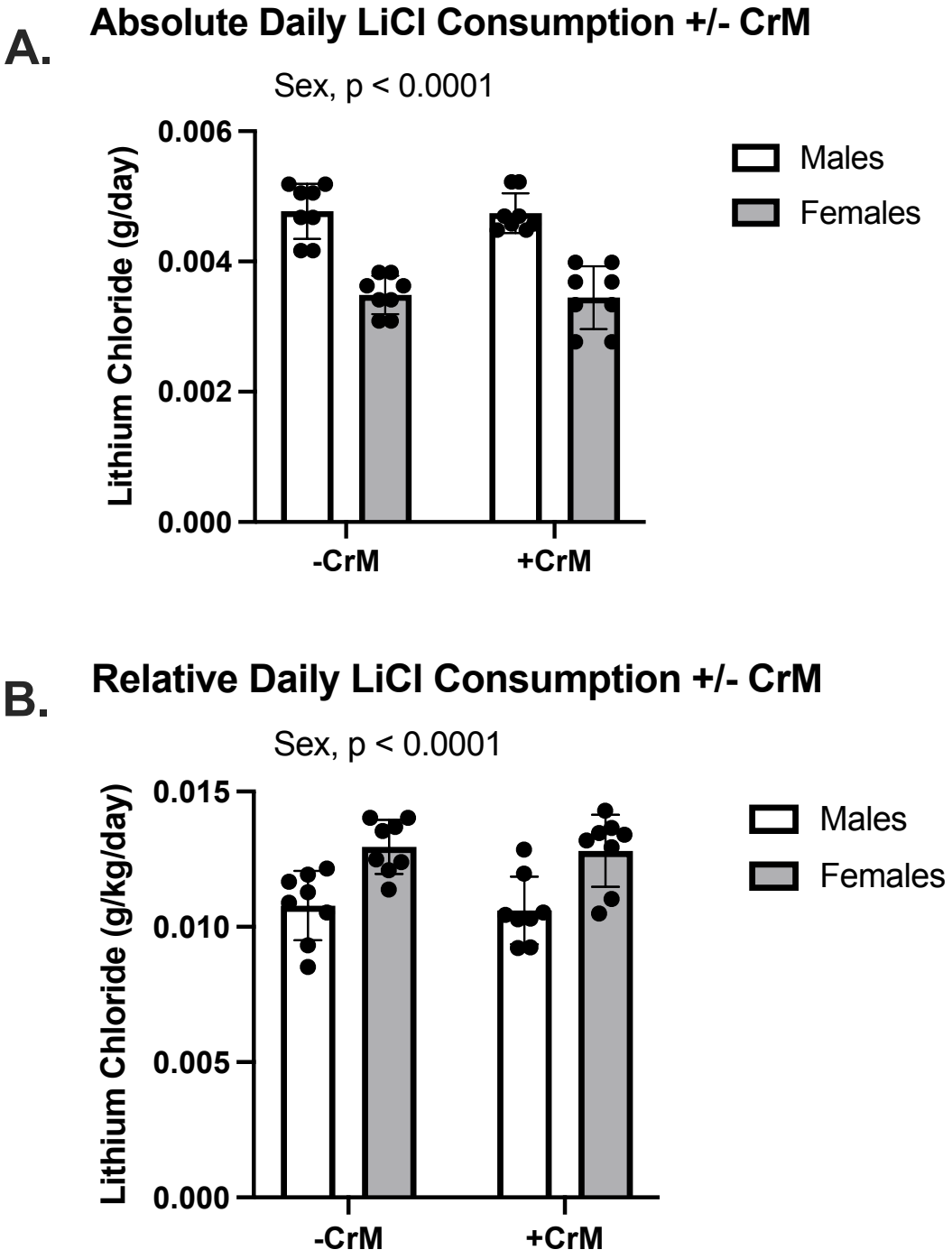


**Figure 11. (A)** Relative daily and **(B)** Absolute daily LiCl consumption in grams per kilogram body weight +/- CrM in rats. The average consumption data per cage was used to estimate relative consumption per rat. For A & B, a two-way ANOVA was used to test the main effects of CrM, LiCl, and their potential interaction. Text indicates significant main effects with their corresponding p-values. Data expressed as group means +/- SD with n=8/group.

## 3.4. Brain Response to Supplementation

### 3.4.1. Total Creatine Concentration

TCr brain concentration +/- CrM and LiCl for combined sex had a main effect of CrM ($F(1, 59) = 42.86$, $p<0.0001$), irrespective of LiCl, with +CrM rats (55.48 μmol/g) greater than -CrM (49.43 μmol/g) (Figure 12A). There was also a main effect of LiCl ($F(1, 59) = 16.26$, $p=0.0002$), irrespective of CrM, with +LiCl (54.04 μmol/g) greater than -LiCl (49.43 μmol/g) (Figure 12A). There was no interaction between CrM and LiCl ($F(1, 59) = 2.099$, $p=0.1527$).

Within males, brain [TCr] +/- CrM and LiCl had a main effect of CrM ($F(1, 27) = 27.47$, $p<0.0001$), irrespective of LiCl, with +CrM (56.54 μmol/g) greater than -CrM (47.11 μmol/g) (Figure 10B). There was also a main effect present for LiCl ($F(1, 27) = 11.07$, $p=0.0025$), irrespective of CrM, with +LiCl (54.82 μmol/g) greater than -LiCl (48.83 μmol/g) for brain [TCr] (Figure 12B). There was no interaction present between CrM and LiCl ($F(1, 27) = 0.9142$, $p=0.3475$).

Within females, there was a main effect of CrM ($F(1, 27) = 15.66$, $p=0.0005$), irrespective of LiCl, with +CrM (54.53 μmol/g) greater than -CrM (48.88 μmol/g) (Figure 12C). There was also a main effect of LiCl ($F(1, 27) = 5.480$, $p=0.0266$), irrespective of CrM, with +LiCl (53.38 μmol/g) greater than -LiCl (50.04 μmol/g) for brain [TCr] (Figure 12C). There was no interaction present between CrM and LiCl ($F(1, 27) = 1.083$, $p=0.3068$).

The percent change in brain TCr concentrations with LiCl was determined between sex. LiCl led to a ~12% TCr increase in males, whereas females only had a ~7% increase, though this was not statistically significant ($p=0.18$) (Figure 13).

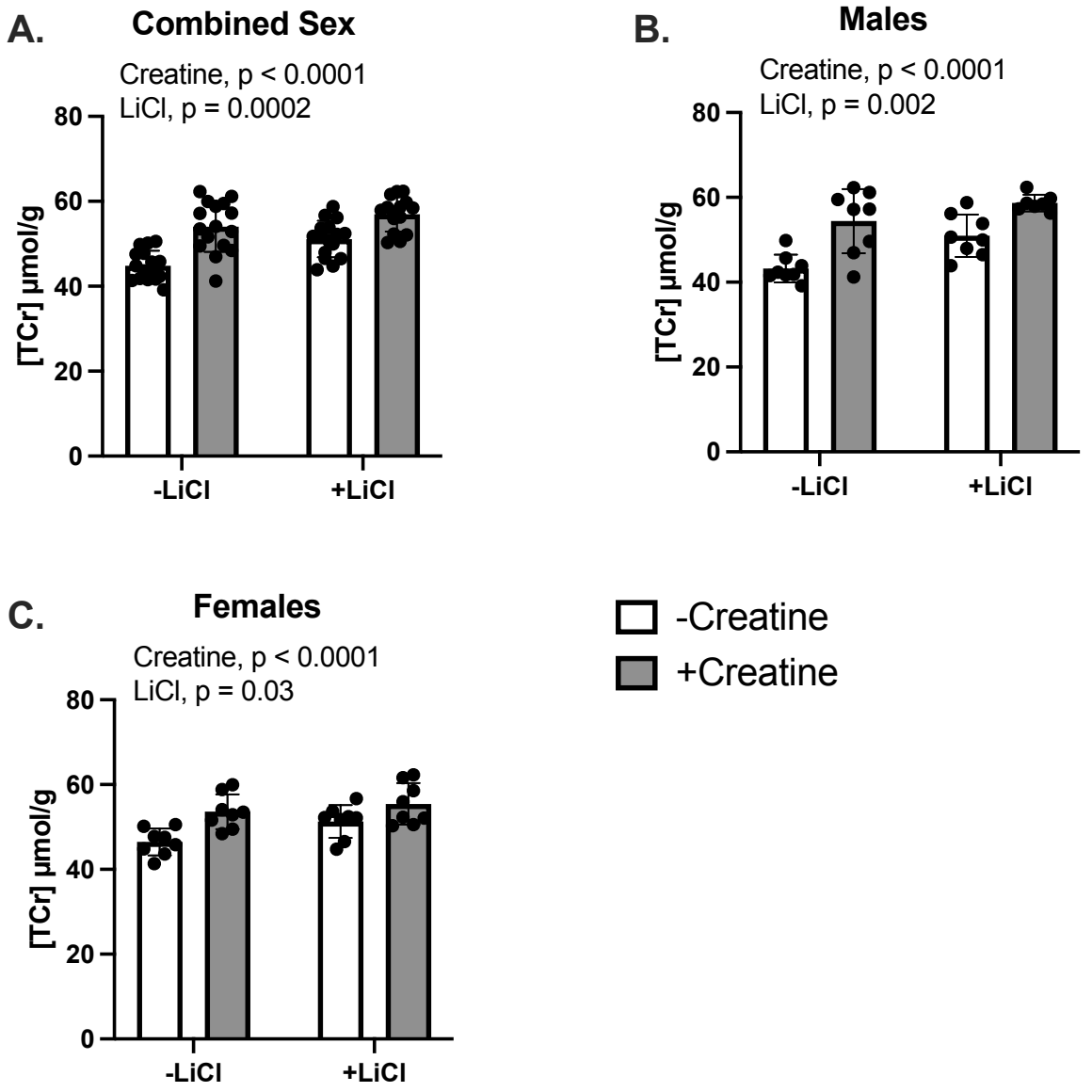


**Figure 12.** TCr concentrations in the frontal lobe of rat brains with (+) and without (-) CrM/LiCl. **(A)** Combined Sex (n=16/group), **(B)** Males (n=8/group), and **(C)** Females (n=8/group). For A-C, a two-way ANOVA was used to test the main effects of Creatine, LiCl, and their potential interaction. Text indicates significant main effects with their corresponding p-values. Data expressed as group means +/- SD.

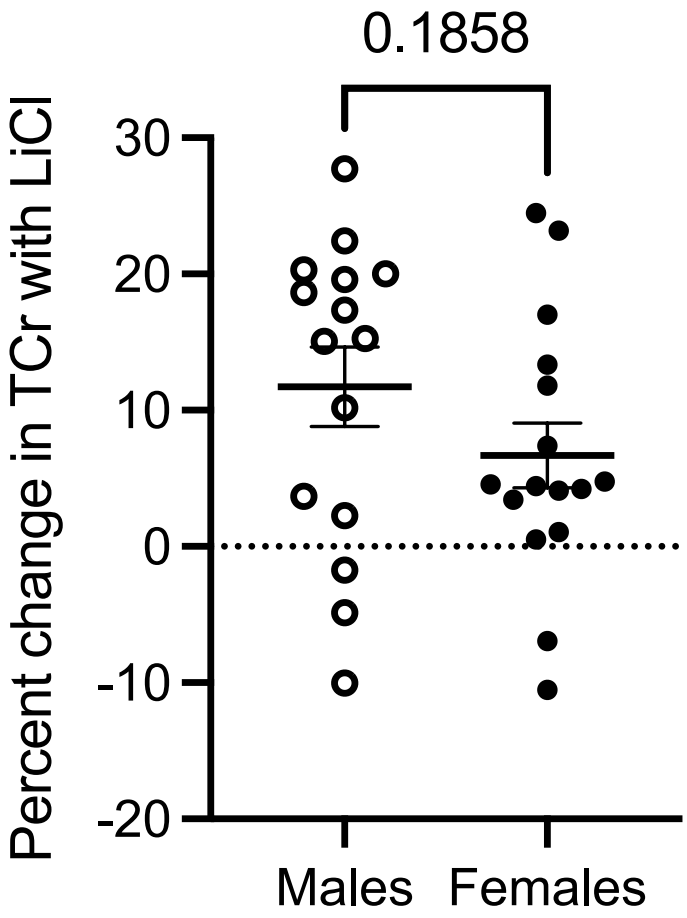


**Figure 13.** Percent change in brain TCr concentrations with LiCl in male vs female rat brains. Text indicates percent difference with their corresponding p-values (Unpaired T-test). Data expressed as group means +/- SD.

### 3.4.2. GSK3 Activity

Total GSK3 activity was compared between each group and sex. There was a significant difference present between sex ($F(1, 39) = 15.19$, $p=0.0004$), with females (5.755 nmol/mg protein/min) exhibiting greater activity than males (4.419 nmol/mg protein/min, $p=0.0004$). No difference was present between groups ($F(3, 39) = 1.467$, $p=0.2385$).

The two-way ANOVA revealed a trend for a main effect of LiCl on GSK3 activity, with reduced GSK3 activity with the consumption of LiCl ($F(1, 43) = 2.613$, $p=0.11$) (Figure 15). There was no main effect for CrM ($F(1, 43) = 0.2835$, $p=0.59$) and no significant interaction was present ($F(1, 43) = 0.0884$, $p=0.77$).

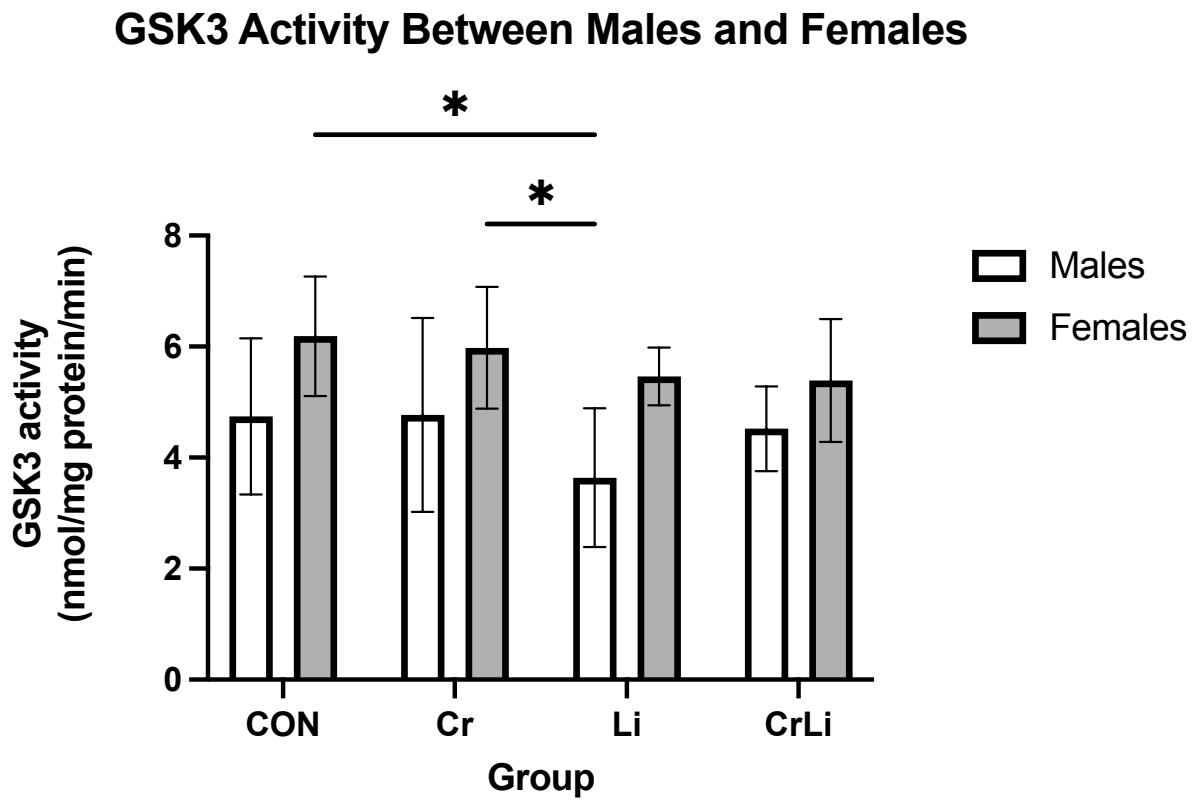


**Figure 14.** GSK3 activity in nanomoles per milligram of protein per minute, between male and female rat brains. Symbols indicate statistical differences between groups: *p<0.05 (Tukey's Test). Data expressed as group means +/- SD with n=6/group.

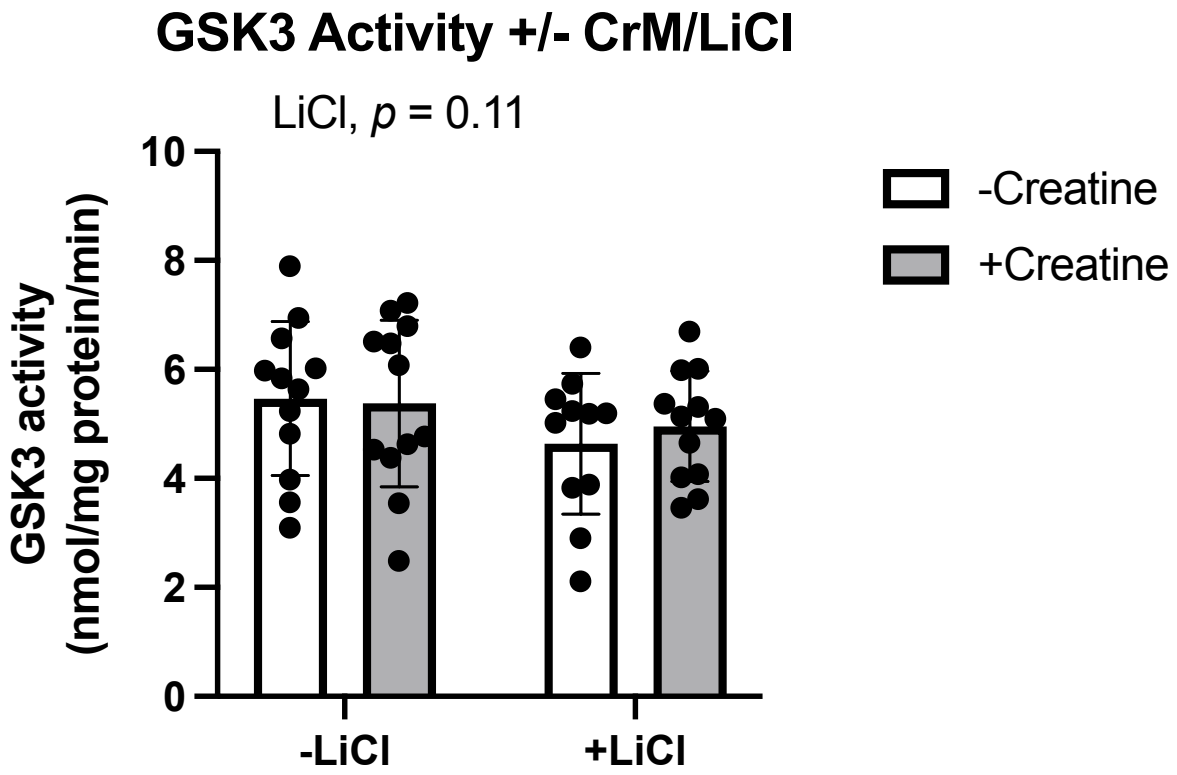


**Figure 15.** GSK3 activity with (+) and without (-) CrM/LiCl in rat brains. Statistical trend present between LiCl groups (p=0.11) (Bonferroni). Data expressed as group means +/- SD with n=12/group.

### 3.4.3. Creatine Transporter mRNA Expression

Relative creatine transporter gene (slc6a8) expression was determined between groups and sex. There were no significant differences between sex ($F(1, 54) = 0.1777$, $p=0.6751$) or group ($F(3, 54) = 2.195$, $p=0.0992$). Additionally, no significant interaction was present between group and sex ($F(3, 54) = 0.5299$, $p=0.6637$). When groups were collapsed across sex, no statistical difference between groups were observed ($F(3, 43) = 0.7941$, $p=0.5039$).

Relative slc6a8 expression +/- CrM/LiCl had a trend for a main effect of LiCl ($F(1, 42) = 2.501$, $p=0.12$), irrespective of CrM, with +LiCl ($1.755\ 2^{-\Delta\Delta CT}$) greater than -LiCl ($1.350\ 2^{-\Delta\Delta CT}$) (Figure 16B). There was no main effect of CrM ($F(1, 42) = 1.529$, $p=0.2232$) and no interaction between CrM and LiCl ($F(1, 42) = 0.0221$, $p=0.8826$).

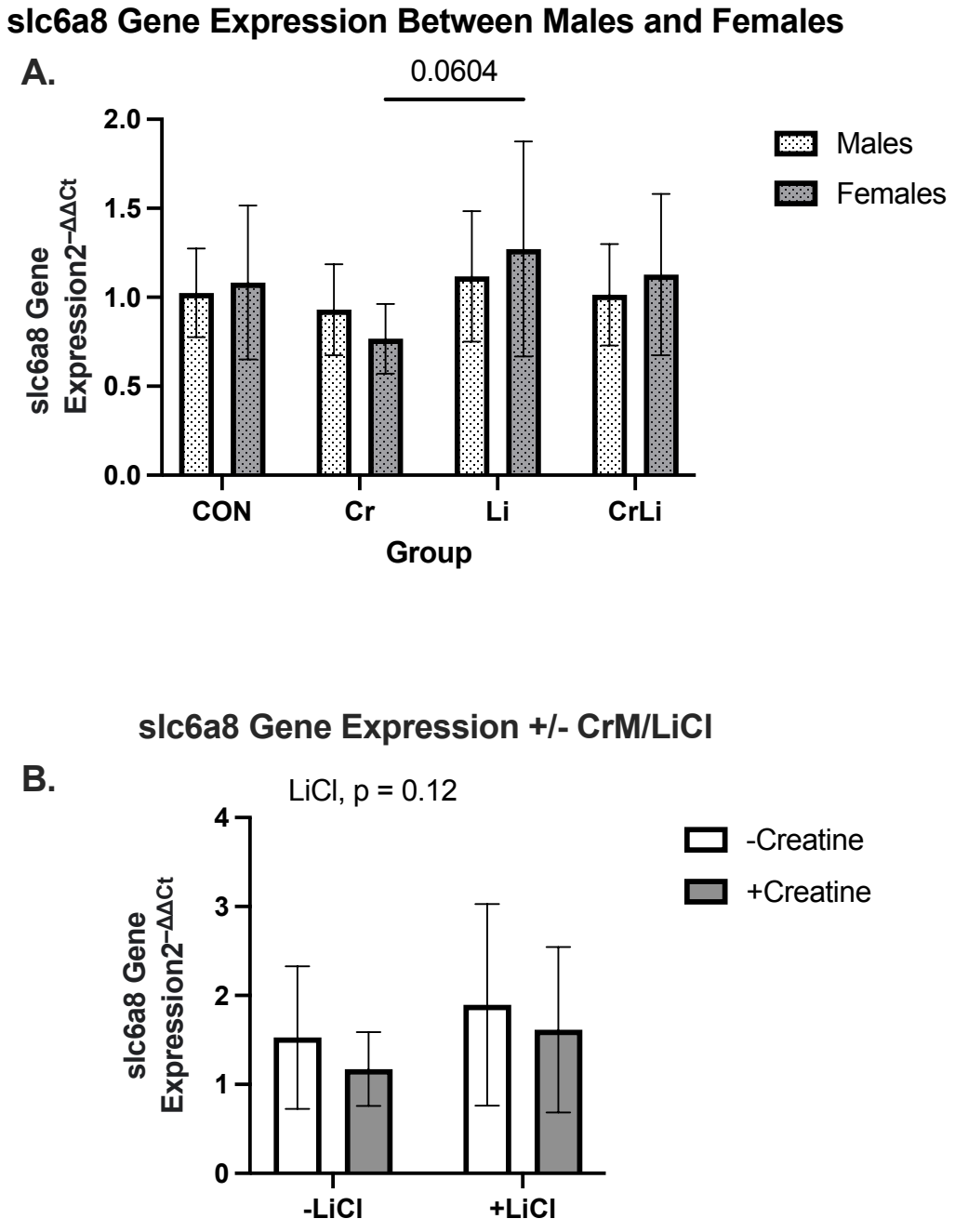


**Figure 16.** Relative gene expression of creatine transporter slc6a8 in rat brains. **(A)** Between males and females (n=8/group) **(B)** With (+) and without (-) CrM/LiCl for combined sex (n=16/group). For A, a statistical trend was present between Cr female and Li female groups (p=0.0604) (Tukey's Test). For B, a two-way ANOVA was used to test the main effects of Creatine, LiCl, and their potential interaction. Text indicates significant main effects with their corresponding p-values. Data expressed as group means +/- SD.

### 3.4.4. GSK3 and β-catenin Protein Expression

Western blotting was used to determine the relative expression of various proteins in both males and females. Data was analyzed using a two-way ANOVA to test the main effects of CrM, LiCl, and their potential interaction with sex combined. Males and females were also separated to determine the main effects of sex, group, and their potential interaction.

With sex combined, pGSK3β content had a main effect of LiCl ($F(1, 40) = 5.613$, $p=0.0227$), irrespective of CrM, with +LiCl (0.04031 A.U.) greater than -LiCl (0.03442) (Figure 17B). There was no main effect of CrM ($F(1, 40) = 0.90200$, $p=0.3480$) or significant interaction between LiCl and CrM ($F(1, 40) = 0.5995$, $p=0.4433$) (Figure 17B). Total GSK3β content had no main effect of LiCl ($F(1, 40) = 0.9652$, $p=0.3318$) and no main effect of CrM ($F(1, 40) = 0.6996$, $p=0.4079$). There was also no significant interaction between LiCl and CrM ($F(1, 40) = 0.9089$, $p=0.3461$) (Figure 17C). The ratio of pGSK3β:GSK3β had a main effect of LiCl ($F(1, 36) = 5.133$, $p=0.0296$), irrespective of CrM, with +LiCl (2.060 A.U.) greater than -LiCl (1.801 A.U.) (Figure 17D). There was no main effect of CrM ($F(1, 36) = 0.0681$, $p=0.7956$) and no significant interaction between LiCl and CrM ($F(1, 36) = 0.3300$, $p=0.5692$) (Figure 17D).

pGSK3α content had a main effect of LiCl ($F(1, 40) = 11.11$, $p=0.0019$), irrespective of CrM, with +LiCl (0.7742 A.U.) greater than -LiCl (0.5844 A.U.) (Figure 17E). There was also a main effect of CrM ($F(1, 40) = 7.064$, $p=0.0113$), irrespective of LiCl, with +CrM (0.7550 A.U.) greater than -CrM (0.6036 A.U.) (Figure 17E). There was no interaction present for pGSK3α between LiCl and CrM ($F(1, 40) = 0.0570$, $p=0.8125$) (Figure 17E). Total GSK3α content had a significant interaction between LiCl and CrM ($F(1, 36) = 4.756$, $p=0.0358$) (Figure 17F). There was no main effect of LiCl ($F(1, 36) = 1.457$, $p=0.2352$) and no main effect of CrM ($F(1, 36) = 0.0414$, $p=0.8398$) (Figure 17F). The ratio of pGSK3α:GSK3α had a main effect of CrM ($F(1, 31)$

= 11.95, p=0.0016), irrespective of LiCl, with +CrM (2.432 A.U.) greater than -CrM (1.785 A.U) (Figure 17G). There was also a trend for a main effect of LiCl (F(1, 31) = 3.748, p=0.0620), irrespective of CrM, with +LiCl (2.289 A.U.) greater than -LiCl (1.927 A.U.) (Figure 17G). There was no significant interaction between LiCl and CrM (F(1, 31) = 0.1046, p=0.7485) (Figure 17G).

With males and females separated, pGSK3β content had no main effect of sex (F(1, 40) = 0.008, p=0.9282), no main effect of group (F(3, 40) = 0.4545, p=0.7155), and no interaction (F(3, 40) = 0.4524, p=0.7170) (Figure 18A). For total GSK3β content there was no main effect of sex (F(1, 39) = 0.3566, p=0.5539), and no main effect of group (F(3, 39) = 0.7974, p=0.5028). There was however a trend towards a interaction between sex and group (F(3, 39) = 2.545, p=0.07) (Figure 18B). No main effects for sex or group and no interactions were observed for the ratio of pGSK3β:GSK3β (F(1, 40) = 0.4216, p=0.5198), (F(3, 40) = 0.3625, p=0.7804), (F(3, 40) = 0.0855, p= 0.9676) (Figure 18C).

No main effect was observed for sex for pGSK3α content (F(1, 40) = 0.0027, p=0.9589), but a trend towards a main effect of group was observed(F(3, 40) = 2.126, p=0.1121), with CrLi (1.430 A.U.) higher than CON (0.9913 A.U.) (Figure 18D). A trend towards a main effect for sex for total GSK3α content was also observed (F(1, 40) = 3.886, p=0.0556), irrespective of group, with females (0.9851 A.U.) greater than males (0.8238 A.U.). There was no main effect of group (F(3, 40) = 0.0855, p=0.9675) for total GSK3α content, but a trend was seen for an interaction between sex and group (F(3, 40) = 1.955, p=0.1363) (Figure 18E). The ratio of pGSK3α:GSK3α also demonstrated a trend for a main effect of sex (F(1, 40) = 2.352, p=0.1330), irrespective of group, with males (1.441 A.U.) greater than females (1.158 A.U.) (Figure 18F). There was no main effect of group (F(3, 40) = 1.649, p=0.1934) and no significant interaction between sex and group (F(3, 40) = 0.9440, p=0.4285) (Figure 18F).

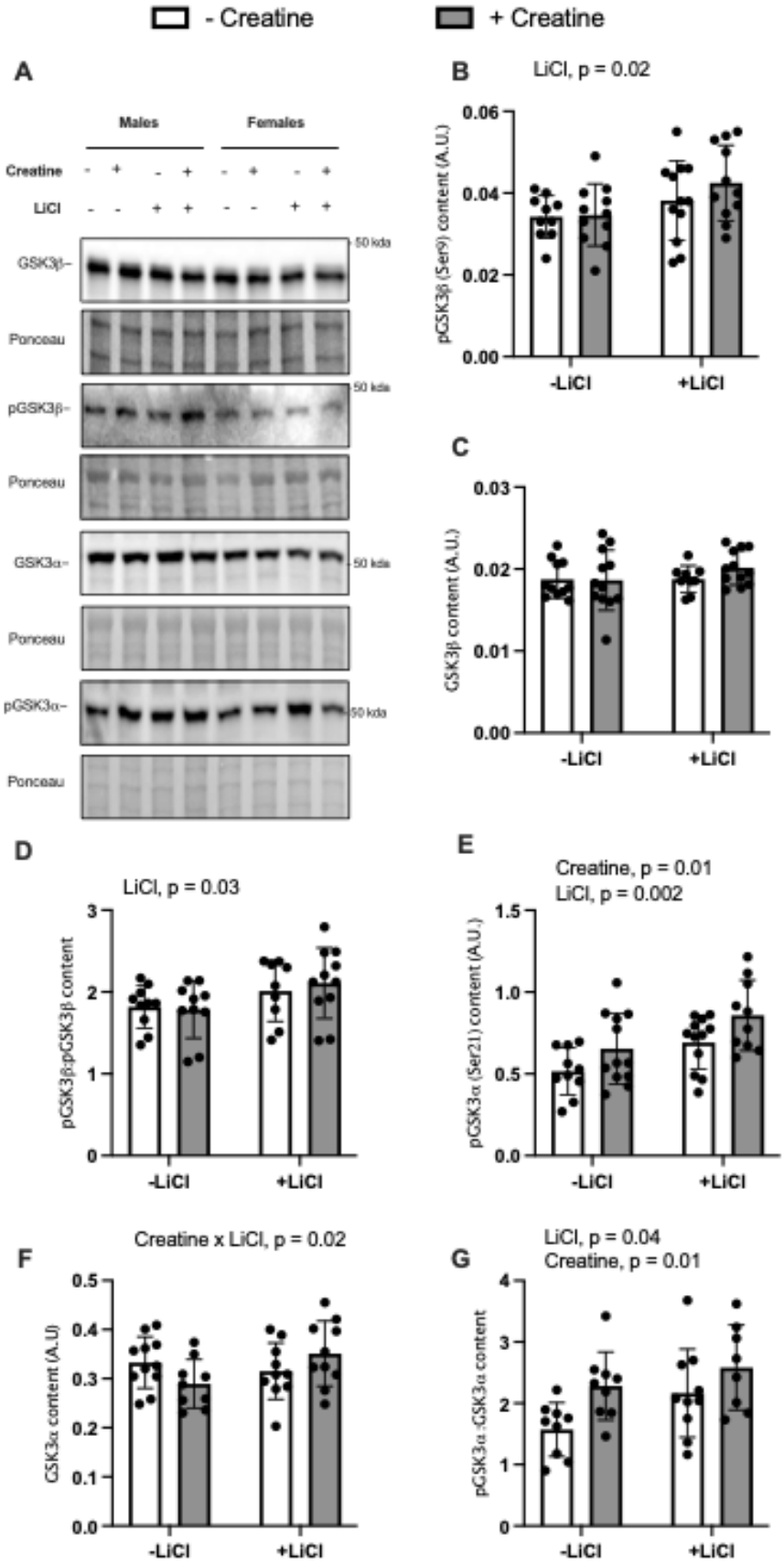
- Creatine
+ Creatine
A
Males
Females
Creatine
LiCl
GSK3β–
Ponceau
pGSK3β–
Ponceau
GSK3α–
Ponceau
pGSK3α–
Ponceau
50 kda
B
LiCl, p = 0.02
pGSK3β (Ser9) content (A.U.)
-LiCl
+LiCl
C
GSK3β content (A.U.)
D
LiCl, p = 0.03
pGSK3β:pGSK3β content
E
Creatine, p = 0.01
LiCl, p = 0.002
pGSK3α (Ser21) content (A.U.)
F
Creatine x LiCl, p = 0.02
GSK3α content (A.U)
G
LiCl, p = 0.04
Creatine, p = 0.01
pGSK3α:GSK3α content

**Figure 17**. **(A)** Western blot representative images for GSK3β, p-GSK3β, GSK3α, and p-GSK3α, along with their corresponding ponceau stains in rat brains. Samples are indicated for each representative blot. Optical density of various proteins. **(B)** p-GSK3β (Ser9) content **(C)** GSK3β content **(D)** p-GSK3β:GSK3β content **(E)** p-GSK3α (Ser21) **(F)** GSK3α **(G)** p-GSK3α:GSK3α. For B-G, a two-way ANOVA was used to test the main effects of CrM, LiCl, and their potential interaction. Text indicates significant main effects with their corresponding p-values. Data expressed as group means +/- SD with n=12/group.

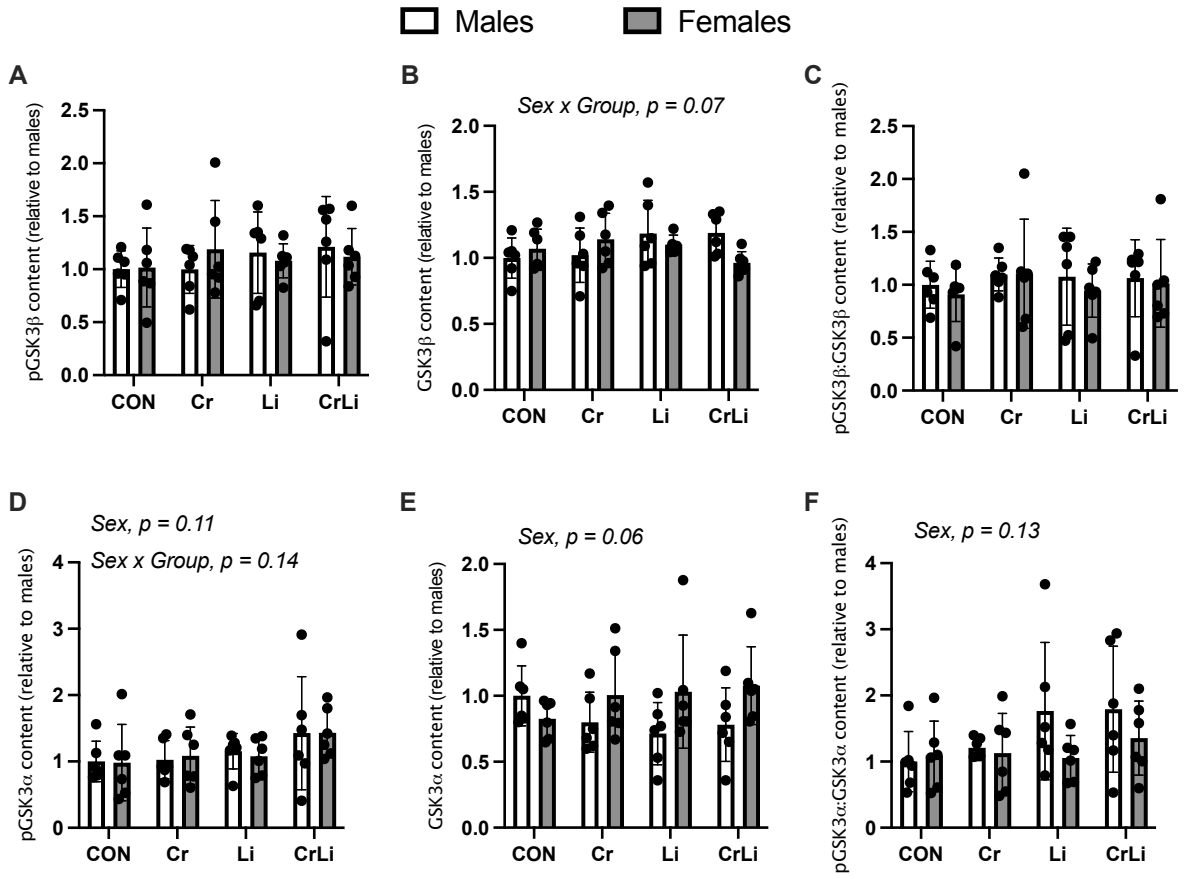


**Figure 18.** Optical density of western blots for both group and sex from rat brains. **(A)** p-GSK3β (Ser9) content **(B)** GSK3β content **(C)** p-GSK3β:GSK3β content **(D)** p-GSK3α (Ser21) **(E)** GSK3α **(F)** p-GSK3α:GSK3α. For A-F, male vs female comparison was normalized to CON males. A two-way ANOVA was used to test the main effects of sex, group, and their potential interaction. Text indicates significant main effects with their corresponding p-values. Data expressed as group means +/- SD with n=6/group.

# 4. Discussion

## 4.1. Brain TCr Concentrations

The purpose of this study was to investigate the individual and combined influences of creatine monohydrate and lithium chloride on creatine concentrations in the *in vivo* rat brain. This study determined that rats supplemented with 5g/L CrM demonstrated a significant increase in brain TCr concentrations compared to rats who were not fed CrM. This held true for combined sex, as well as within each sex alone. LiCl fed rats at 0.2g/L also had a significant increase in brain TCr concentrations for both combined sex and with sex separated. This suggests that LiCl is capable of independently increasing TCr concentrations, as increases were observed irrespective of CrM. Although CrM and LiCl independently increased brain TCr concentrations, there was no combined or synergistic effect for rats who were co-supplemented. This is the first known study to examine brain TCr concentrations following supplementation with LiCl. Furthermore, the investigation of co-supplementation with CrM and LiCl on brain TCr concentrations is novel to this field.

Increases in brain TCr concentrations have been previously reported in rats of middle to late adolescent age (12-20 weeks old) after 8 weeks of supplementation using the same dose of 5g/L CrM (Dunham et al., 2021). The current study therefore suggests that a shorter supplementation of 6 weeks of 5g/L CrM is also adequate to increase TCr concentrations in the brain of young rats. Animal and human investigations on brain TCr concentrations following supplementation with CrM in the literature are consistent with the current findings. Both male and female Cr groups demonstrated significantly greater brain TCr levels compared to their CON counterparts.

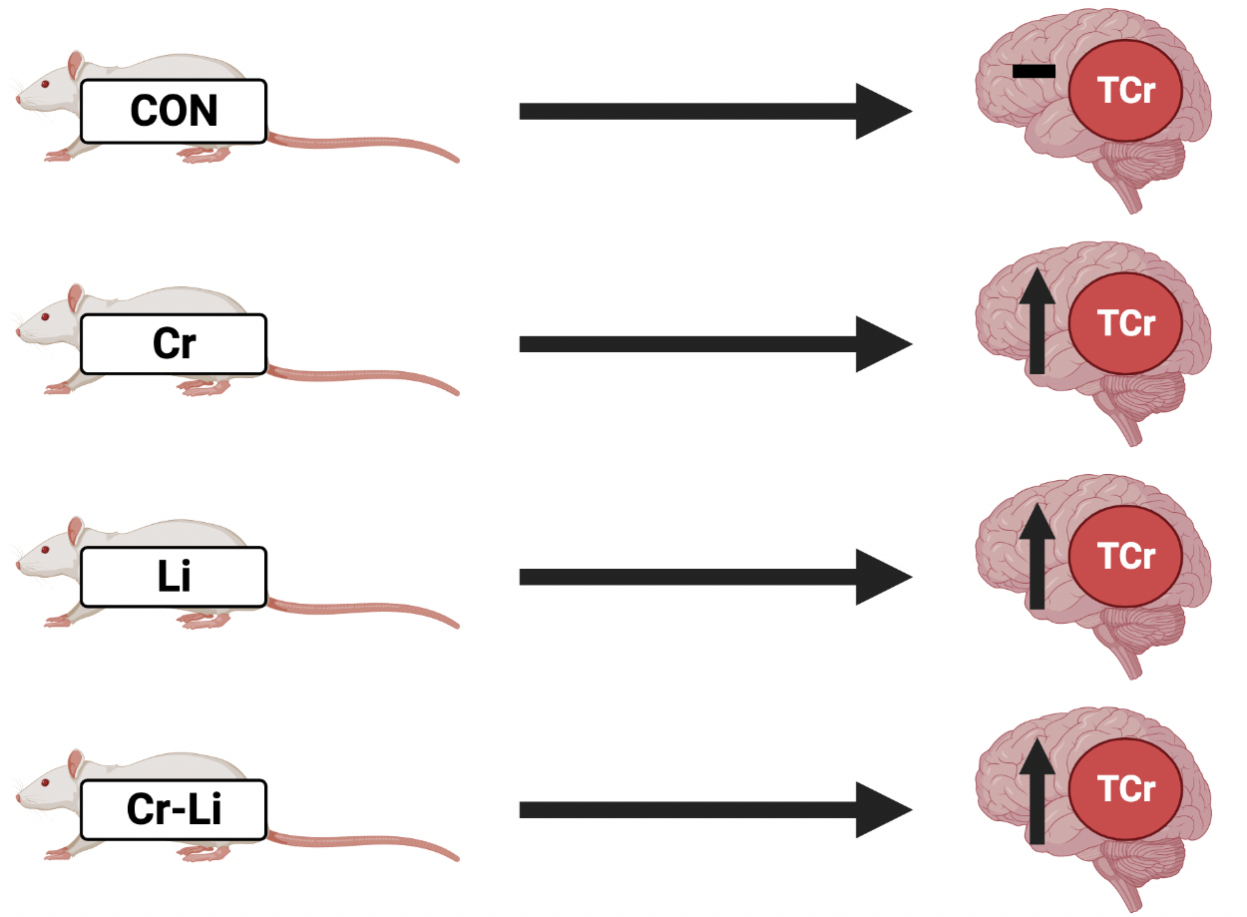


**Figure 19.** Outcome of brain [TCr] between supplementation groups. The Cr, Li, and Cr-Li groups each independently increased brain TCr concentrations compared to the CON group.

Multiple studies have observed increased TCr in the brain following CrM supplementation. A study conducted on 6-week old female mice and rats supplemented drinking water with 2g/kg/day CrM for 2, 4, or 8 weeks (Ipsiroglu et al., 2001). Five of each animal was included in the supplementation group, and five assigned to the control group. High performance liquid chromatography (HPLC) determined TCr measurements were significantly higher in the supplemented mice after 2, 4, and 8 weeks compared to baseline. In rats, TCr measurements were significantly higher after both 4- and 8-week periods. These findings are supportive of the brain TCr increase observed in young rats in the current study following a 6-week supplementation period.

Dechent et al., 1999, measured TCr brain concentrations in humans following oral supplementation of 5g CrM 4 times a day for 4 weeks. Proton magnetic resonance spectroscopy (MRS) was used to measure brain TCr concentrations in vivo of six volunteers aged 26-28 (4 female, 2 male). Findings indicated a statistically significant increase in brain TCr concentrations when averaged across brain regions and subjects (Dechent et al., 1999). A follow up conducted 3 months post-study yielded the previously observed TCr increase to be reversible in all brain regions when not supplementing with CrM (Dechent et al., 1999). This study also supports our observations of brain TCr increase with creatine supplementation.

Another clinical study examined the effect of CrM supplementation on brain TCr levels during oxygen deprivation. Recruitment included 15 participants (10 male, 5 female) with a mean age of 31. Participants first underwent a baseline assessment spending 30 minutes doing cognitive tests under normal conditions, followed by 30 minutes in a hypoxic environment measuring blood pressure, heart rate, and oxygen saturation. They were then randomized into a CrM supplemented group or control group given placebo. The CrM group was given 5g of CrM four times daily (20g/day) for one week. Following the supplemented period, participants underwent imaging and MRS measures of brain creatine before completing cognitive tasks under hypoxic conditions. A wash-out period involving no supplements then took place for 5 weeks. A second round of the 7-day dietary intervention and experimental session involving cognitive testing was then completed. Findings indicated the 7-day period of CrM supplementation increased brain TCr concentration on average by 9.2%. Furthermore, attentional capacity and corticomotor excitability, previously affected by hypoxic conditions, were restored when participants were creatine supplemented. (Turner, Byblow, & Gant, 2015).

### 4.2. Sex Differences in Brain TCr Concentrations

The current study design also allowed for an initial investigation into possible sex differences in the response to the interventions. In males, the main effect of LiCl on brain TCr was highly significant (p=0.002), whereas statistical significance was attenuated in female rats (p=0.03). This may be indicative of a sex difference in sensitivity or responsivity to LiCl, despite females consuming more LiCl relative to their body mass. When comparing the percent change in TCr, with LiCl versus without LiCl, and with both -CrM and +CrM included in the model, we find that LiCl led to a ~12% increase in males, whereas females only had a ~7% increase, though this was not statistically significant (p=0.18).

Male rats consumed more absolute LiCl, but less relative to their body weight compared to females, irrespective of CrM. This additionally suggests a potential greater response in the males, despite consuming less LiCl relative to their size, as they had a more robust response in TCr in both lithium groups compared to control. Furthermore, the females consumed significantly greater amounts of CrM relative to their body weight than males, irrespective of LiCl. This suggests the possibility that the benefit of increased brain [TCr] was saturated with the CrM consumption in the females, and the benefit of LiCl was potentially masked.

In the study previously discussed by Dechent et al., 1999, the two male subjects demonstrated smaller changes in TCr concentrations with a 3.5-5.8% change, compared to the females who had a 8.6-13.3% change. Despite this observation, they did not further investigate whether this difference was due to hormonal factors or if the lesser response in the males was due to their higher body mass (80.5 kg) compared to the females (64.0 kg). This further supports the current suggestion of lithium eliciting a higher response in male brain TCr concentrations as Dechent et al., 1999, only supplemented with CrM resulting in a higher response in females.

A previous study conducted by our lab reported TCr sex differences in tissues other than the brain. White gastrocnemius (WGAS) TCr concentrations were increased in female rats following 8 weeks of 5g/L CrM supplementation (Dunham et al., 2021). There were no differences observed for females fed 2.5g/L or 10g/L CM. Male WGAS TCr concentrations were not observed to be responsive to CrM at any of these doses. Furthermore, female TCr concentrations in cardiac tissue (HRT) responded to both 5g/L and 10g/L supplementation, while no response was observed in males (Dunham et al., 2021). This suggests a potential greater response among females to CrM in tissues other than the brain. The reasoning for these potential sex difference responses to CrM and LiCl is currently unknown and future work is warranted.

### 4.3. Lithium's role in CRT regulation

Findings in the current study present an interesting finding in the expression of the creatine transporter gene (slc6a8), with LiCl consumption resulting in a trend for increased expression ($p=0.12$), irrespective of CrM. There was also a trend for gene expression between the Li and Cr females, with the Li group trending higher ($p=0.06$). Greater expression of the CRT gene could suggest higher levels of CRT expression or activity through interaction with GSK3. It is therefore possible that supplementation with lithium can inhibit the activation of GSK3, which in turn leads to an increased expression of the transporter gene. This is further supported by the current GSK3 activity data, with a trend for LiCl consumption having decreased activity ($p=0.11$), irrespective of CrM.

A study conducted by Fezai et al., 2016, investigated the relationship between GSK3β and the CRT in a Xenopous laevis oocyte model. PKB/Akt, a known inhibitor of GSK3β through phosphorylation, was examined further, as well as the effects of lithium. In *Xenopus laevis* oocytes expressing CRT, GSK3β in its active form resulted in a decreased creatine induced current,

suggesting decreased transport. Further exposing these cells to 24h of lithium significantly increased the creatine generated current, suggesting increased transport (Fezai et al., 2016). The downregulation effect of GSK3β on CRT was determined to be reversed by treatment with lithium (Fezai et al., 2016). This is therefore supportive of the current data suggesting Li supplementation results in a possible upregulation of slc6a8, through suppression of GSK3.

At the protein level for GSK3 isoforms, there was differences observed in content with supplementation. LiCl fed rats had greater protein levels of pGSK3β and the ratio of pGSK3β:GSK3β, irrespective of CrM. There was also increased pGSK3α content, and a greater ratio of pGSK3α:GSK3α with the presence of LiCl. This is supportive of Li leading to diminished activity of GSK3 at the protein level, as GSK3 becomes inactive in its phosphorylated state for both α and β isoforms.

CrM also appeared to have an effect on pGSKα and the ratio of pGSK3α:GSK3α as supplementation with CrM led to increases in these protein levels irrespective of LiCl. This suggests that CrM may also play a part in GSK3 inactivation, but this was only observed for the α isoform.

Collectively, these observations highlight the need for future work examining the relationship between GSK3 and the CRT, as there appears to be a downregulation effect based on the previous literature and current study. It is suggested that this effect can be further reversed by lithium, as lithium is a direct inhibitor of GSK3. Other than the current observations and the study done by Fezai et al., 2016, there is no other known work investigating this relationship. Future work may benefit from the use of a larger sample size providing more statistical power for the gene measurements, and future work should also include protein and transport measurements. Past work has been cast in doubt in regard to CRT protein expression however, as there has been

difficulty in establishing an effective antibody for CRT (Tarnopolsky, Parshad, Walzel, Schlattner, & Wallimann, 2001).

### 4.4. Sex Differences in Consumption

Food and water consumption were measured three times weekly in the current investigation. Males consumed more absolute food and water compared to the females. This difference in absolute food and water consumption was expected due to the higher mass on average of the males. Similar differences in mass were previously reported in the work by Dunham et al., 2021, who also observed higher absolute food consumption in the males (Dunham et al., 2021). Despite the differences in absolute food intake, it was also reported in this study that females had a higher food intake relative to their body weight than males (Dunham et al., 2021). This was also observed in the current investigation. In the current study, we also observed higher relative water consumption in the females. This was not previously observed by Dunham et al., 2021, as no significant difference was determined. It was however, reported by McGivern et al., 1996, that female Sprague-Dawley rats housed in groups consumed more than males beginning at 6 weeks of age (McGivern, Henschel, Hutcheson, & Pangburn, 1996). They further ruled out gonadal steroids to be the cause of this observed sex difference through castration of males at birth (McGivern et al., 1996). Santollo et al., 2017, suggested sex difference in fluid intake may be related to the Renin-Angiotensin-Aldosterone-System (RAAS), more specifically angiotensin II (Santollo, 2017). Future work is recommended to explore this area further as there is conflicting data.

For both sexes, CON and Cr rats consumed more water than both Li and Cr-Li groups. There are several possibilities for the water consumption decline containing LiCl. The first possibility is due to the taste of the compound. Nachman et al., 1963, analyzed the drinking habits

of male albino rats with access to water containing various salts. Rats given a 10 minute trial of access to water containing LiCl drank significantly less after 2-3 minutes compared to control rats (Nachman, 1963). It was suggested that this may be due to an unpleasant aftertaste (Nachman, 1963). Since these findings, LiCl has been used as an unconditioned stimulus to establish taste aversion to other substances (Loy & Hall, 2002; Manuelian, Albanell, Rovai, Caja, & Guitart, 2015; Nachman & Ashe, 1973). Another possibility for the decreased consumption in drinking water containing LiCl may be due to feelings of nausea. In a follow-up study conducted by Nachman et al., 1973, they learned aversions to LiCl occurred with intraperitoneal, subcutaneous, and stomach tube administration of LiCl (Nachman & Ashe, 1973). This suggests taste may not be the reason for the avoidant behaviour as LiCl produced aversion regardless of administration. Another study examined the relationship between the area postrema (AP), an area of the brain associated with nausea and vomiting, and LiCl behaviour in rats. Changes in behaviour following LiCl supplementation in rats who were given lesions of their AP were observed. Typical responses associated with LiCl fed rats, such as lying on their belly and delayed stomach emptying, were decreased in rats with AP lesions. These behaviours are indicative of nausea in rats as they cannot vomit. This further suggests a potential nauseating aspect of LiCl, explaining its avoidance in the current study (Bernstein, Chavez, Allen, & Taylor, 1992).

The higher relative water consumption in females further led to them consuming more relative CrM and LiCl than their male counterparts, irrespective of LiCl. This difference in CrM consumption between sex was not previously observed in the study by Dunham, et al., 2021. It is recommended in future studies to control for the supplemented amount consumed. This could be achieved by using alternative administration techniques, such as intraperitoneal or subcutaneous administration based on the weight of each individual rat or using a pair-feeding model.

Post-supplementation body mass in the current study was different between the male groups. CON males were significantly heavier than both Li and Cr-Li groups. There was also a trend present between CON and Cr males, suggesting CON males may have weighed more on average. This may be related to the food consumption of the males, as CON males consumed more absolute food than both Li and Cr-Li groups. This is different from the females as there were no differences between female groups in weight or food consumption.

The lower weight and food consumption in male rats supplemented with LiCl may be due to a chain of events stemming from the disruption of circadian rhythms. GSK3β, which lithium is known to inhibit, phosphorylates several core clock proteins associated with maintaining circadian rhythm (Noguchi, Lo, Diemer, & Welsh, 2016). Due to this downstream effect, Li has been reported in several cell culture studies to increase the amplitude of circadian rhythms and further lengthen its period (Abe, Herzog, & Block, 2000; Johansson, Brask, Owe-Larsson, Hetta, & Lundkvist, 2011). Disruption of circadian rhythms, whether shortened or lengthened, can lead to reduced sleep and lower quality of sleep. This disruption can further lead to other health complications such as impaired cognitive function, altered hormonal function, and gastrointestinal complaints (Vitaterna, Takahashi, & Turek, 2001). Potential health complications associated with this disruption are a possibility leading to the decreased food and water consumption in the male rats of the current study. Another possibility of the lower consumption may be due to a lack of general physical activity in response to tiredness from low sleep quality. It is unknown whether this is the case for the current study as activity levels, cognition, hormone levels, and gastrointestinal function was not mentioned. There are also no known investigations examining this connection in a preclinical or clinical model.

## 4.5. Strengths and Limitations

There are several strengths to the current study. The first strength to recognize is the use of an already established dose of 5g/L CrM in rats. Previous work done by Dunham et al., 2021, examined various doses of CrM supplementation on TCr response in several tissues. It was concluded that 5g/L of CrM in water to effectively increase brain TCr concentrations in a rat model (Dunham et al., 2020). Further building off this past work with an *n* of 32, sample size in the current study was doubled for a total *n* of 64. This included 16 rats in each of the supplementation groups with 8 males and 8 females each. This increase in sample size allowed for higher statistical power in the current study. Also, longitudinal measurements of body mass, as well as food and water intake - three times weekly – allowed for growth and consumption to be closely monitored throughout the study. Another strength of the current work is the adolescent-aged model that underwent supplementation. Given the high incidence of TBIs experienced at this age, this is a potential target population in terms of clinical care. The capacity for developmental delay due to injury further makes the adolescent aged brain of importance when looking into preventative and treatment regimes. Inclusion of both male and female rats is another strength of the current investigation. Males and females differ biologically and often behaviourally. For clinical investigations to be conducted regarding supplementation, work is required *in vitro* and *in vivo* preclinical models. Without the inclusion of both sexes in the current model, future work is less likely to move towards a clinical model due to the differences between sex in medicine. Sex differences affect the manifestation, pathophysiology, and epidemiology of injuries and diseases. The inclusion of both males and females is therefore more effective than a *one size fits all* approach.

There are several areas of limitation in the current investigation. The first being that serum lithium concentrations following supplementation were not determined. Previous studies involving

LiCl supplementation in rodent drinking water accounted for this measure to ensure the uptake of lithium into the bloodstream and possible tissues. Since this was not determined in the current study, the exact amount of lithium uptake cannot be confirmed. Lithium consumption can only be assumed based on the 0.2g/L lithium concentration in the drinking water and consumption of water recorded per cage. Rats in the current study were housed in pairs due to their social nature and reduced stress levels (Manuelian et al., 2015). This housing arrangement with *ad libitum* access to food and water requires acquiring cage consumption data, and assuming each rat consumed half the total amount. This negates the ability to determine outliers specific to the individual rat in terms of food and water consumption. It further leads to the assumption that the CrM/LiCl consumption was equal between the cage pairs based on water consumption. However, housing rats alone is considered unethical due to the levels of stress that are produced when isolated. A possible way to control for the supplement amount consumed in the future is to do so through intraperitoneal or subcutaneous injection.

Another limitation of this investigation was related to the measurements for the CRT. Although the gene expression of slc6a8 was determined using RT-PCR, this likely does not directly reflect the amount or the activity of the actual transporters. The trend involving Li females expressing higher levels of the slc6a8 gene compared to the Cr group does not necessarily reflect the actual transporter number or activity. However, it does suggest that LiCl may influence the expression of slc6a8 and further research is warranted, more specifically examination of the CRT at the protein level.

### 4.6. Influence of Chloride on CRT

The CRT is a sodium-chloride (NaCl) cotransporter that transports 2 sodium ($Na^+$) and 1 chloride ($Cl^-$) along with every Cr that enters the cell (Li et al., 2010). Supplementation with LiCl

in the current study may have had an effect on the CRT due to the chloride present in some of the groups. It is unclear if increasing chloride intake through LiCl may promote Cr transport into the brain through CRT. A previous study by Peral, Vázquez-Carretero, & Ilundain, (2010), determined the CRT in rat synaptosomes to be NaCl dependent, as the presence of both ions were required in the incubation buffer for the transporter to function. They also demonstrated the CRT to be electrogenic, as its activity was inhibited by a decrease in voltage across the membrane (Peral et al., 2010). Although this is the first study examining LiCl supplementation on brain Cr, it is recommended for future work to examine Li coupled to several different molecules to see if the increased availability of $Cl^-$ plays a role by increasing Cr transport.

## 4.7. Conclusions and Future Work

In conclusion, this study is the first pre-clinical *in vivo* model to show that supplementation with LiCl significantly increased brain TCr concentrations. Furthermore, this study demonstrated that the combination of CrM and LiCl supplementation can increase TCr, but not in an additive or synergistic manner. Although CrM supplementation has demonstrated potential protective effects in hypoxic situations, Li supplementation may also offer similar benefits. Dietary supplementation of LiCl inhibited GSK3 activity through an increase in pGSK3β and pGSK3α, and trended with reduced total GSK3 activity ($p=0.12$). The increases in TCr with LiCl was presumably due to a reduction in GSK3 activation, possibly influencing CRT, as we also observed a trend for increased CRT gene expression with LiCl. Our observations suggest that a decrease in GSK3 activity may be at least partially underlying the increase in TCr.

The current work highlights the need to further explore the possible protective effects of increase in brain TCr concentrations by Cr, Li, and co-supplementation of Cr-Li during hypoxic

and traumatic brain situations. Future work should continue to examine sex differences in response to CrM and LiCl, as well as sex differences observed in reported consumption data.

# References

Abe, M., Herzog, E. D., & Block, G. D. (2000). Lithium lengthens the circadian period of individual suprachiasmatic nucleus neurons. *NeuroReport*, *11*(14), 3261–3264. https://doi.org/10.1097/00001756-200009280-00042

Agoston, D. V. (2017, March 17). How to translate time? The temporal aspect of human and rodent biology. *Frontiers in Neurology*. Frontiers Research Foundation. https://doi.org/10.3389/fneur.2017.00092

Allahyar, R., Akbar, A., & Iqbal, F. (2017). Effect of creatine monohydrate supplementation on learning, memory and neuromuscular coordination in female albino mice. *Acta Neuropsychiatrica*, *29*(1), 27–34. https://doi.org/10.1017/neu.2016.28

Alraddadi, E. A., Lillico, R., Vennerstrom, J. L., Lakowski, T. M., & Miller, D. W. (2018). Absolute oral bioavailability of creatine monohydrate in rats: Debunking a myth. *Pharmaceutics*, *10*(1), 1–13. https://doi.org/10.3390/pharmaceutics10010031

Andres, R. H., Ducray, A. D., Schlattner, U., Wallimann, T., & Widmer, H. R. (2008). Functions and effects of creatine in the central nervous system. *Brain Research Bulletin*, *76*(4), 329–343. https://doi.org/10.1016/j.brainresbull.2008.02.035

Annoni, F., Peluso, L., Bogossian, E. G., Creteur, J., Zanier, E. R., & Taccone, F. S. (2021). Brain protection after anoxic brain injury: Is lactate supplementation helpful? *Cells*, *10*(7), 1–11. https://doi.org/10.3390/cells10071714

Antonio, J., Candow, D. G., Forbes, S. C., Gualano, B., Jagim, A. R., Kreider, R. B., … Ziegenfuss, T. N. (2021, February 8). Common questions and misconceptions about creatine supplementation: what does the scientific evidence really show? *Journal of the International Society of Sports Nutrition*. BioMed Central. https://doi.org/10.1186/s12970-

021-00412-w

Arain, M., Haque, M., Johal, L., Mathur, P., Nel, W., Rais, A., … Sharma, S. (2013). Maturation of the adolescent brain. *Neuropsychiatric Disease and Treatment*. Dove Press. https://doi.org/10.2147/NDT.S39776

Balestrino, M. (2021, April 1). Role of creatine in the heart: Health and disease. *Nutrients*. Multidisciplinary Digital Publishing Institute (MDPI). https://doi.org/10.3390/nu13041215

Barth, J. T., Freeman, J. R., Broshek, D. K., & Varney, R. N. (2001). Acceleration-Deceleration Sport-Related Concussion: The Gravity of It All. *Journal of Athletic Training*, *36*(3), 253–256. Retrieved from www.journalofathletictraining.org

Bernstein, I. L., Chavez, M., Allen, D., & Taylor, E. M. (1992). Area postrema mediation of physiological and behavioral effects of lithium chloride in the rat. *Brain Research*, *575*(1), 132–137. https://doi.org/10.1016/0006-8993(92)90432-9

Borchel, A., Verleih, M., Kühn, C., Rebl, A., & Goldammer, T. (2019). Evolutionary expression differences of creatine synthesis-related genes: Implications for skeletal muscle metabolism in fish. *Scientific Reports*, *9*(1), 5429. https://doi.org/10.1038/s41598-019-41907-6

Braissant, O. (2012). Creatine and guanidinoacetate transport at blood-brain and blood-cerebrospinal fluid barriers. *Journal of Inherited Metabolic Disease*, *35*(4), 655–664. https://doi.org/10.1007/s10545-011-9433-2

Brasure, M., Lamberty, G. J., Sayer, N. A., Nelson, N. W., MacDonald, R., Ouellette, J., … Wilt, T. J. (2012). Executive Summary. Retrieved from https://www.ncbi.nlm.nih.gov/books/NBK98999/

Brekke, T. D., Steele, K. A., & Mulley, J. F. (2018). Inbred or outbred? Genetic diversity in laboratory rodent colonies. *G3: Genes, Genomes, Genetics*, *8*(2), 679–686.

https://doi.org/10.1534/g3.117.300495

Brosnan, J. T., da Silva, R. P., & Brosnan, M. E. (2011, May 9). The metabolic burden of creatine synthesis. *Amino Acids*. Springer. https://doi.org/10.1007/s00726-011-0853-y

Brosnan, M. E., & Brosnan, J. T. (2016). The role of dietary creatine. *Amino Acids*, *48*(8), 1785–1791. https://doi.org/10.1007/s00726-016-2188-1

Bulmer, T., Volders, D., & Kamal, N. (2021). Analysis of Thrombolysis Process for Acute Ischemic Stroke in Urban and Rural Hospitals in Nova Scotia Canada. *Frontiers in Neurology*, *12*(March), 1–15. https://doi.org/10.3389/fneur.2021.645228

Caffes, N., Kurland, D. B., Gerzanich, V., & Marc Simard, J. (2015). Glibenclamide for the treatment of ischemic and hemorrhagic stroke. *International Journal of Molecular Sciences*. https://doi.org/10.3390/ijms16034973

Casey, B. J., Jones, R. M., & Hare, T. A. (2008). The adolescent brain. *Annals of the New York Academy of Sciences*, *1124*, 111–126. https://doi.org/10.1196/annals.1440.010

Centers for Disease Control and Prevention. (2019). TBI: Get the Facts | Concussion | Traumatic Brain Injury | CDC Injury Center. *U.S. Department of Health & Human Services*, 1–3. Retrieved from https://www.cdc.gov/traumaticbraininjury/get_the_facts.html

Chen, H. R., Zhang-Brotzge, X., Morozov, Y. M., Li, Y., Wang, S., Zhang, H. H., … Kuan, C. Y. (2021). Creatine transporter deficiency impairs stress adaptation and brain energetics homeostasis. *JCI Insight*, *6*(17). https://doi.org/10.1172/jci.insight.140173

Chen, S., Zeng, L., & Hu, Z. (2014). Progressing haemorrhagic stroke: categories, causes, mechanisms and managements. *Journal of Neurology*. https://doi.org/10.1007/s00415-014-7291-1

Choi, S. E., Jang, H. J., Kang, Y., Jung, J. G., Han, S. J., Kim, H. J., … Lee, K. W. (2010).

Atherosclerosis induced by a high-fat diet is alleviated by lithium chloride via reduction of VCAM expression in ApoE-deficient mice. *Vascular Pharmacology*, *53*(5–6), 264–272. https://doi.org/10.1016/j.vph.2010.09.004

Christensen, J., Eyolfson, E., Salberg, S., & Mychasiuk, R. (2021). Traumatic brain injury in adolescence: A review of the neurobiological and behavioural underpinnings and outcomes. *Developmental Review*, *59*, 100943. https://doi.org/10.1016/J.DR.2020.100943

Christie, D. L. (2007). Functional insights into the creatine transporter. *Subcellular Biochemistry*, *46*, 99–118. https://doi.org/10.1007/978-1-4020-6486-9_6

Cooper, R., Naclerio, F., Allgrove, J., & Jimenez, A. (2012, July 20). Creatine supplementation with specific view to exercise/sports performance: An update. *Journal of the International Society of Sports Nutrition*. BioMed Central. https://doi.org/10.1186/1550-2783-9-33

da Silva, R. P., Nissim, I., Brosnan, M. E., & Brosnan, J. T. (2009). Creatine synthesis: hepatic metabolism of guanidinoacetate and creatine in the rat in vitro and in vivo. *American Journal of Physiology-Endocrinology and Metabolism*, *296*(2), E256–E261. https://doi.org/10.1152/ajpendo.90547.2008

Dechent, P., Pouwels, P. J. W., Wilken, B., Hanefeld, F., & Frahm, J. (1999). Increase of total creatine in human brain after oral supplementation of creatine-monohydrate. *American Journal of Physiology - Regulatory Integrative and Comparative Physiology*, *277*(3 46-3). https://doi.org/10.1152/ajpregu.1999.277.3.r698

Dewan, M. C., Mummareddy, N., Wellons, J. C., & Bonfield, C. M. (2016). Epidemiology of Global Pediatric Traumatic Brain Injury: Qualitative Review. *World Neurosurgery*, *91*, 497-509.e1. https://doi.org/10.1016/j.wneu.2016.03.045

Dunham, T. C., Murphy, J. E., MacPherson, R. E. K., Fajardo, V. A., Ward, W. E., & Roy, B. D.

(2021). Sex- and tissue-dependent creatine uptake in response to different creatine monohydrate doses in male and female Sprague-Dawley rats. *Applied Physiology, Nutrition, and Metabolism*, 1–16. https://doi.org/10.1139/apnm-2021-0301

Dunham, T., Murphy, J., Colonna, K., Fajardo, V., MacPherson, R., Ward, W., & Roy, B. (2020). The Effect of Creatine Monohydrate Supplementation on Tissue Creatine Concentrations in Male and Female Rats. *The FASEB Journal*, *34*(S1), 1–1. https://doi.org/10.1096/fasebj.2020.34.s1.04833

Dunn, J., & Grider, M. H. (2020). *Physiology, Adenosine Triphosphate (ATP)*. *StatPearls*. StatPearls Publishing. Retrieved from http://www.ncbi.nlm.nih.gov/pubmed/31985968

Fezai, M., Jemaà, M., Fakhri, H., Chen, H., Elsir, B., Pelzl, L., & Lang, F. (2016). Down-Regulation of the Na + ,Cl - Coupled Creatine Transporter CreaT (SLC6A8) by Glycogen Synthase Kinase GSK3ß. *Cellular Physiology and Biochemistry*, *40*(5), 1231–1238. https://doi.org/10.1159/000453177

Freland, L., & Beaulieu, J.-M. (2012). Inhibition of GSK3 by lithium, from single molecules to signaling networks. *Frontiers in Molecular Neuroscience*, *5*, 14. https://doi.org/10.3389/fnmol.2012.00014

Fu, T. S., Jing, R., McFaull, S. R., & Cusimano, M. D. (2015). Recent trends in hospitalization and in-hospital mortality associated with traumatic brain injury in Canada: A nationwide, population-based study. *The Journal of Trauma and Acute Care Surgery*, *79*(3), 449–454. Retrieved from http://www.ncbi.nlm.nih.gov/pubmed/26535433

Galgano, M., Toshkezi, G., Qiu, X., Russell, T., Chin, L., & Zhao, L. R. (2017, July 1). Traumatic brain injury: Current treatment strategies and future endeavors. *Cell Transplantation*. SAGE Publications Ltd. https://doi.org/10.1177/0963689717714102

Ginsburg, J., & Huff, J. S. (2011). Closed Head Trauma. In *Encyclopedia of Child Behavior and Development* (pp. 374–374). Springer US. https://doi.org/10.1007/978-0-387-79061-9_6270

Giza, C. C., & Hovda, D. A. (2001a). The Neurometabolic Cascade of Concussion. *Journal of Athletic Training*, *36*(3), 228–235. Retrieved from http://www.ncbi.nlm.nih.gov/pubmed/12937489

Giza, C. C., & Hovda, D. A. (2001b). The Neurometabolic Cascade of Concussion. *Journal of Athletic Training*, *36*(3), 228–235. Retrieved from http://www.ncbi.nlm.nih.gov/pubmed/12937489

Giza, C. C., & Hovda, D. A. (2014). The new neurometabolic cascade of concussion. *Neurosurgery*, *75*, S24–S33. https://doi.org/10.1227/NEU.0000000000000505

Guimarães-Ferreira, L. (2014). Role of the phosphocreatine system on energetic homeostasis in skeletal and cardiac muscles. *Einstein (Sao Paulo, Brazil)*, *12*(1), 126–131. https://doi.org/10.1590/S1679-45082014RB2741

Hamstra, S. I., Kurgan, N., Baranowski, R. W., Qiu, L., Watson, C. J. F., Messner, H. N., … Fajardo, V. A. (2020). Low-dose lithium feeding increases the SERCA2a-to-phospholamban ratio, improving SERCA function in murine left ventricles. *Experimental Physiology*, *105*(4), 666–675. https://doi.org/10.1113/EP088061

Hanna-El-Daher, L., & Braissant, O. (2016). Creatine synthesis and exchanges between brain cells: What can be learned from human creatine deficiencies and various experimental models? *Amino Acids*, *48*(8), 1877–1895. https://doi.org/10.1007/s00726-016-2189-0

Hedya, S. A., Avula, A., & Swoboda, H. D. (2020). *Lithium Toxicity*. *StatPearls*. StatPearls Publishing. Retrieved from http://www.ncbi.nlm.nih.gov/pubmed/29763168

Ilie, G., Trenholm, M., Boak, A., Mann, R. E., Adlaf, E. M., Asbridge, M., … Cusiman, M. D.

(2020). Adolescent traumatic brain injuries: Onset, mechanism and links with current academic performance and physical injuries. *PLoS ONE*, *15*(3). https://doi.org/10.1371/journal.pone.0229489

Ipsiroglu, O. S., Stromberger, C., Ilas, J., Höger, H., Mühl, A., & Stöckler-Ipsiroglu, S. (2001). Changes of tissue creatine concentrations upon oral supplementation of creatine-monohydrate in various animal species. *Life Sciences*, *69*(15), 1805–1815. https://doi.org/10.1016/S0024-3205(01)01268-1

Ishii, N., & Terao, T. (2018). Trace lithium and mental health. *Journal of Neural Transmission*, *125*(2), 223–227. https://doi.org/10.1007/S00702-017-1824-6

Iverson, L., & Bryan, J. (2020). Glasgow Coma Scale Issues of Concern Clinical Signi cance, 1–5. Retrieved from https://pubmed.ncbi.nlm.nih.gov/30020670/

Jäger, R., Purpura, M., Shao, A., Inoue, T., & Kreider, R. B. (2011). Analysis of the efficacy, safety, and regulatory status of novel forms of creatine. *Amino Acids*. https://doi.org/10.1007/s00726-011-0874-6

Jivan, K., Ranchod, K., & Modi, G. (2013). Management of ischaemic stroke in the acute setting: Review of the current status. *Cardiovascular Journal of Africa*. https://doi.org/10.5830/CVJA-2013-001

Johansson, A. S., Brask, J., Owe-Larsson, B., Hetta, J., & Lundkvist, G. B. S. (2011). Valproic acid phase shifts the rhythmic expression of PERIOD2::LUCIFERASE. *Journal of Biological Rhythms*, *26*(6), 541–551. https://doi.org/10.1177/0748730411419775

Kelly-Hayes, M. (2010). Influence of age and health behaviors on stroke risk: Lessons from longitudinal studies. *Journal of the American Geriatrics Society*. https://doi.org/10.1111/j.1532-5415.2010.02915.x

Kurgan, N., Bott, K. N., Helmeczi, W. E., Roy, B. D., Brindle, I. D., Klentrou, P., & Fajardo, V. A. (2019). Low dose lithium supplementation activates Wnt/β-catenin signalling and increases bone OPG/RANKL ratio in mice. *Biochemical and Biophysical Research Communications*, *511*(2), 394–397. https://doi.org/10.1016/J.BBRC.2019.02.066

Langlois, J.; Rutland-Brown, W.; Thomas, K. (2006). Traumatic Brain Injury in the United States: Emergency Department Visits, Hospitalizations, and Deaths. *Centers for Disease Control and Prevention, National Center for Injury Prevention and Control*, *2*. Retrieved from /http://www.cdc.gov/ncipc/factsheets/tbi.htmS.

Lee, B., & Newberg, A. (2005). Neuroimaging in traumatic brain imaging. *NeuroRx*, *2*(2), 372–383. https://doi.org/10.1602/neurorx.2.2.372

Li, H., Thali, R. F., Smolak, C., Gong, F., Alzamora, R., Wallimann, T., … Hallows, K. R. (2010a). Regulation of the creatine transporter by AMP-activated protein kinase in kidney epithelial cells. *American Journal of Physiology-Renal Physiology*, *299*(1), F167–F177. https://doi.org/10.1152/ajprenal.00162.2010

Li, H., Thali, R. F., Smolak, C., Gong, F., Alzamora, R., Wallimann, T., … Hallows, K. R. (2010b). Regulation of the creatine transporter by AMP-activated protein kinase in kidney epithelial cells. *American Journal of Physiology - Renal Physiology*, *299*(1). https://doi.org/10.1152/AJPRENAL.00162.2010

Liang, M. H., & Chuang, D. M. (2006). Differential roles of glycogen synthase kinase-3 isoforms in the regulation of transcriptional activation. *Journal of Biological Chemistry*, *281*(41), 30479–30484. https://doi.org/10.1074/jbc.M607468200

Livak, K. J., & Schmittgen, T. D. (2001). Analysis of relative gene expression data using real-time quantitative PCR and the 2-ΔΔCT method. *Methods*, *25*(4), 402–408.

https://doi.org/10.1006/meth.2001.1262

Loy, I., & Hall, G. (2002). Taste aversion after ingestion of lithium chloride: An associative analysis. *Quarterly Journal of Experimental Psychology Section B: Comparative and Physiological Psychology*, *55*(4), 365–380. https://doi.org/10.1080/02724990244000070

Manuelian, C. L., Albanell, E., Rovai, M., Caja, G., & Guitart, R. (2015). Kinetics of lithium as a lithium chloride dose suitable for conditioned taste aversion in lactating goats and dry sheep. *Journal of Animal Science*, *93*(2), 562–569. https://doi.org/10.2527/jas.2014-8223

Marsh, J. D., & Keyrouz, S. G. (2010). Stroke prevention and treatment. *Journal of the American College of Cardiology*, *56*(9), 683–691. https://doi.org/10.1016/j.jacc.2009.12.072

McGivern, R. F., Henschel, D., Hutcheson, M., & Pangburn, T. (1996). Sex difference in daily water consumption of rats: Effect of housing and hormones. *Physiology and Behavior*, *59*(4–5), 653–658. https://doi.org/10.1016/0031-9384(95)02017-9

Menon, D. K., Schwab, K., Wright, D. W., & Maas, A. I. (2010). Position statement: Definition of traumatic brain injury. *Archives of Physical Medicine and Rehabilitation*, *91*(11), 1637–1640. https://doi.org/10.1016/j.apmr.2010.05.017

Mitchell, P. B. (2000). Therapeutic drug monitoring of psychotropic medications. *British Journal of Clinical Pharmacology*, *49*(4), 303. https://doi.org/10.1046/J.1365-2125.2000.00174.X

Nachman, M. (1963). Learned aversion to the taste of lithium chloride and generalization to other salts. *Journal of Comparative and Physiological Psychology*, *56*(2), 343–349. https://doi.org/10.1037/h0046484

Nachman, M., & Ashe, J. H. (1973). Learned taste aversions in rats as a function of dosage, concentration, and route of administration of LiCl. *Physiology and Behavior*, *10*(1), 73–78. https://doi.org/10.1016/0031-9384(73)90089-9

Naidech, A. M. (2011). Intracranial hemorrhage. *American Journal of Respiratory and Critical Care Medicine*, *184*(9), 998–1006. https://doi.org/10.1164/rccm.201103-0475CI

Navis, A., Garcia-Santibanez, R., & Skliut, M. (2019). Epidemiology and Outcomes of Ischemic Stroke and Transient Ischemic Attack in the Adult and Geriatric Population. *Journal of Stroke and Cerebrovascular Diseases*, *28*(1), 84–89. https://doi.org/10.1016/j.jstrokecerebrovasdis.2018.09.013

Noguchi, T., Lo, K., Diemer, T., & Welsh, D. K. (2016). Lithium effects on circadian rhythms in fibroblasts and suprachiasmatic nucleus slices from Cry knockout mice. *Neuroscience Letters*, *619*, 49–53. https://doi.org/10.1016/j.neulet.2016.02.030

Ohtsuki, S., Tachikawa, M., Takanaga, H., Shimizu, H., Watanabe, M., Hosoya, K. ichi, & Terasaki, T. (2002). The blood-brain barrier creatine transporter is a major pathway for supplying creatine to the brain. *Journal of Cerebral Blood Flow and Metabolism*, *22*(11), 1327–1335. https://doi.org/10.1097/01.WCB.0000033966.83623.7D

Olivieri, B., Rampakakis, E., Gilbert, G., Fezoua, A., & Wintermark, P. (2021). Myelination may be impaired in neonates following birth asphyxia. *NeuroImage: Clinical*, *31*, 102678. https://doi.org/10.1016/j.nicl.2021.102678

Peral, M. J., Vázquez-Carretero, M. D., & Ilundain, A. A. (2010). Na+/Cl-/creatine transporter activity and expression in rat brain synaptosomes. *Neuroscience*, *165*(1), 53–60. https://doi.org/10.1016/j.neuroscience.2009.10.001

Petrea, R. E., Beiser, A. S., Seshadri, S., Kelly-Hayes, M., Kase, C. S., & Wolf, P. A. (2009). Gender differences in stroke incidence and poststroke disability in the framingham heart study. *Stroke*, *40*(4), 1032–1037. https://doi.org/10.1161/STROKEAHA.108.542894

Prass, K., Royl, G., Lindauer, U., Freyer, D., Megow, D., Dirnagl, U., … Priller, J. (2007).

Improved reperfusion and neuroprotection by creatine in a mouse model of stroke. *Journal of Cerebral Blood Flow and Metabolism*, *27*(3), 452–459. https://doi.org/10.1038/sj.jcbfm.9600351

Press, P. (1987). Newton ' s Third Law and Universal Gravity Author ( s ): I . Bernard Cohen Source : Journal of the History of Ideas , Oct . - Dec ., 1987 , Vol . 48 , No . 4 ( Oct . - Dec ., Published by : University of Pennsylvania Press Stable URL : https://www.jstor.o, *48*(4), 571–593.

Prince, C., & Bruhns, M. (2017). Evaluation and Treatment of Mild Traumatic Brain Injury: The Role of Neuropsychology. *Brain Sciences*, *7*(8), 105. https://doi.org/10.3390/brainsci7080105

Rae, C., Digney, A. L., McEwan, S. R., & Bates, T. C. (2003). Oral creatine monohydrate supplementation improves brain performance: A double-blind, placebo-controlled, cross-over trial. *Proceedings of the Royal Society B: Biological Sciences*, *270*(1529), 2147–2150. https://doi.org/10.1098/rspb.2003.2492

Randolph, S. A. (2016). Ischemic Stroke. *Workplace Health and Safety*, *64*(9), 444. https://doi.org/10.1177/2165079916665400

Saab, A. S., Tzvetanova, I. D., & Nave, K. A. (2013). The role of myelin and oligodendrocytes in axonal energy metabolism. *Current Opinion in Neurobiology*, *23*(6), 1065–1072. https://doi.org/10.1016/J.CONB.2013.09.008

Santollo, J. (2017). Sex differences in angiotensin II-stimulated fluid intake. *Experimental Physiology*, *102*(11), 1380–1384. https://doi.org/10.1113/EP086518

Schlattner, U., Tokarska-Schlattner, M., & Wallimann, T. (2013). Metabolite Channeling: Creatine Kinase Microcompartments. In *Encyclopedia of Biological Chemistry* (pp. 80–85).

Elsevier. https://doi.org/10.1016/B978-0-12-378630-2.00283-8

Schlattner, Uwe, Tokarska-Schlattner, M., & Wallimann, T. (2006, February 1). Mitochondrial creatine kinase in human health and disease. *Biochimica et Biophysica Acta - Molecular Basis of Disease*. Elsevier. https://doi.org/10.1016/j.bbadis.2005.09.004

Schrauzer, G. N. (2002). Lithium: Occurrence, Dietary Intakes, Nutritional Essentiality. *Journal of the American College of Nutrition*, *21*(1), 14–21. https://doi.org/10.1080/07315724.2002.10719188

Sennfält, S., Norrving, B., Petersson, J., & Ullberg, T. (2019). Long-Term Survival and Function after Stroke: A Longitudinal Observational Study from the Swedish Stroke Register. *Stroke*, *50*(1), 53–61. https://doi.org/10.1161/STROKEAHA.118.022913

Shah, M. K., Al-Adawi, S., Dorvlo, A. S. S., Burke, D. T., S H A H Y, Samir A L -A D A W I Yz, R. K., & Dorvlo} A N D D A V I, A. S. S. (2004). Brain Injury Functional outcomes following anoxic brain injury: a comparison with traumatic brain injury Functional outcomes following anoxic brain injury: a comparison with traumatic brain injury. *BRAIN INJURY*, *18*(2), 111–117. https://doi.org/10.1080/0269905031000149551

Silverberg, N. D., Iaccarino, M. A., Panenka, W. J., Iverson, G. L., McCulloch, K. L., Dams-O'Connor, K., … Weyer Jamora, C. (2020). Management of Concussion and Mild Traumatic Brain Injury: A Synthesis of Practice Guidelines. *Archives of Physical Medicine and Rehabilitation*, *101*(2), 382–393. https://doi.org/10.1016/j.apmr.2019.10.179

Sullivan, P. G., Geiger, J. D., Mattson, M. P., & Scheff, S. W. (2000). Dietary supplement creatine protects against traumatic brain injury. *Annals of Neurology*, *48*(5), 723–729. https://doi.org/10.1002/1531-8249(200011)48:5<723::AID-ANA5>3.0.CO;2-W

Tarnopolsky, M. A., & Parise, G. (1999). Direct measurement of high-energy phosphate

compounds in patients with neuromuscular disease. *Muscle & Nerve*, *22*(9), 1228–1233. https://doi.org/10.1002/(sici)1097-4598(199909)22:9<1228::aid-mus9>3.3.co;2-y

Tarnopolsky, M. A., Parshad, A., Walzel, B., Schlattner, U., & Wallimann, T. (2001). Creatine transporter and mitochondrial creatine kinase protein content in myopathies. *Muscle and Nerve*, *24*(5), 682–688. https://doi.org/10.1002/mus.1055

The Government of Canada. (2014). *Mapping Connections an Understanding of Neurological Conditions*. Ottawa. Retrieved from http://publications.gc.ca/collections/collection_2014/aspc-phac/HP35-45-2014-eng.pdf

Timothy O'Brien, W., & Klein, P. S. (2009). Validating GSK3 as an in vivo target of lithium action: Table 1 . *Biochemical Society Transactions*, *37*(5), 1133–1138. https://doi.org/10.1042/bst0371133

Turner, C. E., Byblow, W. D., & Gant, N. N. (2015a). Creatine Supplementation Enhances Corticomotor Excitability and Cognitive Performance during Oxygen Deprivation. *Journal of Neuroscience*, *35*(4), 1773–1780. https://doi.org/10.1523/JNEUROSCI.3113-14.2015

Turner, C. E., Byblow, W. D., & Gant, N. N. (2015b). Creatine Supplementation Enhances Corticomotor Excitability and Cognitive Performance during Oxygen Deprivation. *Journal of Neuroscience*, *35*(4), 1773–1780. https://doi.org/10.1523/JNEUROSCI.3113-14.2015

Unnithan, A. K. A., & Mehta, P. (2021). Hemorrhagic Stroke. *StatPearls*. Retrieved from https://www.ncbi.nlm.nih.gov/books/NBK559173/

Vitaterna, M. H., Takahashi, J. S., & Turek, F. W. (2001). Overview of circadian rhythms. *Alcohol Research & Health : The Journal of the National Institute on Alcohol Abuse and Alcoholism*, *25*(2), 85–93. Retrieved from https://pubmed.ncbi.nlm.nih.gov/11584554

Whiteneck, G. G., Cuthbert, J. P., Corrigan, J. D., & Bogner, J. A. (2016). Prevalence of Self-

Reported Lifetime History of Traumatic Brain Injury and Associated Disability. *Journal of Head Trauma Rehabilitation*, *31*(1), E55–E62. https://doi.org/10.1097/HTR.0000000000000140

Whitley, K. C., Hamstra, S. I., Baranowski, R. W., Watson, C. J. F., MacPherson, R. E. K., MacNeil, A. J., … Fajardo, V. A. (2020). GSK3 inhibition with low dose lithium supplementation augments murine muscle fatigue resistance and specific force production. *Physiological Reports*, *8*(14). https://doi.org/10.14814/phy2.14517

Wyss, M., & Kaddurah-Daouk, R. (2000). Creatine and Creatinine Metabolism. *Physiological Reviews*, *80*(3), 1107–1213. https://doi.org/10.1152/physrev.2000.80.3.1107

Yew, K. S., & Cheng, E. (2009a). Acute stroke diagnosis. *American Family Physician*, *80*(1), 33–40. Retrieved from http://www.ncbi.nlm.nih.gov/pubmed/19621844

Yew, K. S., & Cheng, E. (2009b). Acute stroke diagnosis. *American Family Physician*. Retrieved from http://www.ninds.nih.gov/doctors/NIH_Stroke_Scale.pdf

# Appendix I: List of Reagents

| Reagent | Supplier | SKU |
|---|---|---|
| ADP - Adenosine 5′-diphosphate sodium salt | Millipore Sigma | A2754 |
| ATP - Adenosine 5′-triphosphate disodium salt hydrate | Millipore Sigma | A2383 |
| Bicinchoninic Acid solution | Millipore Sigma | B9643 |
| BCA - Bicinchoninic Acid | Millipore Sigma | B9643 |
| BSA - Bovine Serum Albumin | Millipore Sigma | A2153 |
| CHIR | Millipore Sigma | SML1094 |
| Chloroform | BDH | BDH1109-4LG |
| Creatine Kinase | Millipore Sigma | 10736988001 |
| Creatine Monohydrate | Millipore Sigma | C3630 |
| $CuSO_4$ - Sulfuric Acid | BioShop | CUS803 |
| DNA-free Kit | Invitrogen | AM1906 |
| DMSO - Dimethyl sulfoxide | Millipore Sigma | D2650 |
| D.T.T. - DL-Dithiothreitol | Millipore Sigma | 43815 |
| EGTA - Egtazic acid | Millipore Sigma | 4100 |
| G6PDH - Glucose-6-phosphate Dehydrogenase | Millipore Sigma | G8404 |
| Glucose | Millipore Sigma | G8270 |
| HEPES - 4-(2-hydroxyethyl)-1-piperazineethanesulfonic acid | Millipore Sigma | H3375 |
| Hexokinase | Millipore Sigma | H4502 |
| Imidazole | Millipore Sigma | I202 |
| KCl - Potassium chloride | Millipore Sigma | P3911 |

| | | |
|---|---|---|
| $KHCO_3$ - Potassium bicarbonate | Millipore Sigma | 60339 |
| LDH - L-Lactate Dehydrogenase | Millipore Sigma | 10127876001 |
| $MgCl_2$ - Magnesium chloride | Millipore Sigma | M8266 |
| NADH - 1,4-Dihydronicotinamide adenine dinucleotide | Millipore Sigma | 10128023001 |
| NADP - Nicotinamide adenine dinucleotide phosphate | Millipore Sigma | 10128040001 |
| $NaN_3$ - Sodium azide | Millipore Sigma | S2002 |
| PCr - Phosphocreatine disodium salt hydrate | Millipore Sigma | P7936 |
| PEP - Phospho(enol)pyruvic acid trisodium salt hydrate | Millipore Sigma | P7002 |
| PK - Pyruvate Kinase | Millipore Sigma | 10109045001 |
| Protein Standard (Bovine Serum Albumin) | Millipore Sigma | P0834-10X1ML |
| Random Primers | Invitrogen | 48190-011 |
| RNaseOUT | Invitrogen | 10777-019 |
| RNeasy Mini Kit (250) | Qiagen | 74106 |
| Sucrose | Millipore Sigma | S7903 |
| SuperScript II Reverse Transcriptase | Invitrogen | 18064-014 |
| Tris - Trizma® base | Millipore Sigma | T6066 |
| TRIzol | Ambion | 15596018 |
| Zirconia/Silica Beads (1mm) | BioSpec | 11079101z |
| 100mM dNTP Set | Invitrogen | 10297-018 |
| 2-Propanol | Fisher | A426P-4 |

# Appendix II: TCr Concentration

### Step 1: Tissue Lyophilization

1. Get samples from -80ºC storage.
2. Place tubes in column attached to Freeze dryer (*FreeZone 4.5, Labconco).*
3. Freeze dry samples for ~8h to remove any moisture.

### Step 2: Perchloric Acid Extraction

Reagents

0.5M Perchloric Acid (PCA) - Stored

1. Add 400mL of doubly distilled water to a beaker
2. Add 21.5mL of PCA *in fume hood*
3. Top up reagent to 500mL (by adding 78.5mL of doubly distilled water)
4. Transfer to storage container
5. Store in 0-4°C for 1 month

2.3M $KHCO_3$ - Make daily

1. Add 2.3g $KHCO_3$ to a container
2. Add 10mL of doubly distilled water
3. Mix by light vortex
4. Make fresh each day
5. Keep on ice after making

Procedure

1. Crush tissue into very small pieces/powder, using a weigh boat and tweezers
2. Tease out connective tissue and discard (for muscle)
3. Weigh 3-5mg of tissue into new centrifuge tube(s)
4. Add 600uL of precooled 0.5M PCA & place on ice
    a. Extract for 10 minutes while vortexing intermittently (e.g., every 2 mins)
        i. Shake tissue back into acid after vortexing
        ii. Tissue should appear grey in colour
5. Centrifuge for 10 minutes, 0°C at 15,000g
6. Remove 540uL supernatant and place at -20°C for 15 minutes to refreeze, in new tube(s)
7. Add 135uL of 2.3M KHCO3 to the FROZEN supernatant, then vortex until liquid
    a. PCA will precipitate out of solution and appear as a white cloud powder
    b. Open cap between vortexing
8. Centrifuge for 10 minutes, 0°C at 15,000g
9. Remove ~550uL of supernatant to assay metabolites
    a. Place in new tube for storage and store at -80ºC

**Step 3: Fluorometric Assays**

**ATP/PCr Assay**

$$PCr + ADP \xleftrightarrow{Creatine\ Kinase} Creatine + ATP$$

$$ATP + Glucose \xrightarrow{Hexokinase} ADP + Glucose-6-P$$

$$Glucose-6-P + NADP \xleftrightarrow{G6PDH} Glucanolactone + NADPH$$

| **Reagent** | **mg/mL** | **Stock Conc** | **Final Conc** | **V for 25ml** | **V for 50ml** | **V for 100ml** |
|---|---|---|---|---|---|---|
| 1. TRIS pH 8.1 | 121.140 | 1.0M | 50.0 mM | 1.25mL | 2.5mL | 5mL |
| 2. $MgCl_2$ | 95.210 | 1.0M | 1.0mM | 25uL | 50uL | 100uL |
| 3. D.T.T. | 77.125 | 0.50M | 0.5mM | 25uL | 50uL | 100uL |
| 4. Glucose | 18.016 | 100.0mM | 100uM | 25uL | 50uL | 100uL |
| 5. NADP | 39.369 | 50mM | 50uM | 25uL | 50uL | 100uL |
| | | | | | | |
| 6. G6PDH | | 350U/mL | 0.02U/mL | 2.5uL | 5uL | 10uL |
| | | | | | | |
| 7. Hexokinase | | 280U/mL | 0.14U/mL | | | |
| 8. ADP | | | | | | |
| 9. CK | | | 3.6U/mL | | | |
| | | | | | | |
| ATP Standard | 551.14g/mol | 50µM | | | | |
| PCr Standard | 255.08g/mol | 500µM | | 63.77mg in 500mL | | |
| 10% BSA | | >=98% | | 1g in 10mL | | |

<u>Steps Prior to Starting Assay</u>

Reagent

1. Locate pre-made reagents + make daily reagents in 1.5mL tubes
2. Add regents 1 to 5
3. Bring to volume with water (ex. 47.3mL for 50mL)

4. pH to 8.1
5. Add reagents 6

Dilute enzymes - **#1 HK**

1. Add 2mL of reagent
2. Add 10µL of HK and mix by inversion.

Dilute enzymes - **#2 CK**

1. Mix 3mL of reagent with 30uL of 10% BSA and 6mg ADP.
2. Add 6mg of CK to solution and mix by inversion.

Assay

1. Use 3 tubes for each sample, 3 tubes for 'standard' and 3 tubes for 'blanks'
2. Add water, ATP standard, PCr standard, or sample to respective tubes
    a. Add 10uL of doubly distilled water to 'blank' tubes.
    b. Add 10uL of 50uM ATP standard to 'ATP standard' tubes.
    c. Add 10uL of 500uM PCr standard to 'PCr standard' tubes.
    d. Add 10uL of sample to appropriate tubes.
3. Add 1mL dilute reagent to all tubes.
4. Cover with parafilm & gently vortex
5. Read as point 1 (R1) using fluorometer
6. Add 25uL of dilute hexokinase (**#1-HK**) to all tubes.
7. Cover with parafilm & gently vortex
8. Place in dark for 60 min
9. Read as point 2 (R2) using fluorometer
    a. R2-R1 reflects the ATP in the extract.
10. Add 20uL of dilute CK (**#2-CK**) to all tubes.
11. Place in dark for 105 min
12. Read as point 3 (R3)
    a. R3-R2 reflects the PCr in the extract.

**Cr Assay**

$$Creatine + ATP \xleftrightarrow{Creatine\ Kinase} ADP + PCr$$

$$ADP + P - Pyruvate \xrightarrow{Pyruvate\ Kinase} ATP + Pyruvate$$

$$Pyruvate + NADH \xleftrightarrow{LDH} Lactate + NAD$$

| **Reagent** | **mg/1mL** | **Stock Conc** | **Final Conc** | **V for 25mL** | **V for 50mL** | **V for 100mL** |
|---|---|---|---|---|---|---|
| 1.Imidazole | 68.080 | 1M | 50mM | 1.25mL | 2.5mL | 5mL |
| 2.$MgCl_2$ | 95.210 | 1M | 5mM | 125uL | 250uL | 500uL |
| 3.KCl | 74.550 | 1M | 30mM | 0.75mL | 1.5mL | 3mL |

| | | | | | | |
|---|---|---|---|---|---|---|
| 4.PEP | 2.340 | 10mM | 25uM | 60uL | 120uL | 240uL |
| 5.ATP | | | 200uM | 3mg | 6mg | 12mg |
| 6.NADH | 10.641 | 15mM | 45uM | 75uL | 150uL | 300uL |
| | | | | | | |
| 7.LDH | At Stock Conc. | 2750U/mL | 0.24U/mL | 2.5uL | 5uL | 10uL |
| 8.Pyruvate Kinase | At Stock Conc. | 2000u/mL | 0.75U/mL | 10uL | 20uL | 40uL |
| | | | | | | |
| 9.Creatine Kinase | | | 3.6U/mL | | | |
| | | | | | | |
| 10.Creatine standard (Creatine Monohydrate) | 149.15g/mol | 500µM | | 37.288mg in 500mL | | |
| 11. 10% BSA | | >/= 98% | | 1g in 10mL | | |

Steps Prior to Starting Assay

Reagent

1. Locate pre-made reagents + make daily reagents in 1.5mL tubes
2. Add regents 1 to 6
3. Bring to volume with water (45.48mL for 50mL SOL)
4. pH to 7.5
5. Add reagents 7 and 8

Dilute Enzyme - **#1CK**

1. Mix 2mL of reagent and 20uL of 10% BSA
2. Add 10mg of creatine kinase to solution and mix by inversion.

Assay

1. Use 3 tubes for each sample, 3 tubes for 'standard' and 3 tubes for 'blanks'
2. Add water, Cr standard or sample to respective tubes
    a. Add 10uL of water to the blank tubes
    b. Add 10uL of 500uM creatine standard to the standard tubes
    c. Add 10uL of sample to the appropriate tubes.
3. Add 1mL of dilute reagent to all of the tubes.
4. Cover with parafilm & gently vortex
5. Wait 15 minutes
6. Read as point 1 (R1) using fluorometer
    a. Wipe bottoms of tubes before reading
7. Add 25uL of dilute creatine kinase **(#1-CK**) to all of the tubes.
8. Cover with parafilm & gently vortex
9. Place in the dark for 60 minutes
10. Read as point 2 (R2) using fluorometer
    a. Wipe bottoms of tubes before reading

# Appendix III: RT-qPCR

**Step one: RNA Extraction**

Procedure:

1. Prep 2mL homogenization tubes with just enough silica beads to cover the sample
2. Take samples from -80°C and keep in liquid nitrogen throughout homogenization
3. Weigh tissue in a weigh boat, while keeping sample frozen with liquid nitrogen
    a. Brain: 20-40mg
    b. Muscle: 10-30mg
4. Place samples in homogenization tubes with silica beads
5. In the fume hood, add 1mL TRIzol Reagent to homogenization tubes and tighten the tube caps as much as possible
6. In fume hood, place tubes in the Fast Prep and make sure to secure them tightly using the allen key. Homogenize for 45 seconds at speed 6.5 or until fully liquefied (some connective tissue may remain and is unavoidable)
7. In fume hood, transfer homogenate into 1.5mL tubes.
8. Centrifuge samples at 12,000xg (RCF setting) for 10 min at 4°C.
9. Return to fume hood and transfer supernatant to new 1.5mL tubes, incubate for 5 minutes at room temp.
10. Add 200uL chloroform to the tube and shake vigorously by hand for 15 seconds.
11. Incubate at room temperature for 15 minutes.
12. Centrifuge at 12,000xg for 15 minutes at 4°C.
13. Return to fume hood and transfer the upper clear phase to a new 1.5mL tube being sure not to take up any of the middle white or bottom pink layers.
14. Add 600uL isopropanol and invert by hand until thoroughly mixed (15 or so times).
15. Transfer 700uL of sample at a time into a Qiagen RNeasy spin column (700uL is maximum capacity for the spin column, the remainder of the solution will be added to the column after it is spun)
16. Centrifuge at 12,000xg for 1 min, discard flow-through in fume hood and pat the bottom of the column dry with a Kimwipe.
17. Add any remaining sample into the column and centrifuge at 12,000xg for 1 min.
18. Discard flow-through, pat bottom of column and add 350uL of Wash Buffer RW1 to the column and centrifuge at 12,000xg for 1 min.
19. Discard flow-through, pat bottom of column and add 350uL of Wash Buffer RW1 to the column and centrifuge at 12,000xg for 1 min
20. Transfer column to a new collection tube, add 500uL of buffer RPE (containing ethanol) and centrifuge for 1 min at 12,000xg
21. Discard flow-through and add 500uL of Buffer RPE and spin at 12,000xg for 2 minutes
22. Transfer column to a new collection tube and add 30-40uL (ex/ 35uL) of RNAse-free H20 to the column, incubate at room temperature for 1 minute and then centrifuge at 12,000xg for 1.5 minutes.

Optional DNA Free Steps:

1. Get DNA-free treatment out and allow it to thaw
2. Transfer flow-through to new 1.5mL tube

3. Add 0.1x volume of 10x DNAse buffer (ex/ 3.5uL) Mix by pipette.
4. Add 1uL of rDNAse to this solution
5. Incubate for 20 minutes at 37°C
6. Add 0.1 volume DNAse Inhibitor (ex/ 3.5uL), mix gently and centrifuge for 1.5 minutes at 10,000xg
7. Remove supernatant making sure to stay clear of the pellet which will contaminate the sample
8. Measure the sample for concentration (ng/µL) and absorption (A260/280) via Nanodrop Spectrophotometer and then store sample at -80°C.

**Step 2: cDNA Creation**

1. Label PCR tubes on lid and side with appropriate sample names.
2. Dilute each RNA sample to 1µg in new tube based on concentration obtained from nanodrop.
    a. Add appropriate volume of RNase free water ($C_1V_1=C_2V_2$)
    b. Add appropriate volume of RNA
3. Make primer mix.
    a. Add 1µL per number of samples of Random Primers to 1.5mL tube.
    b. Add 1µL per number of samples of dNTP (base pairs) to same 1.5mL tube.
    c. *Can add 1µL extra of each to account for pipette error.
4. Add 2µL of primer mix to each diluted RNA sample.
5. Put samples into thermocycler and run using pre-set protocol (MacPherson RT1) for 5 minutes.
6. Make Master Mix (multiply the values below by the number of samples).
    a. Add 4µL of 5x FSB to 1.5mL tube.
    b. Add 2µL of Dithiothreitol (DTT) to mix.
    c. Add 1µL of RNase Out to mix.
    d. Add 1µL of Superscript II (SSII) to mix.
    e. *Can add extra of each to account for pipette error.
7. Add 8µL of Master Mix to each sample.
8. Put samples into thermocycler and run using pre-set protocol (MacPherson protocol RT2) for 1h15min.
9. Remove samples from thermocycler and store at -20ºC until further use.

**Step 3: RT-qPCR Analysis**

1. Dilute cDNA samples.
    a. Mix 20µL of cDNA with 80µL of RNase free water.
    b. Total yield = 100µL.
2. Make Master Mix (multiply the values below by the number of samples in duplicate).
    a. Add 10µL of Quanta (Taqman master mix) to 1.5mL tube.
    b. Add 4µL RNAse free water to mix.
    c. Add 1µL gene expression (SLC6A8 or GAPDH) to mix.
3. Add 15µL of Master Mix to 96 well-plate
    a. Number of wells = number of samples*2

4. Add 5µL of diluted cDNA to wells in duplicate.
5. Seal 96 well-plate with plastic cover.
6. Spin 96 well-plate using *Labnet Mini Plate Reader*
7. Use *Applied Biosciences RT-PCR System* to run samples for ~1h20.
8. Dispose of well-plate after transferring data output to personal file.

# Appendix IV: GSK3β Activity Assay

**Step 1: Homogenize Tissue**

1. Prep 2mL homogenization tubes with just enough *Silica beads* to cover the sample
2. Take samples from -80°C and keep in liquid nitrogen throughout homogenization
3. Weigh tissue in a weigh boat, while keeping sample frozen with liquid nitrogen
    a. Brain: 20-30mg (*for rat tissue).
    b. Calculate buffer needed to dilute each sample by 1:20 dilution factor
4. Place samples in homogenization tubes with silica beads.
5. Mix cell lysis buffer (amounts below are for 10mL buffer).
    a. 10mL cell lysis buffer
    b. Add 50µL of Pi
    c. Add 34µL of PMSF
6. Add appropriate amount of mixed cell lysis buffer to samples in 2mL homogenization tubes.
7. Put tubes in *Fast Prep* and run at 6.5 speed for 45sec.
8. Remove solution from tubes and place into 1.5mL tubes.
    a. Avoid *Silica beads.*
9. Centrifuge samples 10,000g for 10min at 4ºC.
10. Remove supernatant and place in new 1.5mL tube.
11. Store homogenate at -80ºC.

**Step 2: Prepare $Ca^{2+}$ ATPase Buffer:**

1. Add the following reagents and the bring to desired volume with doubly distilled water.
2. Bring the pH to 7.
3. Store at -20ºC.

| **Reagent** | **Molecular Weight (g/mol)** | **Final Concentration** |
|---|---|---|
| KCl | 74.55 | 200mM |
| HEPES | 238.30 | 20mM |
| $NaN_3$ | 65.01 | 10mM |
| EGTA | 380.35 | 1mM |
| $MgCl_2$ | 203.3 | 15mM |
| ATP | 605.19 | 5mM |
| PEP | 465.6 | 10mM |

**Step 3: Run Assay**

1. Add 20µL of homogenate samples in duplicate to 1.5mL tubes.
    a. Add 2.5µL of DMSO to half.
    b. Add 2.5µL of CHIR to half.
    c. Incubate on ice for 1 hour and vortex every 15 minutes.
2. Master Mix:
    a. Calculate desired amount (# samples in duplicate x 300µL)
    b. Add desired amount from above calculation of $Ca^{2+}$ ATPase buffer to tube.
    c. Add PK (36µL for 10mL solution).
    d. Add LDH (29µL for 10mL solution).
3. Vortex and pipette 300µL of master mix to each sample tube.
4. Vortex and pipette 90µL of each sample to a 96-well plate in triplicate.
5. Read using M2 Multimode Reader, Molecular Devices set to 37ºC at 340nm.
6. Add 4µL of NADH to each well using repeater pipette.
7. Add 5µL of GSK3β to each well using repeater pipette.
8. Read using M2 Multimode Reader, Molecular Devices set to 37ºC at 340nm.

# Appendix V: Western Blots

**Step 1: Homogenize Tissue**

1. Prep 2mL homogenization tubes with just enough *Silica beads* to cover the sample
2. Take samples from -80°C and keep in liquid nitrogen throughout homogenization
3. Weigh tissue in a weigh boat, while keeping sample frozen with liquid nitrogen
    a. Brain: 20-30mg (*for rat tissue).
    b. Calculate buffer needed to dilute each sample by 1:20 dilution factor
4. Place samples in homogenization tubes with silica beads.
5. Mix cell lysis buffer (amounts below are for 10mL buffer).
    a. 10mL cell lysis buffer
    b. Add 50µL of Pi
    c. Add 34µL of PMSF
6. Add appropriate amount of mixed cell lysis buffer to samples in 2mL homogenization tubes.
7. Put tubes in *Fast Prep* and run at 6.5 speed for 45sec.
8. Remove solution from tubes and place into 1.5mL tubes.
    a. Avoid *Silica beads.*
9. Centrifuge samples 10,000g for 10min at 4ºC.
10. Remove supernatant and place in new 1.5mL tube.
11. Store homogenate at -80ºC.

**Step 2: Semi-Dry Transfer Blotting with pre-made Gels**

1. Obtain prepped samples from -80ºC and appropriate gels.
2. Set up cassette:
    a. Put gels in cassette.

   b. Remove gel combs.
3. Pour small amount of running buffer (10x Tris/Glycine buffer), make sure there are no leaks.
4. Sample prep:
   a. Add 4µL of appropriate ladder to first lane.
   b. Add 5µL of each sample to the remaining lanes.
   c. Add 5µL of control/reference sample to the last lane.
5. Running gels:
   a. Put cassettes in electrophoresis tank.
   b. Fill tank and cassettes with running buffer.
   c. Run using for 22 minutes at 240V, 3A, 300W.
6. Membrane prep (PVDF):
   a. Cut square/triangle from top corner.
   b. Place in washing dish on rocker in methanol for ~5 minutes to activate.
   c. Pour off methanol and put on rocker in transfer buffer (5x Trans-Blot Turbo).
7. Get stacks to make sandwich:
   a. Stack - membrane - gel - stack.
8. Run for 3 minutes (x2) with Trans-Blot Turbo Transfer System to transfer to membranes.
9. Blocking membranes:
   a. Transfer membranes to washing dish.
   b. Add appropriate blocking solution.
   c. Put on rocker for 1 hour.
10. Primary antibody:
   a. Dump blocking solution.
   b. Add new blocking solution.
   c. Add correct amount of primary antibody.
   d. Put in fridge on rocker overnight.
11. Secondary antibody:
   a. Put primary in tubes and store at -20ºC for later use.
   b. Wash 3 x 5 minutes in TBST.
   c. Add secondary antibody and blocking solution.
   d. Place on rocker for 1 hour.
12. Imaging:
   a. Wash 3 x 5 minutes TBST.
   b. Add 500µL Millipore Immobilon Chemiluminescent HRP Substrate.
   c. Add 500µL Clarity Max HRP substrate.
   d. Visualize using BioRad Chemi Doc Imager.
13. Analyze using ImageLab.

# Appendix VI: BCA Protein Assay

1. Serial dilute protein standard BSA (1 mg/ml, 0.5, 0.25, 0.125, 0).
   a. Put 100µL of 1 mg/mL standard into 1.5mL tube and vortex.
   b. Take 50µL of 1 mg/mL standard and dilute with 50µL of distilled water to make 0.5 mg/mL and vortex.

    c. Take 50µL of 0.5 mg/mL standard and dilute with 50µL of distilled water to make 0.25 mg/mL and vortex.
    d. Continue until serially diluted standards are made.
    e. For the 0 mg/mL standard, place 50µL of distilled water into 1.5mL tube.
2. Take an aliquot of the protein extract to dilute.
    a. For muscle/brain 1:50 dilution.
    b. Take 1µL of homogenate and dilute in 49µL of distilled water.
3. Plate 10µL of protein standards and diluted samples in 96 well plate in triplicate.
4. Calculate the amount of working reagent you need. Each will receive 200µL of working reagent.
5. Add 200µL of sulfuric acid ($CuSO_4$) and BCA reagent to filled wells.
6. Incubate plate at 37ºC for 30min.
7. Place plate in Spectramax M2 to read at 527nm.
8. Assign the appropriate wells using template editor and read the plate.